Song et al. 2018/04/12

The authors' response file includes: response to anonymous referee #1, #2, and Nenes et al, as well as the change-tracked manuscript for acp-2018-6.

Response to Anonymous Referee #1

Song et al.

Comments are in black and responses are in blue.

This manuscript needs minor reversion before acceptance for publication.

Our responses to specific comments are provided below.

(1) As the authors stated, some papers reported the aerosol pH in Beijing, I suggest it should be declared clearly what are the correct results in the abstract and conclusion, also to let the readers know, which method is correct to estimate a reasonable aerosol pH.

The abstract and conclusion have been revised to highlight the appropriate applications of thermodynamic modeling and the reasonable range of aerosol water pH inferred from such method.

Revisions made in the manuscript:

> ***"Abstract.*** *pH is an important property of aerosol particles but is difficult to measure directly. Several studies have estimated the pH values for fine particles in North China winter haze using thermodynamic models (i.e., E-AIM and ISORROPIA) and ambient measurements. The reported pH values differ widely, ranging from close to 0 (highly acidic) to as high as 7 (neutral). In order to understand the reason for this discrepancy, we calculated pH values using these models with different assumptions with regard to model inputs and particle phase states. We find that the large discrepancy is due primarily to differences in the model assumptions adopted in previous studies. Calculations using only aerosol phase composition as inputs (i.e., reverse mode) are sensitive to the measurement errors of ionic species and inferred pH values exhibit a bimodal distribution with peaks between −2 and 2 and between 7 and 10, depending on whether anions or cations are in excess. Calculations using total (gas plus aerosol phase) measurements as inputs (i.e., forward mode) are affected much less by these measurement errors. In future studies, the reverse mode should be avoided whereas the forward mode should be used. Forward mode calculations in this and previous studies collectively indicate a moderately acidic condition (pH from about 4 to about 5) for fine particles in North China winter haze, indicating further that ammonia plays an important role in determining this property. The particle phase state assumed, either stable (solid plus liquid) or metastable (only liquid), does not significantly impact pH predictions. The unrealistic pH values of about 7 in a few previous studies (using the standard ISORROPIA model and stable state assumption) resulted from coding errors in the model, which have been identified and fixed in this study."*

> ***"Conclusions.*** *This study suggests that the significant discrepancy of fine particle pH, ranging from about 0 (highly acidic) to about 7 (neutral), calculated in previous studies of North China winter haze is due primarily to differences in the ways in which the E-AIM and ISORROPIA thermodynamic equilibrium models have been applied. The reverse mode calculations (only using aerosol phase composition as inputs) lead to erroneous results of pH since they are strongly affected by ionic measurement errors (especially under ammonia-rich conditions), and therefore should be avoided in future winter haze studies. The forward mode calculations (using the total (gas plus aerosol phase) compositions as inputs) account for additional constraints imposed by the partitioning of semi-volatile species and are affected much less by the measurement errors, and therefore, should be used in future studies. The forward mode calculations in this and previous studies collectively indicate, during North China winter haze events, that aerosol particles are moderately acidic with pH values ranging from about 4 to about 5. The assumed particle phase state (stable or metastable) does not significantly affect the pH calculations of ISORROPIA after coding errors in its standard model being fixed. A few previous studies, in which the standard ISORROPIA model was used and the stable state was assumed, predicted unrealistic pH values of around 7, and should be re-evaluated. In agreement with previous studies, we confirm that ammonia plays an important role in determining particle pH under winter haze conditions in northern China."*

(2) The "forward stable" module was modified by the authors, although I did not read it in detail, the results seem more reasonable than previous runs. If possible, please contact GIT group to confirm it.

Our modification of the ISORROPIA source code for the "forward stable" mode has been confirmed by its developers.

(3) Some recent studies declared the aerosol pH could be close to 7 due to the high ammonia level, please use the sensitivity test to show if it is possible. The implications of aerosol pH should be very important for atmospheric reactions.

The sensitivity of pH to ammonia concentration levels has been examined in a few previous winter haze studies (e.g., Liu et al., 2017 and Guo et al., 2017). Thus, in this study we cited their results in Sect. 3.2.3 in the revised manuscript and also provided a similar sensitivity test. Our conclusions are the same as those from these previous studies.

Revisions made in the manuscript:

> *"By analyzing the sensitivity of pH to ammonia concentrations, recent studies have emphasized the important role of ammonia in determining winter haze particle pH (Guo et al., 2017b; Liu et al., 2017a). It was suggested, under ammonia-rich conditions, that a 10-fold increase in gas phase NH_3 concentrations roughly corresponds to one unit increase in pH (i.e., a 10-fold decrease in H^+ activity) (Guo et al., 2017b). This is obvious, since the equilibrium of dissolution and dissociation of ammonia in water can be expressed as: $NH_{3(g)} + H^+_{(aq)} \leftrightarrow NH^+_{4(aq)}$. These sensitivity tests have also indicated that atmospheric relevant ammonia concentrations are not high enough to achieve a fully neutralized condition (pH of around 7) for aerosol particles (Guo et al., 2017b; Liu et al., 2017a). The sensitivity tests conducted in this study are consistent with these previous studies (Fig. S9 in the Supplement)."*

Liu, M., Song, Y., Zhou, T., Xu, Z., Yan, C., Zheng, M., Wu, Z., Hu, M., Wu, Y., and Zhu, T.: Fine particle pH during severe haze episodes in northern China, Geophys. Res. Lett., 44, 5213-5221, doi:10.1002/2017GL073210, 2017a.

Guo, H., Weber, R. J., and Nenes, A.: High levels of ammonia do not raise fine particle pH sufficiently to yield nitrogen oxide-dominated sulfate production, Sci. Rep., 7, 12109, doi:10.1038/s41598-017-11704-0, 2017b.

(4) Please have some discussion on the aerosol water content effects on pH values especially when RH was high.

In the revised manuscript, we have added more discussion in Sect. 3.2.3 on the effects of ammonia concentrations and RH on the pH values predicted by ISORROPIA and E-AIM. We think it does not make much sense to directly compare aerosol water content and pH values, because the aerosol water content predicted by the thermodynamic equilibrium models depends on the amount of chemical species and RH values in the input. If the input RH and excess ammonia remain constant, increasing the amount of chemical species would increase aerosol water content but would not change predicted pH values significantly. On the other hand, if the excess ammonia and the amount of chemical species in the input remain constant, increasing RH values would affect predicted pH values, but this effect is different for E-AIM and ISORROPIA. Thus we choose to evaluate the effect of changing RH on the predicted pH values.

Below is a new figure in the supplement of the revised manuscript. It shows the sensitivity of pH to NH_x concentrations and RH. The model inputs include total H_2SO_4 = 30 μg m^{-3}, total HNO_3 = 51 μg m^{-3}, temperature = 278 K, and varying RH (from 30% to 90%) and total NH_x concentrations (from 25 to 100 μg m^{-3}). The inputs are calculated from our field measurements during haze episodes (RH > 60%) as the average temperature and average concentrations of total H_2SO_4, and HNO_3. Na^+ and K^+ are accounted for as equivalent NH_4^+, and Cl^- as equivalent NO_3^-. The required NH_x concentrations calculated for the input total H_2SO_4 and HNO_3 concentrations are about 24 μg m^{-3}. The curves in panels (c and d) show the average pH in each bin for NH_x concentrations or RH.

Panel (d) of this figure shows the relationship of RH and pH. We find that the pH from ISORROPIA is insensitive to RH and the variability of pH is less than 0.3 unit. On the other hand, pH from E-AIM increases by 0.8 unit with increasing RH from 30% to 90%. The reason for this difference in pH between ISORROPIA and E-AIM remains unclear, and is discussed briefly in Sect. 3.2.1.

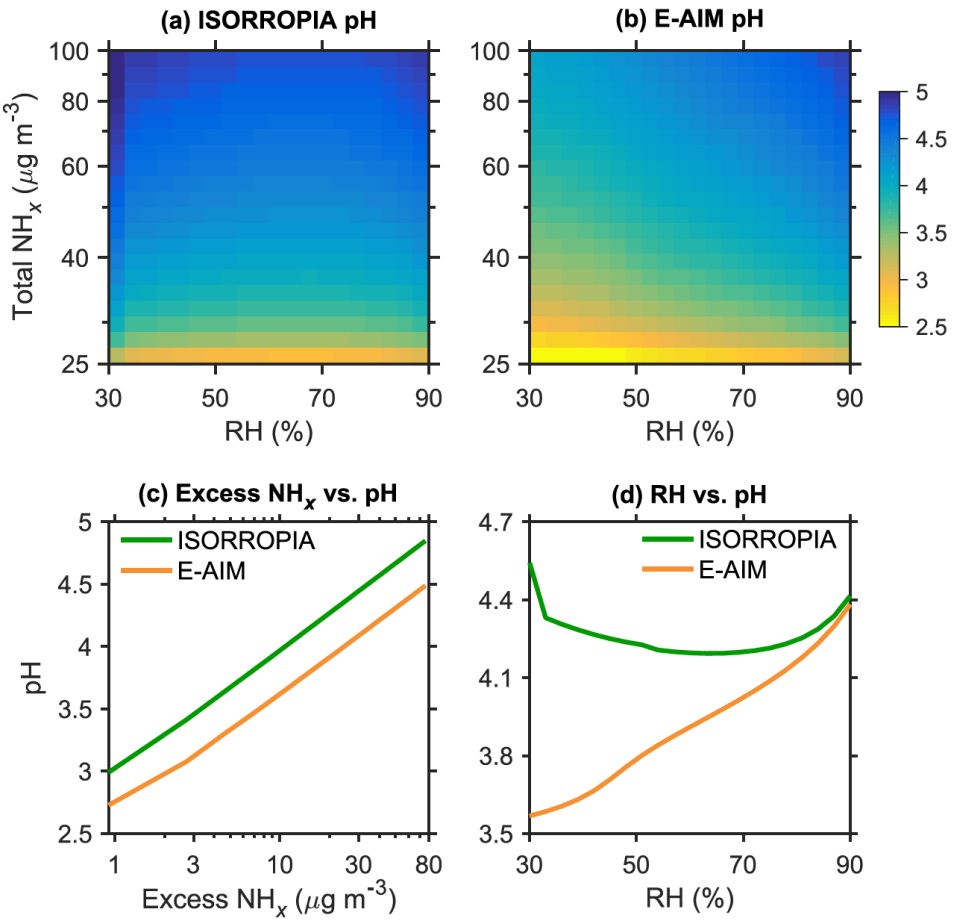
(a) ISORROPIA pH
(b) E-AIM pH
Total NH$_x$ (μg m^{-3})
RH (%)
(c) Excess NH$_x$ vs. pH
ISORROPIA
E-AIM
pH
Excess NH$_x$ (μg m^{-3})
(d) RH vs. pH

Response to Anonymous Referee #2

Song et al.

Comments are in black and responses are in blue.

This paper provides insight into the acidity of aerosols in Beijing. Table 1 provides a nice summary of previously published values which range from very acidic (-1) to basic (7.6). The paper uses ISORROPIA and E-AIM to estimate pH and provides discussion on how organic compounds may modify pH. The paper is well written, fairly thorough, and detailed. The Monte Carlo approach provides additional confidence in the results. A number of (mostly clarifying) comments are listed below.

Thanks for these positive comments for our manuscript. Our responses to specific comments are provided below.

One role for organic compounds in modifying pH was missing from the discussion. Specifically, on page 11, the authors list three ways in which organics can modify pH: (1) adding aerosol water, (2) participating in charge balance (e.g. dissociation of organic acids), and (3) by changing the aerosol phase state. The third area could use clarification (see detailed comments), but a fourth way (that seemed to be missing) is through modification of the chemical environment and therefore by modifying the activity coefficients of the inorganic species. This could be scoped out using the AIOMFAC model.

It is a very good comment. E-AIM assumes that the inorganic ions and organic solutes do not influence each other. Their molality-based activity coefficients are thus equal to those calculated for the systems water + inorganic ions only, and water + organic solutes only (Clegg et al., 2001). In the revised manuscript, we add the fourth way in Sect. 3.4 when discussing the effect of organics on particle pH calculation. Specifically, we modified this sentence to "*Organics may affect particle pH in several ways: (1) by increasing the absorption of aerosol water; (2) by participating in the charge balance and modifying the activity coefficients of inorganic ions in the aqueous phase; and (3) by changing the aerosol phase state (liquid-liquid phase separation)*", and added "*Note that E-AIM assumes that the organics in the aqueous solution do not affect the activity coefficients of inorganic ions (Clegg et al., 2001). Using the AIOMFAC model (web.meteo.mcgill.ca/aiomfac), Pye et al. (2018) recently showed that the interaction of inorganic ions with water-soluble organic compounds resulted in a 0.1 unit increase in pH for aerosols in the southeast United States*".

S. L. Clegg, J. H. Seinfeld, and P. Brimblecombe (2001) Thermodynamic modelling of aqueous aerosols containing electrolytes and dissolved organic compounds. J. Aerosol Sci. 32, 713-738.

Pye, H. O. T., Zuend, A., Fry, J. L., Isaacman-VanWertz, G., Capps, S. L., Appel, K. W., Foroutan, H., Xu, L., Ng, N. L., and Goldstein, A. H.: Coupling of organic and inorganic aerosol systems and the effect on gas–particle partitioning in the southeastern US, Atmos. Chem. Phys., 18, 357-370, doi:10.5194/acp-18-357-2018, 2018.

The authors should also be more forceful in their statements regarding what is a reasonable pH calculation and what is likely erroneous (see specific comment 1).

The abstract and conclusion have been revised to highlight the appropriate applications of thermodynamic modeling and the reasonable range of aerosol water pH inferred from such method. Revisions made in the manuscript:

> ***"Abstract.*** *pH is an important property of aerosol particles but is difficult to measure directly. Several studies have estimated the pH values for fine particles in North China winter haze using thermodynamic models (i.e., E-AIM and ISORROPIA) and ambient measurements. The reported pH values differ widely, ranging from close to 0 (highly acidic) to as high as 7 (neutral). In order to understand the reason for this discrepancy, we calculated pH values using these models with different assumptions with regard to model inputs and particle phase states. We find that the large discrepancy is due primarily to differences in the model assumptions adopted in previous studies. Calculations using only aerosol phase composition as inputs (i.e., reverse mode) are sensitive to the measurement errors of ionic species and inferred pH values exhibit a bimodal distribution with peaks between −2 and 2 and between 7 and 10, depending on whether anions or cations are in excess.*

Calculations using total (gas plus aerosol phase) measurements as inputs (i.e., forward mode) are affected much less by these measurement errors. In future studies, the reverse mode should be avoided whereas the forward mode should be used. Forward mode calculations in this and previous studies collectively indicate a moderately acidic condition (pH from about 4 to about 5) for fine particles in North China winter haze, indicating further that ammonia plays an important role in determining this property. The particle phase state assumed, either stable (solid plus liquid) or metastable (only liquid), does not significantly impact pH predictions. The unrealistic pH values of about 7 in a few previous studies (using the standard ISORROPIA model and stable state assumption) resulted from coding errors in the model, which have been identified and fixed in this study."

***"Conclusions.** This study suggests that the significant discrepancy of fine particle pH, ranging from about 0 (highly acidic) to about 7 (neutral), calculated in previous studies of North China winter haze is due primarily to differences in the ways in which the E-AIM and ISORROPIA thermodynamic equilibrium models have been applied. The reverse mode calculations (only using aerosol phase composition as inputs) lead to erroneous results of pH since they are strongly affected by ionic measurement errors (especially under ammonia-rich conditions), and therefore should be avoided in future winter haze studies. The forward mode calculations (using the total (gas plus aerosol phase) compositions as inputs) account for additional constraints imposed by the partitioning of semi-volatile species and are affected much less by the measurement errors, and therefore, should be used in future studies. The forward mode calculations in this and previous studies collectively indicate, during North China winter haze events, that aerosol particles are moderately acidic with pH values ranging from about 4 to about 5. The assumed particle phase state (stable or metastable) does not significantly affect the pH calculations of ISORROPIA after coding errors in its standard model being fixed. A few previous studies, in which the standard ISORROPIA model was used and the stable state was assumed, predicted unrealistic pH values of around 7, and should be re-evaluated. In agreement with previous studies, we confirm that ammonia plays an important role in determining particle pH under winter haze conditions in northern China."*

Specific comments:

1. Page 1, line 29: The authors indicate reverse mode calculations "exhibit a bimodal distribution with peaks between -2 and 2 and between 7 and 10." This reads as if these peaks are plausible values. Consider adding "depending on whether cations or anions were in excess" to highlight that the bimodal values are artifacts.

Revised accordingly.

2. Page 1, line 34-35 "The phase state assumed, which can be either stable (solid plus liquid) or metastable (only liquid), does not significantly impact pH predictions of ISORROPIA." Presumably this is true only at high RH? Figure 4a does not provide "stable" pH estimates below 60% RH and Figure 4b indicates the metastable and stable aerosol water differs (and is nonzero) between 40 and 70%.

This statement is true for a large RH range. In Figure 4b, the predicted metastable and stable aerosol water contents are zero for 30% and 40% RH bins (the *x* and *y* axis is not intersected at zero). For the RH bin at 50% (i.e., 45%-55%), the aerosol water content is 2.8 μg m^{-3} (a small value but nonzero). We did not show in Figure 4a the pH estimates for this RH range because there were many cases with no liquid phase in the stable state (the mutual deliquescence RH is around 50%). The average pH value for this RH range is 4.3 for the stable state (calculated using the available cases), which is ~0.2 unit smaller compared to that for the metastable state. Thus we think phase state does not *significantly* (compared to the reported 3 to 4 units' difference in some previous studies) impact pH predictions of ISORROPIA. We added a supplementary figure in the revised manuscript in order to clarify and emphasize this point and please see the details in the responses to Nenes et al.

3. Page 3, line 27-30. The collection efficiency of the AMS is known to be a function of the ammonium to sulfate ratio (e.g. Middlebrook et al., 2012 https://www.tandfonline.com/doi/pdf/10.1080/02786826.2011.620041). Was this factored in?

The several factors described in Middlebrook et al. (2012) which may affect the collection efficiency (CE) of the AMS have been considered when the CE of 0.5 was chosen in our AMS analysis. One sentence has been added here: "*A*

constant collection efficiency of 0.5 was chosen because (1) particles were dried before being analyzed, (2) the mass fraction of NH_4NO_3 was smaller than 0.4, and (3) the particle acidity was not high enough to affect CE substantially".

4. Page 4, line 12: What effects of organic compounds does E-AIM consider? Dissociation of acids? Does it treat the effects of organics on inorganic activity coefficients?

E-AIM considers the dissociation of organic acids and treats the produced organic anions by the Pitzer, Simonson and Clegg (PSC) equations. E-AIM assumes that the inorganic ions and organic solutes do not influence each other. Their molality-based activity coefficients are thus equal to those calculated for the systems water + inorganic ions only, and water + organic solutes only (Clegg et al., 2001).

S. L. Clegg, J. H. Seinfeld, and P. Brimblecombe (2001) Thermodynamic modelling of aqueous aerosols containing electrolytes and dissolved organic compounds. J. Aerosol Sci. 32, 713-738.

The above information has been added in the revised manuscript.

5. Page 5, equations: Add "charge equivalent" before "measured ion concentrations" to indicate that sulfate, Ca, Mg have been multiplied by 2.

Revised accordingly.

6. Section 3.2.1 and Figure 2: Do E-AIM and ISORROPIA predict different H+ concentrations? To what degree? How much of the difference between ISORROPIA and E-AIM is due to including gamma_H+ different than 1 in reporting pH vs the activity coefficient of H+ actually modifying the thermodynamics? In other words, if you plotted E-AIM and ISORROPIA and set the activity coefficient to 1 in both for plotting purposes only, what would the difference be?

We have provided a detailed response to this question in the response to Nenes et al. Please refer to that.

7. Figure 3: Could ISORROPIA or E-AIM predictions be overlaid on the plot? What measurement technique is the measured NH_4^+ fraction from? Is it different than the AMS value?

In the revised manuscript, we have added the average pH values from different model calculations to this figure. It is now noted in the caption of this figure that "*the measured average aqueous fraction … is calculated with the gas phase NH_3 and $PM_{2.5}$ NH_4^+ concentrations*." The AMS pH value is similar, although it is not shown.

8. Page 10, before section 3.4: Emphasize and clearly state what your best estimate of aerosol pH is.

One more sentence has been added: "*The appropriate applications of thermodynamic modeling indicate a moderately acidic condition (pH from about 4 to about 5) for fine particles in North China winter haze.*"

9. Page 11, line 6-8: See above comment about a missing organic modification to pH.

See our responses to the general comment about the impacts of organics on pH above.

10. Page 11, line 17: What fraction of the total aerosol water is due to organic compounds?

The data has been added in the revised manuscript: "*we find that the aerosol water associated with these species is only about 14 ± 3% (median ± median absolute deviation) of that associated with inorganic salts*".

11. Page 12, near line 7. What is your hypothesis regarding liquid-liquid phase separation and the effect on pH? Isn't your default configuration essentially liquid-liquid phase separation into and organic-rich and inorganic-rich phase? This ties in with the fourth possible way organics affect pH (via activity coefficients if organic compounds coexist in the inorganic phase).

The aerosol solution under liquid-liquid phase separation can be separated into two phases: organic-rich and inorganic-rich, which may have different pH values (although such effect remains unclear). The study we cited here (Dallemagne et al., 2016) showed that the organic-rich phase had a pH value higher by 0.4 unit compared to the single phase situation. This effect is not the same as the fourth possible way, which is the influence of water-soluble organics on the activity coefficients of inorganic ions in the aqueous phase (inorganic-rich).

12. In the supporting information, can you provide the exact ISORROPIA file names and line numbers and what the content was modified?

The standard ISORROPIA source code is password protected at *http://isorropia.eas.gatech.edu/index.php?title=Code_Repository*, but there is a version of ISORROPIA-II implemented by Pye et al. (2009) in the GEOS-Chem chemical transport model and fully publicly accessible at: *http://acmg.seas.harvard.edu/geos/doc/man/*. The ISORROPIA-II code is under the directory *ISOROPIA/*. Thus we have published bug fixes for ISORROPIA-II stable mode and the exact line numbers and contents can be found at: *http://wiki.seas.harvard.edu/geos-chem/index.php/ISORROPIA_II*

Pye, H. O. T., H. Liao, S. Wu, L. J. Mickley, D. J.Jacob, D. K. Henze, and J. H. Seinfeld, Effect of changes in climate and emissions on future sulfate-nitrate-ammonium aerosol levels in the United States, J. Geophys. Res., 114, D01205, 2009.

The above information has been added in the revised manuscript and the supplement.

Response to A. Nenes, H. Guo, A. Russell and R. Weber

Song et al.

Comments are in black and responses are in blue.

We would like to commend Song et al. for their extensive analysis that goes deep into the model code and data. The importance of understanding aerosol pH is key to understanding of aerosol growth and impacts, as has been demonstrated in a growing body of literature. This literature, however, also exposes knowledge gaps. Following are some comments and thoughts about the analysis that in our opinion require attention, especially on the impact and importance of the H^+ activity coefficient. Addressing these points, may require considerable rewriting and refocusing of the paper, but we feel it will eventually substantially enhance the contribution.

We thank Nenes et al. for their comments, which are very useful for improving the quality of this manuscript. The comments on the H^+ activity coefficients are especially helpful. Our responses to the specific points raised by Nenes et al. are given below.

Algorithm changes to ISORROPIA-II routines.

We would like to thank the authors for their very detailed explanation of the pH calculation issue, and the resolution provided. This clearly shows the value of having open source codes so that they are continuously used and tested by the community. The alternative approach in the standard code was used in the routines identified, because loss in precision in calculating the SQRT function (at low concentrations of aerosol precursors and when solid precipitates formed, e.g., NH_4Cl), made partitioning calculations at times inaccurate and noisy. Although the alternative approach captured partitioning, pH was clearly not, so adopting the standard calculation approach used in the subcases with higher RH values is appropriate; however, provision still needs to be shown to avoid loss of precision (e.g., Taylor expansion approximations or renormalization instead of SQRT). We will address this in the upcoming version of ISORROPIA-II.

We thank Nenes for sharing us the source codes of ISORROPIA, which allowed us to examine and identify the coding errors in the model.

Application of thermodynamic models when interpreting data.

We were very pleased to see that the analysis of Beijing data carried out here fully supports our prior work on how to use observational data to constrain pH, namely: *i*) avoiding usage of molar ratios and ion balances as pH proxies (Guo et al., 2015; Hennigan et al., 2015; Guo et al., 2016; Weber et al., 2016; Guo et al., 2017b), and, *ii*) the large pH errors that can result when aerosol-only concentrations from observations are used in open-system thermodynamic calculations (i.e., "reverse mode" calculations that are not subject to a global constraint of mass balance (Pilinis et al., 2000; Hennigan et al., 2015)).

We agree with Nenes et al. on this.

It should also be noted that the secondary effect of water-soluble organics on aerosol pH is also consistent with the recent work of Pye et al. (2017). Note that the reference to Pye et al. (2017) should refer to the following publication: Coupling of organic and inorganic aerosol systems and the effect on gas–particle partitioning in the southeastern US, Atmos. Chem. Phys., 18, 357-370, https://doi.org/10.5194/acp-18-357-2018, 2018.

The effect of water-soluble organic compounds is discussed in more detail in the revised manuscript. Please see the responses to anonymous reviewer #2.

One conclusion that the authors come to is that the pH calculations are not sensitive to the assumption of metastable and stable state. As presented, this can be misinterpreted by the reader that partitioning evaluations are not valuable for constraining aerosol pH. Partitioning calculations can sufficiently constrain pH, but only when predictions of aerosol water and semivolatile partitioning (of NH_3-NH_4^+, HNO_3-NO_3^-, and HCl-Cl^- if possible) are reproduced by

observations (as shown in e.g., Guo et al. (2015) and other studies) – and a sufficient fraction of the partitioned aerosol species is associated with the aqueous phase. When aerosol water measurements are lacking or too uncertain, then showing that when **aqueous phase semivolatile partitioning by itself** (i.e., provided by the metastable solution) reproduces aerosol observations, aerosol pH is sufficiently constrained. **The pH values calculated for the metastable solution, for cases where partitioning is consistent with observations, provide the most plausible estimates of acidity.** pH values for the stable solution, especially when the liquid water content becomes very small (hence aqueous-phase partitioning a secondary contribution to the total partitioning), are subject to considerably more uncertainty – even if the pH corresponding to the metastable and stable solutions agree.

We partially disagree with Nenes et al. on this.

We think partitioning evaluations are important for evaluating the rationality of pH calculations in thermodynamic modeling. A good model–observation comparison of semivolatile species partitioning is a necessary condition for a good estimate of pH, but not a sufficient condition. When using the standard source codes, although model calculations can well reproduce the partitioning of semivolatile species for both particle phase states, the predicted pH values can be significantly different, for example, on average 4.6±0.4 (metastable) and 7.0±1.3 (stable) during 2012 winter in Xi'an, China (Wang et al., 2018). On the other hand, when using the revised source codes of ISORROPIA, model calculations under both states can well reproduce the partitioning of semivolatile species and also predict very similar pH values.

It is important to note that the predicted partitioning of semivolatile species is almost identical for both particle phase states. Guo et al. (2017c) mentioned that the partitioning of aerosol inorganic concentrations (e.g., NH_4^+, NO_3^-) using the metastable mode agreed better with the observations, when compared to those using the stable mode. We believe that the model–observation comparisons in Figure S1 of Guo et al. (2017c) were conducted inappropriately for the stable mode because only aqueous phase concentrations were used. However, the total particle phase (aqueous + solid) concentrations should be used in order to be consistent with ambient observations. The same results were also given in a recent study by Wang et al. (2018). In fact, since the forward thermodynamic calculations take the measured total (gas + particle) concentrations as model inputs, good model–observation comparisons for gas phase concentration (e.g., NH_3(g)) definitely mean that the model can well reproduce the observed particle phase concentrations (e.g., NH_4^+(p)).

We think thermodynamic model calculations with either stable or metastable state assumption can provide reasonable estimates of aerosol water pH, and the predicted pH values for the stable solution are NOT subject to "considerably more uncertainty" when the aerosol water content is small, at least for the winter haze conditions considered in our study. In order to better describe our point of view, here we conduct some more model calculations using ISORROPIA. The inputs are the average temperature and the average concentrations of total H_2SO_4, HNO_3, and NH_3 from our field measurements during haze episodes, and varied RH values from low to high. Figure R1 shows the comparisons of the predicted pH, AWC, ionic strength, and partitioning of NH_3 for both stable and metastable solutions.

As shown in Figure R1a–b, the predicted pH values for the stable and metastable solutions are exactly the same when the RH is larger than about 80% (when the RH is larger than the deliquescence RH for all the salts and both of the solution includes an aqueous phase only). When the RH is between about 60% and about 80% (when both aqueous and solid phases are present for the stable solution), the predicted pH values for the stable solution are on average 0.02 ± 0.00 greater than those for the metastable solution. This difference in pH is small relative to the uncertainty resulting from other factors (e.g., measurements of gas and aerosol species and meteorological parameters). Note that in Figure R1c for some cases the AWC in the stable solution is more than one order of magnitude lower than that in the metastable solution, and that for the same cases in the stable solution the "aqueous-phase partitioning a secondary contribution to the total partitioning", as can be seen in Figure R1e–f.

We also would like to emphasize that there has been no observational evidence so far to suggest whether the Beijing winter haze fine particles are in a metastable or stable state. It is also unlikely to figure out particle phase states from theoretical calculations because of the very large variability of ambient RH (see Section 2.2 of our paper) and the difficulty in estimating the efflorescence RH for multicomponent salts (Seinfeld and Pandis, 2016 Chapter 10). Therefore, at the current stage, a practical approach is to predict the aerosol water content and pH for both stable and

metastable states, which can provide a way to estimate the uncertainty of these variables due to the assumption of different phase states.

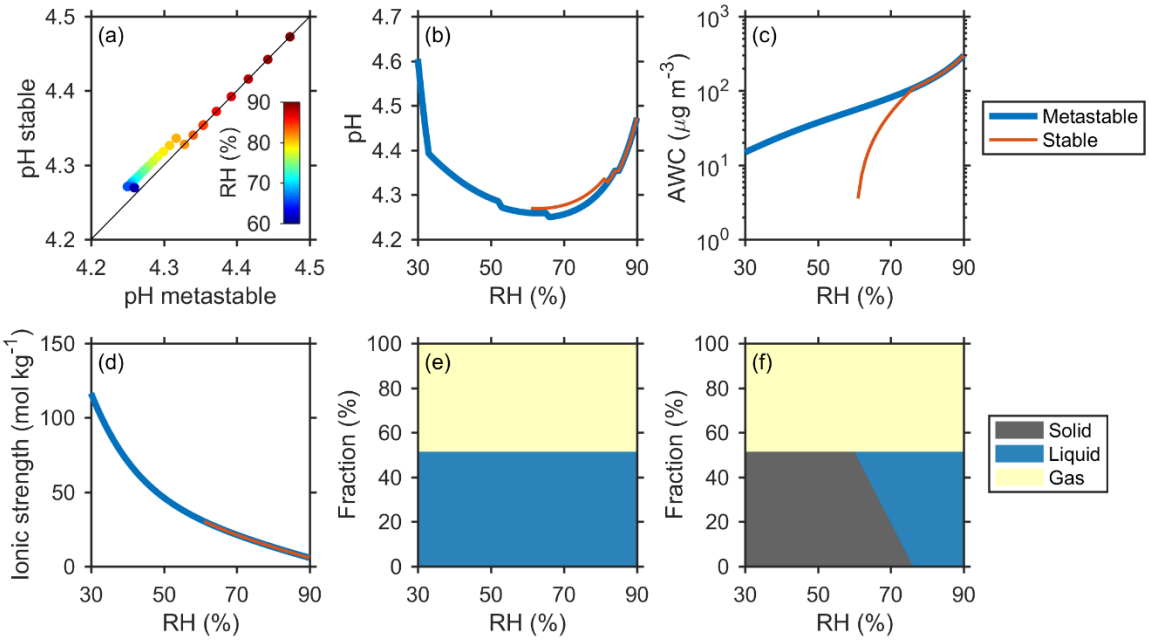

Figure R1. Comparisons of the ISORROPIA-predicted pH (a–b), AWC (c), ionic strength (d), and partitioning of NH_3 (e–f) under assumptions of the metastable and stable phase states. The model inputs include total H_2SO_4 = 30 μg m^{-3}, total HNO_3 = 51 μg m^{-3}, total NH_3 = 47 μg m^{-3}, temperature = 278 K, and varied RH. The inputs are calculated from our field measurements during haze episodes (RH > 60%) as the average temperature and the average concentrations of total H_2SO_4, HNO_3, and NH_3. Na^+ and K^+ are accounted for as equivalent NH_4^+, and Cl^- as equivalent NO_3^-.

Activity coefficient discussion

The authors extensively comment on the usage of $\gamma_{H+} = 1$ in some of the calculations behind ISORROPIA-II. In fact, the assumption that $\gamma_{H+} = 1$ is thought to be a major source of pH discrepancy between ISORROPIA and E-AIM (it's even stated in the abstract). The data presented does not really support this for the following reasons:

1. γ_{H+} varies by ±0.2 units over the ionic strengths considered (0-20), Figure 2b, while pH differences between the models are typically larger than 0.2 units.

2. The correlation of pH discrepancy between ISORROPIA-II (as calculated with the formula of Guo et al. (2015)) and E-AIM with γ_{H+} *does not* indicate a causal relationship.

3. If $\gamma_{H+} = 1$ was indeed the reason for the discrepancy, then at an ionic strength of ~20, when γ_{H+} ~1, the pH discrepancy between ISORROPIA and E-AIM should be zero (Figure 2b). This is not the case at all.

Considering points 1, 2, 3 together, one can actually conclude that about 0.2 pH units discrepancy between ISORROPIA-II and E-AIM may arise from the assumption of $\gamma_{H+} = 1$ for the RH (ionic strength) range considered, while the rest of the discrepancy may be related to the predicted concentration of H^+. This may even suggest that $\gamma_{H+} = 1$ is not a leading cause of discrepancy. In support of this, we find it very interesting that when one compares the γ_{H+} values from E-AIM (Figure 2c) and from AIOMFAC (Figure S6), $\log(\gamma_{H+})$ differs by about 0.6 units at an ionic strength of 20 M (E-AIM gives 0.1 and AIOMFAC gives -0.5; note the -0.6 difference in $\log(\gamma_{H+})$ means +0.6 pH compared to E-AIM), which seems to be consistent with the 0.6 higher pH comparing ISORROPIA to E-AIM at the same ionic strength. Could it just be then that the calculation of γ_{H+} by E-AIM is more uncertain than implied? The Beijing haze polluted period has an ionic strength close to 40 M, which brings γ_{H+} close to 1 according to Figure S6.

Assuming γ_{H+} = 1 to diagnose pH from ISORROPIA (single point) translates to an uncertainty of less than 0.5 pH units over a large range of RH or ionic strength (Figure S6).

We agree with Nenes et al. that our data analysis does not support the statement in the original manuscript that the assumption of γ_{H+} = 1 is the major source of pH discrepancy between E-AIM and ISORROPIA. The Section 3.2.1 has been extensively revised and this statement has been removed from the abstract and conclusion. In the revised manuscript, we conduct additional model calculations using E-AIM version II (for H^+ - NH_4^+ - SO_4^{2-} - NO_3^- - H_2O aerosol), because this version can be used assuming a metastable state and thus predict pH at low RH values. It was not insightful to introduce a third model, AIOMFAC, to help explain the differences in predicted pH between ISORROPIA and E-AIM. Figure R2 below the difference in pH predicted by ISORROPIA and E-AIM as well as several other parameters. What we find from this additional data analysis is that the difference in predicted pH is: (1) systematic and related to RH, (2) related to both H^+ concentrations and activity coefficients, and (3) smaller than one unit for the cases tested. We note in the revised manuscript that "*The exact factors contributing to ΔpH remain unclear, since these two thermodynamic models differ in many ways (e.g., their methods in calculating the activity coefficients for ionic species other than H^+)*", and that "*the above analysis is based on the data sets collected in Beijing winter and may not apply to other conditions*".

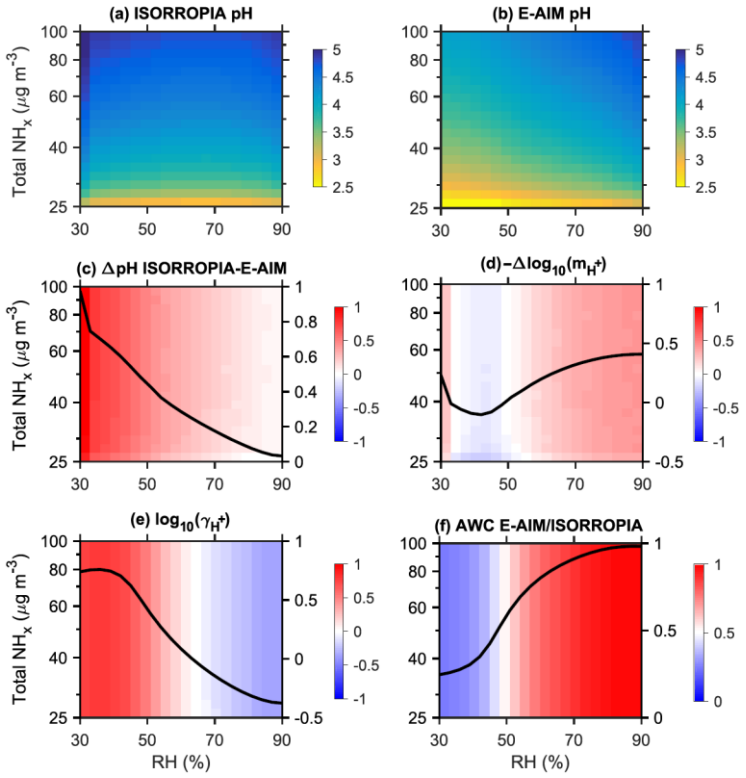

Figure R2. Comparison of predicted pH values and several other parameters from ISORROPIA and E-AIM (version II) under typical Beijing winter haze conditions (NH_x-rich). The curve in each panel (c–f) shows the average value for each bin of RH. The model inputs include total H_2SO_4 = 30 μg m^{-3}, total HNO_3 = 51 μg m^{-3}, temperature = 278 K, and varied RH (from 30% to 90%) and total NH_x concentrations (from 25 to 100 μg m^{-3}). The inputs are calculated from our field measurements during haze episodes (RH > 60%) as the average temperature and average concentrations of total H_2SO_4 and HNO_3. Na^+ and K^+ are accounted for as equivalent NH_4^+, and Cl^- as equivalent NO_3^-.

There is a lack of discussion on the effects of the other ionic species as sources of discrepancy between E-AIM and ISORROPIA-II, which is surprising, given that E-AIM uses the single ion activity approach, while ISORROPIA uses mean activity coefficients of ion pairs. Predictions from the two types of activity coefficient models do show important differences (e.g., Kim et al., 1993).

We agree that the different methods in calculating activity coefficients for ionic species may be a source of difference in predicted pH between E-AIM and ISORROPIA (Kim et al., 1993; Zhang et al., 2000).

The configuration used in ISORROPIA-II (Kusik-Meisner binary activity coefficients with the Bromley mixing rule for multicomponent aerosol) has been shown to provide stable solutions for ionic strengths that far exceed 30, the limit where Pitzer coefficients have been shown to work well (Kim et al., 1993). The latter point of course is quite relevant for the discussion raised by the authors concerning the applicability of the activity coefficient models used by ISORROPIA-II and E-AIM when applied to the high ionic strengths corresponding to RH below 70%.

The Pitzer, Simonson, and Clegg (PSC) method, which is used in E-AIM, overcomes the limitation of molar-based ionic strength and is applicable the over entire concentration range (Zaveri et al., 2005).

Given the above, unless a thorough analysis of how all the activity coefficients water uptake and equilibrium constants contribute to the pH differences between ISORROPIA-II and E-AIM, one cannot really state how much uncertainty in pH arises from the assumption of $\gamma_{H+} = 1$, though it appears to be bounded and much less than the difference in the predicted pH's between the two models. Perhaps it would be better to just plot the predicted particle phase fractions ("$\varepsilon(NH_4^+)$ and "$\varepsilon(NO_3^-)$ as a function of pH) by each model and compare them against the data (following the approach of Guo et al., 2017a). Then one will have a better sense of the pH uncertainty (given by the range between models) for a given value of (observed) ε".

We agree that the pH differences between ISORROPIA and E-AIM cannot be completely explained unless a thorough comparative analysis is made. The main goal of this manuscript is to explain the large pH discrepancy (from about 0 to 7) reported in previous North China winter haze studies. The pH difference in the forward ISORROPIA and E-AIM model calculations is much smaller compared to the other factors (i.e., forward vs. reverse, metastable vs. stable of the standard ISORROPIA) and thus a thorough analysis on this relatively small pH difference between the forward ISORROPIA and E-AIM calculations goes beyond the focus of this manuscript. Both ISORROPIA and E-AIM show a moderately acidic condition for Beijing winter haze particles. It is noted in Figure 1 and Figure S5 that ISORROPIA and E-AIM predict nearly identical $\varepsilon(NH_4^+)$ and $\varepsilon(NO_3^-)$ and both can well capture the observed gas-particle partitioning. Therefore, we think that the difference between ISORROPIA and E-AIM may provide an estimate for the uncertainty of pH.

Specific (but important) comments

- The authors note early in the manuscript that the discrepancy in calculated pH when assuming $\gamma_{H+} = 1$ can be multiple units. This is not supported by the supplementary figure (γ_{H+} from AIOMFAC), where for an ionic strength range of 0-100, log γ_{H+} (hence the contribution of assuming $\gamma_{H+} = 1$ to pH discrepancy) varies within 1 unit. This has always been, by the way, our view – so it is nice to see this confirmed by the analysis presented! Also noted throughout is that pH is overestimated when assuming $\gamma_{H+} = 1$. This is not always true as well; as noted by the supplementary figure (γ_{H+} from AIOMFAC), pH can be underestimated or overestimated by assuming $\gamma_{H+} = 1$, but not more than half a unit.

  Please see the responses to the general comments of activity coefficients above.

- In fact, the average pH estimated by ISORROPIA-II is *actually lower* than that reported for E-AIM (4.2 vs 5.4, for ISORROPIA-II vs E-AIM respectively) inconsistent with pH trends stated above.

  Wrong numbers of pH are quoted from the manuscript. As shown in Section 3.3, the mean pH values of 5.4 (E-AIM) and 4.2 (ISORROPIA) are for the *reverse mode* calculations. The average pH values are 4.0 (E-AIM) and 4.6 (ISORROPIA) for the *forward mode* calculations.

- In ISORROPIA-II, the non-ideal interactions of H+ with all the ions in solution (especially NO3, Cl, HSO4, SO4) is explicitly considered by the Kusik-Meisner and Bromely formulations. $\gamma_{H+} = 1$ is only invoked when the singe ion activity is required. This is not sufficiently noted in the text.

We noted in Section 2.2 that "With ISORROPIA, γ_{H^+} and γ_{OH^-} are assumed equal to unity, whereas the activity coefficients for the other ionic pairs (e.g., H^+–Cl^-) are calculated (Fountoukis and Nenes, 2007)."

- The authors understandably treat NVC (i.e. Ca, Mg, K, Na) as equivalent sodium, because E-AIM cannot explicitly treat Ca, Mg and K. The impact of this assumption can lead to important differences in the predicted thermodynamic state, owing to the strong nonideality of divalent ions and different water uptake characteristics of sodium salts vs. their other counterparts (e.g., Fountoukis et al., 2009).

  We noted in Figure 2 of the original manuscript that K^+ was accounted for as equivalent Na^+ in ISORROPIA, and therefore, for the comparison of pH for E-AIM and ISORROPIA, the model inputs are the same.

- What constitutes a "large/important" and "small/minor" different in pH depends on the context in which the pH is used. Constraining "absolute" pH for ambient aerosol to within less than 0.5 units may prove to be extremely challenging (e.g., the difference in log γ_{H+} between E-AIM and AIOMFAC, the effects of organics on activity and water uptake and so on); so it may most likely be necessary to use a consistent pH calculation method and thermodynamic model when comparing aerosol acidities between models and/or observations.

  Such qualitative expressions have been avoided in the revised manuscript when comparing E-AIM and ISORROPIA.

- The authors caution about the predictions of ISORROPIA-II in metastable mode (for RH below the mutual deliquescence point) owing to the large ionic strengths of the solutions. Although we agree the ionic strengths are high, literature supports that the activity coefficient models used in ISORROPIA-II are stable for ionic strengths above 30, a situation that is also not the case for the Pitzer method (Kim et al., 1993).

  The Pitzer, Simonson, and Clegg (PSC) method, which is used in E-AIM, overcomes the limitation of molar-based ionic strength and is applicable over the entire concentration range (Zaveri et al., 2005).

In closing, we very much appreciate the analysis and it demonstrates an increasing sophistication of which the community is both understanding and discussing the thermodynamics of aerosols and the important topic of aerosol acidity. We also hope that the comments provided here add insight that will considerably strengthen the paper, and provide ideas for future work on the important topic of aerosol acidity.

The authors thank Nenes et al. again for the above comments, which were helpful in improving the quality of this manuscript.

References

Fountoukis, C., Nenes, A., Sullivan, A., Weber, R., VanReken, T., Fischer, M., Matias, E., Moya, M. Farmer, D., and Cohen, R.: Thermodynamic characterization of Mexico City Aerosol during MILAGRO 2006, Atmos. Chem. Phys., 9, 2141-2156, 2009.

Guo, H., et al.: Fine-particle water and pH in the southeastern United States, Atmos. Chem. Phys., 15, 5211-5228, doi: 10.5194/acp-15-5211-2015, 2015.

Guo, H., et al.: Fine particle pH and the partitioning of nitric acid during winter in the northeastern United States, Journal of Geophysical Research: Atmospheres, 121, 10355-10376, doi: 10.1002/2016jd025311, 2016.

Guo, H., Liu, J., Froyd, K. D., Roberts, J. M., Veres, P. R., Hayes, P. L., Jimenez, J. L., Nenes, A., and Weber, R. J.: Fine particle pH and gas–particle phase partitioning of inorganic species in Pasadena, California, during the 2010 CalNex campaign, Atmos. Chem. Phys., 17, 5703-5719, doi: 10.5194/acp-17-5703-2017, 2017a.

Guo, H., Nenes, A., and Weber, R. J.: The underappreciated role of nonvolatile cations on aerosol ammonium-sulfate molar ratios, Atmospheric Chemistry and Physics Discussions, 1-19, doi: 10.5194/acp-2017-737, 2017b.

Guo, H., Weber, R. J., and Nenes, A.: High levels of ammonia do not raise fine particle pH sufficiently to yield nitrogen oxide-dominated sulfate production, Sci. Rep., 7, 12109, doi:10.1038/s41598-017-11704-0, 2017c.

Hennigan, C. J., Izumi, J., Sullivan, A. P., Weber, R. J., and Nenes, A.: A critical evaluation of proxy methods used to estimate the acidity of atmospheric particles, Atmos. Chem. Phys., 15, 2775-2790, doi: 10.5194/acp-15-2775-2015, 2015.

Kim, Y.P., Seinfeld, J.H. and Saxena, P: Atmospheric gas-aerosol equilibrium. 2. Analysis of common approximations and activity-coefficient calculation methods, Aer.Sci.Tech., 19, 182-198, 1993

Pilinis, C., Capaldo, K.P., Nenes, A., Pandis, S.N.: MADM - A New Multicomponent Aerosol Dynamics Model, Aerosol Sci. Tech., 32(5), 482-502, 2000

Pye, H. O. T., et al.: On the implications of aerosol liquid water and phase separation for organic aerosol mass, Atmos. Chem. Phys., 17, 343-369, doi: 10.5194/acp-17-343-2017, 2017.

Pye, H. O. T., Zuend, A., Fry, J. L., Isaacman-VanWertz, G., Capps, S. L., Appel, K. W., Foroutan, H., Xu, L., Ng, N. L., and Goldstein, A. H.: Coupling of organic and inorganic aerosol systems and the effect on gas–particle partitioning in the southeastern US, Atmos. Chem. Phys., 18, 357-370, doi:10.5194/acp-18-357-2018, 2018.

Seinfeld, J. H., and Pandis, S. N.: Atmospheric chemistry and physics: from air pollution to climate change, Third ed., John Wiley & Sons, Inc., Hoboken, New Jersey, 2016.

Wang, G., Zhang, F., Peng, J., Duan, L., Ji, Y., Marrero-Ortiz, W., Wang, J., Li, J., Wu, C., Cao, C., Wang, Y., Zheng, J., Secrest, J., Li, Y., Wang, Y., Li, H., Li, N., and Zhang, R.: Particle acidity and sulfate production during severe haze events in China cannot be reliably inferred by assuming a mixture of inorganic salts, Atmos. Chem. Phys. Discuss., 2018, 1-23, doi:10.5194/acp-2018-185, 2018.

Weber, R. J., Guo, H., Russell, A. G., and Nenes, A.: High aerosol acidity despite declining atmospheric sulfate concentrations over the past 15 years, Nature Geoscience, 9, 282-285, doi: 10.1038/ngeo2665, 2016.

Zaveri, R. A., Easter, R. C., and Wexler, A. S.: A new method for multicomponent activity coefficients of electrolytes in aqueous atmospheric aerosols, J. Geophys. Res., 110, D02201, doi:10.1029/2004JD004681, 2005.

Zhang, Y., Seigneur, C., Seinfeld, J. H., Jacobson, M., Clegg, S. L., and Binkowski, F. S.: A comparative review of inorganic aerosol thermodynamic equilibrium modules: similarities, differences, and their likely causes, Atmos. Environ., 34, 117-137, doi:10.1016/S1352-2310(99)00236-8, 2000.

Fine particle pH for Beijing winter haze as inferred from different thermodynamic equilibrium models

Shaojie Song[1,*], Meng Gao[1,*], Weiqi Xu[2], Jingyuan Shao[3,4], Guoliang Shi[5], Shuxiao Wang[6], Yuxuan Wang[7,8], Yele Sun[2,9], Michael B. McElroy[1,10]

[1]School of Engineering and Applied Sciences, Harvard University, Cambridge, Massachusetts 02138, USA
[2]State Key Laboratory of Atmospheric Boundary Physics and Atmospheric Chemistry, Institute of Atmospheric Physics, Chinese Academy of Sciences, Beijing 100029, China
[3]Laboratory for Climate and Ocean-Atmosphere Studies, Department of Atmospheric and Oceanic Sciences, School of Physics, Peking University, Beijing 100871, China
[4]Department of Atmospheric Sciences, University of Washington, Seattle, Washington 98195, USA
[5]State Environmental Protection Key Laboratory of Urban Ambient Air Particulate Matter Pollution Prevention and Control, College of Environmental Science and Engineering, Nankai University, Tianjin 300071, China
[6]State Key Joint Laboratory of Environmental Simulation and Pollution Control, School of Environment, Tsinghua University, Beijing 100084, China
[7]Department of Earth and Atmospheric Sciences, University of Houston, Houston, Texas 77004, USA
[8]Department of Earth System Science, Tsinghua University, Beijing 100084, China
[9]University of Chinese Academy of Sciences, Beijing 100049, China
[10]Department of Earth and Planetary Sciences, Harvard University, Cambridge, Massachusetts 02138, USA
[*]These authors contributed equally to this work.

Correspondence to: Shaojie Song (songs@seas.harvard.edu), Michael B. McElroy (mbm@seas.harvard.edu), Yele Sun (sunyele@mail.iap.ac.cn)

Abstract. pH is an important property of aerosol particles but is difficult to measure directly. Several studies have estimated the pH values for fine particles in North China winter haze using thermodynamic models (i.e., E-AIM and ISORROPIA) and ambient measurements. The reported pH values differ widely, ranging from close to 0 (highly acidic) to as high as 7 (neutral). In order to understand the reason for this discrepancy, we calculated pH values using these models with different assumptions with regard to model inputs and particle phase states. We find that the large discrepancy is due primarily to differences in the model assumptions adopted in previous studies. Calculations using only aerosol phase composition as inputs (i.e., reverse mode) are sensitive to the measurement errors of ionic species and inferred pH values exhibit a bimodal distribution with peaks between −2 and 2 and between 7 and 10, depending on whether anions or cations are in excess. ~~.~~ Calculations using total (gas plus aerosol phase) measurements as inputs (i.e., forward mode) are affected much less by these ~~the~~ measurement errors. In future studies, the reverse mode should be avoided whereas the forward mode should be used. ~~, and results are thus superior to those obtained from the reverse mode calculations.~~ Forward mode calculations in this and previous studies collectively indicate a moderately acidic condition (pH from about 4 to about 5) for fine particles in North China winter haze, indicating further that ammonia plays an important role in determining this property. ~~The differences in pH predicted by the forward mode E-AIM and ISORROPIA calculations may be attributed mainly to differences in estimates of activity coefficients for hydrogen ions.~~ The particle phase state assumed, ~~which can be~~ either stable (solid plus liquid) or metastable (only liquid), does

not significantly impact pH predictions ~~of ISORROPIA~~. The unrealistic pH values of about 7 in a few previous studies (using the standard ISORROPIA model and stable state assumption) resulted from coding errors in the model, which have been identified and fixed in this study.

1 Introduction

Aerosols in the atmosphere are reported to be associated with respiratory and cardiovascular diseases, and affect climate and ecosystems via aerosol-radiation-cloud interactions (Ramanathan et al., 2001; Lim et al., 2012; Ma et al., 2016). Liquid water is a ubiquitous component of aerosols (Nguyen et al., 2016). The hydrogen ion activity expressed on a logarithmic scale, pH, is an essential property describing the acidity of aqueous aerosols and has been suggested to influence particle formation, toxicity, and nutrient delivery. pH plays a role in the formation of sulfate and secondary organic aerosols (Jang et al., 2002; Xu et al., 2015a; Cheng et al., 2016), and also changes the gas-particle partitioning of semi-volatile species (Keene et al., 2004; Guo et al., 2016; Weber et al., 2016). It affects the solubility of trace metals and thus aerosol toxicity (Ghio et al., 2012; Fang et al., 2017). Low pH may enhance iron mobility in dust and impact ocean productivity (Meskhidze et al., 2003).

In spite of its significance, ambient particle pH is still poorly constrained. The direct filter sampling approach is challenged by the nature of hydrogen ion in that its concentration in a solution does not scale in proportion to the level of dilution, and is also subject to sampling errors (Hennigan et al., 2015). A few studies have determined the pH of laboratory generated particles using colorimetry/spectrometry and Raman microspectroscopy (Li and Jang, 2012; Rindelaub et al., 2016; Craig et al., 2017), but such techniques have not been applied to ambient particles partly due to their much more complex chemical and physical properties. Therefore, an indirect (or proxy) method—thermodynamic equilibrium modeling—has been widely used to estimate particle pH for many regions of the world (Yao et al., 2007; Zhang et al., 2007; Bougiatioti et al., 2016; Guo et al., 2017a; Murphy et al., 2017; Parworth et al., 2017). A number of thermodynamic models have been developed, subject to the principle of minimizing the Gibbs energy of the multi-phase aerosol system, leading to a computationally intensive optimization problem. Thus these models usually incorporate a variety of simplifications and assumptions in their calculations (Fountoukis and Nenes, 2007).

Formatted: Not Highlight

Over the past few years, several studies have estimated values of fine particle pH during North China winter haze events using the E-AIM (Friese and Ebel, 2010) and ISORROPIA (Fountoukis and Nenes, 2007) thermodynamic equilibrium models, as summarized in Table 1. The inferred pH values varied significantly, ranging from close to 0 (highly acidic) to about 7 (neutral). The primary goal of this study is to critically examine the reason for such a large discrepancy. In order to address this problem, we calculate particle pH using the ISORROPIA and E-AIM models under different assumptions (e.g., open vs. closed systems and stable vs. metastable states). The measured data on gas and particle compositions and meteorological parameters collected

Formatted: Not Highlight

in Beijing winter serve as model inputs. We have identified and fixed important coding errors in ISORROPIA which are involved with in pH calculations when a closed system and the stable state are assumed (details in the Supplement, Sect. S1). We compare pH values obtained from these different thermodynamic calculations in Sects. 3.1 and 3.2, as well as in Sect. 3.3 with results from previous winter haze studies. The assumptions and limitations of thermodynamic models are discussed in Sect. 3.4.

Formatted: Not Highlight

Formatted: Not Highlight

Formatted: Not Highlight

Formatted: Not Highlight

2 Methods

2.1 Field measurements

During 2014 winter (from 17 November to 12 December), measurements of air pollutants were conducted at an urban site in Beijing (Institute of Atmospheric Physics, Chinese Academy of Sciences, 39°58'N 116°22'E, 49 m ASL). The $PM_{2.5}$ and PM_1 chemical compositions and several semi-volatile gases were measured with high time resolution, as described below. The ambient temperature and relative humidity (RH) were recorded by a Rotronic HC2-S3 probe. Concentrations of carbon monoxide were also measured (Model 48i, Thermo Fisher Scientific Inc., USA).

The concentrations of six water-soluble inorganic ions (i.e., SO_4^{2-}, NO_3^-, Cl^-, NH_4^+, Na^+, and K^+) in $PM_{2.5}$ and three semi-volatile gases (i.e., NH_3, HNO_3, and HCl) were measured with a time resolution of 30 min using a Gas and Aerosol Collector Ion Chromatography (GAC-IC) system. The instrument was modified based on the Steam Jet Aerosol Collector (Khlystov et al., 1995) in order to better apply to the heavily polluted conditions in China. Ambient air was drawn in at a flow rate of 16.7 L min^{-1} through a $PM_{2.5}$ cyclone inlet. Trace gases were absorbed in a wet annular denuder and then the water-soluble ions in the aerosols were extracted with an improved aerosol collector. The samples of aqueous solution were quantified by two ion chromatography analyzers. Details on the GAC-IC performance (including the detection limits for each species) were described in a previous publication (Dong et al., 2012). The measurement uncertainties arise from several inaccuracies such as internal calibration, pressure and flow control, and collection efficiencies. The intercomparison experiments with filter sampling and other online methods (e.g., Monitor for AeRosols and Gases in Ambient Air, MARGA; Metrohm, Switzerland) reveal that the overall relative uncertainties of the GAC-IC system remain within ± 20% for major species (Dong et al., 2012; Young et al., 2016).

An Aerodyne high-resolution time-of-flight aerosol mass spectrometer (referred to as the AMS) was used to measure size-resolved non-refractory submicron aerosol (NR-PM_1) species (DeCarlo et al., 2006). The detailed operations and calibrations of the AMS have been described elsewhere (Xu et al., 2015b; Sun et al., 2016). Briefly, aerosol particles were drawn into the sampling chamber at a flow rate of 10 L min^{-1}, of which ~ 0.1 L min^{-1} was isokinetically sampled into the AMS after being dried with a silica gel dryer. Concentrations were obtained for organics, sulfate, nitrate, ammonium, and chloride. The AMS was calibrated for ionization efficiency using pure NH_4NO_3 particles following standard protocols (Jayne et al., 2000). A

constant collection efficiency of 0.5 was chosen because (1) particles were dried before being analyzed, (2) the mass fraction of NH_4NO_3 was smaller than 0.4, and (3) the particle acidity was not high enough to affect collection efficiency substantially (Sun et al., 2016). ~~, and T~~The default relative ionization efficiencies, except for ammonium that was determined from pure NH_4NO_3, were applied to all of the species for mass quantifications. The overall uncertainties for each species were estimated following Bahreini et al. (2009) with details provided in the Supplement, Sect. S2.

2.2 pH prediction by thermodynamic models

In this study, pH is defined in Eq. (1) as the negative logarithm with base 10 of the hydrogen ion activity on a molality basis, which is recommended by IUPAC (*goldbook.iupac.org/html/P/P04524.html*) and is also consistent with previous studies (Guo et al., 2016; Battaglia et al., 2017; Pye et al., 2018).~~:~~

~~pH is defined as the negative logarithm with base 10 of the hydrogen ion activity (Guo et al., 2016; Battaglia et al., 2017):~~

$$\mathrm{pH} = -\log_{10}\left(\gamma_{H^+} m_{H^+}\right) = -\log_{10} m_{H^+} - \log_{10}\gamma_{H^+}, \quad (1)$$

where m_{H^+} and γ_{H^+} indicate the molality (mol kg^{-1} water) and the molality-based activity coefficient (a factor accounting for deviations from ideal behavior) of hydrogen ions, respectively. ~~In this study,~~Here, particle pH is predicted using the latest E-AIM (version IV; *www.aim.env.uea.ac.uk*) and ISORROPIA (version II; *isorropia.eas.gatech.edu*) thermodynamic equilibrium models. E-AIM is usually considered as a~~n accurate~~ benchmark model (Zaveri et al., 2008; Seinfeld and Pandis, 2016), ~~whereas~~ while ISORROPIA employs a number of simplifications to make it computationally efficient for application in large-scale atmospheric models (Fountoukis and Nenes, 2007; Pye et al., 2009). E-AIM uses the Pitzer, Simonson, and Clegg equations to calculate activity coefficients for water and ions (Pitzer and Simonson, 1986; Clegg et al., 1992; Wexler and Clegg, 2002). With ISORROPIA, γ_{H^+} and γ_{OH^-} are assumed equal to unity, whereas the activity coefficients for the other ionic pairs (e.g., H^+–Cl^-) are calculated (Fountoukis and Nenes, 2007). For both models, the equilibrium state is calculated at a given temperature and RH. E-AIM solves for the equilibrium of an NH_4^+–H^+–Na^+–SO_4^{2-}–NO_3^-–Cl^-–H_2O inorganic aerosol and its precursor gases (HNO_3, NH_3, and HCl), and can also include certain organic compounds. E-AIM assumes that the inorganic ions and organic solutes do not influence each other in the aqueous solution, when estimating their activity coefficients (Clegg et al., 2001). ISORROPIA treats only inorganic aerosols but includes more crustal species (i.e., Ca, K, and Mg) when compared to E-AIM. The two models can solve for either forward (or closed, in which the total (gas + aerosol) concentration of each species is fixed) or reverse (or open, in which the concentration of each species in the aerosol phase is fixed) condition. The model outputs include concentrations for each species in the solid, liquid, and gas phases (Fountoukis and Nenes, 2007).

It is well known that atmospheric aerosol particles can exist in two states of thermodynamic equilibrium, stable and metastable, depending on their chemical composition and RH history (Rood et al., 1989). Particles in the stable state may be solid, solid plus liquid, or liquid as ambient RH increases (liquid phase appears when ambient RH reaches the deliquescence RH). If the

Formatted: Subscript
Formatted: Subscript
Formatted: Not Highlight
Formatted: Font: Italic
Field Code Changed

ambient RH over a completely liquid aerosol decreases below the deliquescence RH, the aerosol may not crystalize immediately but may constitute a supersaturated aqueous solution (i.e., in the metastable state). The ambient RH varies widely over the North China Plain (NCP) in winter. Synoptic weather patterns are dominated by the Siberian high-pressure system (Jia et al., 2015), under which the northerly winds bring dry and clean air into this region with ambient RH often dropping to as low as about 20% (when aerosol particles are most likely solid). When the northerly winds slacken, often occurring during the NCP winter haze events, the atmospheric conditions are characterized by stagnant inversion, weak southerly winds, and rapid accumulation of both air pollutants and water vapor, and the ambient RH often reaches 80–90% (when aerosol particles are most likely liquid) (Zheng et al., 2015; Gao et al., 2016; Sun et al., 2016; Wang et al., 2016; Tie et al., 2017; Yin et al., 2017). So far, there has been no observational evidence to suggest whether Beijing winter haze fine particles are in a metastable or stable state. It is also unlikely to figure out particle phase states from theoretical calculations because of the very large variability of ambient RH and the difficulty in estimating the efflorescence RH for multicomponent salts (Seinfeld and Pandis, 2016). ~~(Seinfeld and Pandis, 2016)~~Thus, a practical approach is to predict pH for both stable and metastable states, which can provide an estimate of its uncertainty due to the phase state assumption. In this study, ~~Recent field measurements of PM_1 in winter Beijing by Liu et al. (2017b) suggested that the phase state of particles was sensitive to ambient RH and that there existed a gradual transition from semisolid at RH of about 20% to liquid at RH of about 60%. Consequently, it is likely that both stable and metastable particles can exist in the atmosphere of the NCP, their relative abundance depending on ambient RH. We estimate~~ pH values are calculated in both stable and metastable states using ISORROPIA, whereas E-AIM (version IV) can only address the stable state condition.

We have~~We also~~ identified~~y~~ and fixed coding errors in the standard ISORROPIA model, which may significantly affect forward stable mode calculations of~~for~~ pH. In this study, the ISORROPIA model with these errors fixed is denoted as the revised ISORROPIA model. Details concerning the revision of ISORROPIA ~~and its influence on pH prediction~~ are provided in the Supplement, Sect. S1. Briefly, in several subregimes of the solution domain, the standard ISORROPIA model fails to consider the partitioning of NH_3 between the gas and aqueous phases, and therefore the predicted particle pH is very often around 7 (neutral). Importantly, we find that Beijing winter haze conditions (ammonia-rich) happen to belong to the subregimes where coding errors exist. For example, as shown in Fig. 1, the standard ISORROPIA predicts a nearly constant pH of 7.6 for most cases when $\frac{\text{total } [NH_x]}{\text{[illegible]}} > \frac{\text{total } [H_2SO_4]}{\text{[illegible]}}$, where total $[NH_x]$ and $[H_2SO_4]$ are the concentrations (gas plus aerosol phase) of the corresponding species. The revised ISORROPIA model predicts pH lower than 7 (acidic), which varies as a function of $[NH_x]$ and $[H_2SO_4]$. Interestingly, these coding errors have little effect on the predicted gas phase NH_3 concentrations ~~of NH_3~~ (Wang et al., 2016; Guo et al., 2017b), and thus cannot be identified by simply comparing the measured and predicted NH_3 phase partitioning (Supplement, Sect. S1). A few previous studies have been affected by these ISORROPIA coding errors (Wang et al., 2016; He et al., 2017).

Formatted: Not Highlight
Formatted: Subscript
Formatted: Font: +Headings (Times New Roman), Not Italic
Formatted: Font: +Headings (Times New Roman), Not Italic
Formatted: Font: +Headings (Times New Roman)
Formatted: Font: +Headings (Times New Roman)
Formatted: Font: +Headings (Times New Roman)
Formatted: Font: +Headings (Times New Roman)
Formatted: Font: +Headings (Times New Roman), Not Italic
Formatted: Font: +Headings (Times New Roman), Not Italic
Formatted: Font: +Headings (Times New Roman), Not Italic
Formatted: Font: +Headings (Times New Roman), Not Italic
Formatted: Subscript
Formatted: (Asian) Chinese (PRC)

~~. In this study, the ISORROPIA model with these errors fixed is denoted as the revised ISORROPIA model. Details concerning the revision of ISORROPIA and its influence on pH prediction are provided in the Supplement, Sect. S1.~~

Formatted: Not Highlight

2.3 Ion balance and equivalent ratio

The ion balance and equivalent ratio are calculated using the charge equivalent measured ion concentrations and Eqs. (2–5):

$$[\text{cations}] = \frac{[NH_4^+]}{18} + \frac{[Na^+]}{23} + \frac{[K^+]}{39} + \frac{[Ca^{2+}]}{20} + \frac{[Mg^{2+}]}{12} \quad (2)$$

$$[\text{anions}] = \frac{[SO_4^{2-}]}{48} + \frac{[NO_3^-]}{62} + \frac{[Cl^-]}{35.5} \quad (3)$$

$$\text{ion balance} = [\text{cations}] - [\text{anions}] \quad (4)$$

$$\text{equivalent ratio} = [\text{cations}]/[\text{anions}] \quad (5)$$

where $[NH_4^+]$, $[Na^+]$, $[K^+]$, $[Ca^{2+}]$, $[Mg^{2+}]$, $[SO_4^{2-}]$, $[NO_3^-]$, and $[Cl^-]$ are the mass concentrations (μg m^{-3}) of these ions in the atmosphere. [cations] and [anions] denote the sum of charge equivalent total molar concentrations (μmol m^{-3}) of cations and anions, respectively. Although they are straightforward to calculate, a few recent studies (Hennigan et al., 2015; Guo et al., 2016; Murphy et al., 2017) have demonstrated that the ion balance and equivalent ratio calculated from ambient particle measurements should not be used to predict the acidity of particles, especially under ammonia-rich conditions ~~(note that high gas phase NH_3 concentrations are measured in North China winter period, as shown in Sect. 2.4 and 3.2.3)~~, for several reasons summarized as follows. (1) This would require all ions other than H^+ and OH^- to be measured with both very high accuracy and precision, conditions unlikely to be achieved in practice. For example, the filter sampling of semi-volatile species (NH_4^+, NO_3^-, and Cl^-) is subject to both positive and negative biases (Pathak et al., 2004; Wei et al., 2015). Organic acid salts which may contribute significantly to charge balance are usually ignored. In ammonia-rich environments, H^+ commonly accounts for only a tiny fraction of the total concentrations of ions and hence its concentration falls within the range of the accumulated analytical uncertainties for measured ions. (2) The dissociation states of many potentially important ionic species (e.g., HSO_4^- and organic acids) are not considered. (3) The activity coefficients of ionic species are unknown.

Formatted: Not Highlight

2.4 Overview of measurements and model calculations

In the measurement period exhibited here, there were five pollution episodes characterized by high particulate matter (PM) concentrations and RH (Fig. S4). The chemical measurements, along with ambient temperature and RH, are converted to hourly averages and used as inputs to E-AIM and ISORROPIA. This study mainly uses $PM_{2.5}$ data because water-soluble ions are measured and more chemical species (Na^+ and K^+) are available. The pH values of PM_1 are also estimated for comparison. SO_4^{2-}, NO_3^-, Cl^-, and NH_4^+ are identified as the major inorganic ions and their concentrations are positively correlated with RH. With respect to measurements of semi-volatile gases, the mixing ratios of NH_3 (18 ± 9 ppb, median ± median absolute deviation) are high whereas HNO_3 (0.08 ± 0.04 ppb) and HCl (0.25 ± 0.07 ppb) are observed to be ~~very~~ low, consistent with

Formatted: Not Highlight

Liu et al. (2017a). With Eqs. (6–8), we can calculate the total (gas NH_3 + particle NH_4^+) NH_x concentrations, the NH_x concentrations required for the overall (gas + particle phases) charge balance, and the excess NH_x concentrations.

$$\text{Total } NH_x = 17\times\left(\frac{[NH_4^+]}{18}+\frac{[NH_3]}{22.4}\right) \quad (6)$$

$$\text{Required } NH_x = 17\times\left(\frac{[SO_4^{2-}]}{48}+\frac{[NO_3^-]}{62}+\frac{[Cl^-]}{35.5}+\frac{[HNO_3]}{22.4}+\frac{[HCl]}{22.4}-\frac{[Na^+]}{23}-\frac{[K^+]}{39}-\frac{[Ca^{2+}]}{20}-\frac{[Mg^{2+}]}{12}\right) \quad (7)$$

$$\text{Excess } NH_x = \text{Total } NH_x - \text{Required } NH_x \quad (8)$$

where $[NH_4^+]$, $[Na^+]$, $[K^+]$, $[Ca^{2+}]$, $[Mg^{2+}]$, $[SO_4^{2-}]$, $[NO_3^-]$, and $[Cl^-]$ are the measured concentrations (μg m^{-3}) of these ions, and $[HNO_3]$, $[HCl]$, and $[NH_3]$ are the mixing ratios (ppb) of these gases. If Excess $NH_x > 0$ (Total $NH_x >$ Required NH_x), the system is considered to be NH_x-rich. If Excess $NH_x < 0$ (Total $NH_x <$ Required NH_x), the system is considered to be NH_x-poor. The field measurements in this and previous studies (Wang et al., 2016; Liu et al., 2017a) collectively indicate that the Beijing winter haze fine particles are nearly always in an NH_x-rich region, as shown in Fig. 2.

The inputs for the forward mode calculations involve the measured total (gas plus aerosol) concentrations of NH_3, H_2SO_4, HCl, HNO_3, Na^+, and K^+. For the reverse mode calculations, the inputs involve the measured aerosol phase concentrations of NH_4^+, SO_4^{2-}, NO_3^-, Cl^-, Na^+, and K^+. Note that for E-AIM, the measured concentrations of K^+ are accounted for as equivalent Na^+. Note also that gaseous HCl concentrations are taken as zero in the forward mode calculations since a large proportion of HCl data is unavailable. But this treatment only has a very small effect owing to the ~~very~~ low concentrations of gaseous HCl. Model calculations are limited to hourly samples meeting the following criteria: (1) SO_4^{2-}, NO_3^-, Cl^-, NH_4^+, and NH_3 (only for the forward mode) are available, and (2) RH > 20%. The number of eligible samples for ISORROPIA calculations is about three hundred, whereas this number for E-AIM is only about one hundred since version IV additionally requires RH > 60%. Moreover, for the ISORROPIA forward mode pH calculations ~~for pH~~, we adopt a Monte Carlo approach to account for the measurement uncertainties of model inputs, including concentrations of ions and gases (uncertainties described in Sect. 2.1), values of temperature (maximum–minimum range of 2 °C), and values of relative humidity (maximum–minimum range of 10%). All of these variables are assumed to follow a uniform distribution and their values are selected randomly and calculated 5000 times for each hourly sample.

3 Results and discussion

3.1 Reverse mode calculations

Figure 3~~1~~ presents the relationship between ion balance and predicted pH values for $PM_{2.5}$ from four model calculations (i.e., ISORROPIA forward metastable, ISORROPIA reverse metastable, E-AIM forward, and E-AIM reverse), as well as a comparison of measured and predicted gas phase NH_3 mixing ratios. As shown in Fig. 3~~1~~a, a good correlation (r = 0.98, n =

Formatted: Subscript
Formatted: Subscript
Formatted: Superscript
Formatted: Font: Italic, Subscript
Formatted: Font: Italic, Subscript
Formatted: Font: Italic, Subscript
Formatted: Font: +Headings (Times New Roman), Not Italic
Formatted: Font: +Headings (Times New Roman), Not Italic
Formatted: Font: +Headings (Times New Roman)
Formatted: Font: +Headings (Times New Roman), Not Italic
Formatted: Font: +Headings (Times New Roman)
Formatted: Font: +Headings (Times New Roman), Not Italic
Formatted: Font: +Headings (Times New Roman)
Formatted: Font: Italic, Subscript
Formatted: Font: +Headings (Times New Roman)
Formatted: Font: Italic, Subscript
Formatted: Not Highlight
Formatted: English (United States)
Formatted: Not Highlight
Formatted: English (United States)
Formatted: Not Highlight
Formatted: Not Highlight

106) is found between the measured cation and anion concentrations and the average cation-to-anion equivalent ratio (0.99 ± 0.18) is close to unity (similar to previous North China winter haze studies, see Table 1). Figure ~~1~~3b shows that the reverse mode pH values (both E-AIM and ISORROPIA) are highly sensitive to whether the ion balance is positive (n = 61) or negative (n = 45). The samples with negative ion balance (cations < anions) usually project pH values below 2 (highly acidic), whereas those with positive ion balance (cations > anions) are identified with pH values above 7.4 (neutral or basic). These features have been demonstrated also by Hennigan et al. (2015) and Murphy et al. (2017) using different observational datasets. Since the inputs to reverse mode calculations include only aerosol phase measurements of ions, the predicted pH values depend largely on the ion balance (Hennigan et al., 2015). On the other hand, the pH values calculated using the forward mode (both E-AIM and ISORROPIA) range from 3.5 to 5.3 and are not as sensitive to the ion balance. This is because the forward mode calculations account for additional constraints imposed by the partitioning of semi-volatile species. The small difference in pH values between the forward mode E-AIM and ISORROPIA calculations is discussed in Sect. 3.2.1. The agreement between the measured and predicted gas phase concentrations of semi-volatile species serves usually as verification of the accuracy of thermodynamic calculations. Figures ~~3~~1c–d compare measured mixing ratios of NH_3 with model outputs. Good agreement is found for the forward mode, but the reverse mode calculations predict either implausibly high (> 1 ppm) or implausibly low (< 1 ppb) values of NH_3, when compared with measurements. The equilibrium partial pressures of NH_3 for the reverse mode are computed based on the predicted pH values with fixed aerosol NH_4^+ concentrations, and hence the extremely large biases of NH_3 reflect a significant deviation of pH with respect to the real values. Similar behavior is found for gas phase HNO_3 and HCl (Fig. S5).

The above results suggest that the reverse mode calculations (only using aerosol quantity as model inputs) are strongly affected by the ion balance and hence the ionic measurement errors are very likely to lead to unreliable estimates of particle pH (Hennigan et al., 2015; Murphy et al., 2017). Furthermore, an equivalent ratio of near unity may not indicate that fine particles of winter haze have a pH of around 7 or close to 7 (Cheng et al., 2016; Wang et al., 2016; Ma et al., 2017). The forward mode calculations (using gas + aerosol quantity as model inputs) are affected much less by the measurement errors and should be used to predict the pH for winter haze particles.

3.2 Forward mode calculations

3.2.1 E-AIM vs. ISORROPIA

As shown in Fig. 3b, ~~T~~the pH values predicted by the forward mode E-AIM and ISORROPIA calculations differ slightly. Their pH difference, ΔpH (ISORROPIA − E-AIM), can be expressed in Eq. (9): ~~(Fig. 1b)~~

$$\Delta pH = pH_I - pH_E = -\Delta \log_{10} m_{H^+} + \log_{10} \gamma_{H^+} \quad (9)$$

where pH_I and pH_E represent the pH predicted by ISORROPIA and E-AIM, respectively. ΔpH can be considered to consist of two parts: difference in their estimated H^+ concentrations, denoted as $-\Delta \log_{10} m_{H^+}$, and difference in H^+ activity coefficients,

Formatted: Not Highlight
Formatted: Not Highlight
Formatted: Not Highlight
Formatted: Not Highlight
Formatted: Not Highlight
Formatted: Not Highlight
Formatted: Not Highlight
Formatted: Not Highlight
Formatted: Not Highlight
Formatted: Not Highlight
Formatted: Superscript

which equals to the estimated $\log_{10}\gamma_{H^+}$ by E-AIM (since γ_{H^+} is assumed to be unity in ISORROPIA). The forward mode model calculations using our field measurements in Beijing suggest, ~~, and we find~~when RH varies from 70% to 90%, that ΔpH ~~the difference, ΔpH (ISORROPIA − E-AIM),~~ is greater than zero, and negatively correlated with RH (~~(~~Fig. 2~~4~~a)~~a),~~ ~~exhibits a significant linear correlation with RH (Fig. 2a).~~ ΔpH would approach approximately zero, if this relationship were maintained as RH ~~tends to~~approaches 100%. ~~This suggests that ISORROPIA may overestimate pH if E-AIM is taken as a benchmark.~~Similarly, Liu et al. (2017a) ~~also~~ found that ~~the~~ pH values ~~from~~ in ISORROPIA were on average 0.3 unit higher ~~(0.3 unit on average)~~ than ~~those from~~ E-AIM ~~(version II)~~ under winter haze conditions. Figure 4b indicates that ΔpH is related to the differences in both H^+ concentrations and activity coefficients.

Since E-AIM (version IV) cannot be used when RH is below 60%, we conduct calculations using E-AIM (version II), in order to examine whether this relationship between ΔpH and RH still holds at relatively low RH values (Fig. S6 in the Supplement). We find, under typical Beijing winter haze conditions (NH_4^+-rich), that pH predicted by ISORROPIA is systematically higher than E-AIM, and ΔpH is negatively related with RH, when RH varies from 30% to 90%. The exact factors contributing to ΔpH remain unclear, because these two thermodynamic models differ in many ways (e.g., their methods in calculating the activity coefficients for H^+ and the other ionic species and in estimating aerosol water contents). Note that ΔpH is less than one unit for the cases tested in this study, which is much smaller than the pH discrepancy reported in previous winter haze studies (up to 8 pH units). Note also that the above analysis is based on the data sets collected in Beijing winter and may not apply to other conditions.

~~Note that $\gamma_{H^\pm}$ is also affected by other factors (e.g., ionic species in solution) and thus the $\gamma_{H^\pm}$–ionic strength relationship derived here should be considered qualitative. In addition, the above analysis is based on the data sets collected in Beijing winter and may not apply to other conditions. The values of $\gamma_{H^\pm}$ and ΔpH are unknown when ambient RH is below 60% since E-AIM cannot be used in this case.~~

~~One assumption in ISORROPIA is that $\gamma_{H^\pm}$ equals unity (Sect. 2.2). Based on the definition of pH in Eq. (1), it is apparent that ΔpH is strongly correlated with the value of $\log_{10}\gamma_{H^\pm}$ from E-AIM (Fig. 2b). $\gamma_{H^\pm}$ depends largely on the ionic strength, and both $\gamma_{H^\pm}$ and ionic strength reflect the non-ideality of aqueous solutions. Accordingly, $\gamma_{H^\pm}$ and ionic strength are both closely correlated with the RH, which equals to the water activity of solution in an equilibrated aerosol system (Fountoukis and Nenes, 2007). Our calculations indicate that both $\gamma_{H^\pm}$ and ionic strength increase as RH decreases from 90% to 70% (Fig. 2c). As RH continues to decrease, the ionic strength predicted by the ISORROPIA metastable model calculations increases exponentially, reaching about 90 M when RH is about 30% (Fig. 2d). The very high ionic strength at a relatively low RH is a result of supersaturation of the aqueous solution.~~

~~The values of $\gamma_{H^\pm}$ and ΔpH are unknown when ambient RH is below 60% since E-AIM cannot be used in this case.~~ ~~The~~ AIOMFAC model (*web.meteo.mcgill.ca/aiomfac*) can estimate the activity coefficients for electrolytes in an aqueous solution

Formatted: Not Highlight
Formatted: Not Highlight
Formatted: Not Highlight
Formatted: Superscript
Formatted: Font: Italic, Subscript
Formatted: Superscript
Formatted: Not Highlight
Formatted: Not Highlight
Formatted: Not Highlight
Formatted: Not Highlight
Formatted: Not Highlight

~~varying from dilute to supersaturated (Zuend et al., 2011), and has been used here to tentatively explore the effect of large ionic strength on γ_{H^+} under winter haze conditions (Fig. S6). The γ_{H^+} ionic strength relationship suggests that $\log_{10}\gamma_{H^+}$ would increase by about 0.9 unit from an ionic strength of 17 M (corresponding to a RH of about 70%) to 90 M (corresponding to a RH of about 30%). A similar $\log_{10}\gamma_{H^+}$ increase of about 0.8 unit can be computed from the extrapolation of the linear relationship in Fig. 2c. The above calculations show that particle pH values predicted by ISORROPIA may be biased high because of the assumption of $\gamma_{H^+} = 1$, with the positive bias particularly large at relatively low RH. Note that γ_{H^+} is also affected by other factors (e.g., ionic species in solution) and thus the γ_{H^+} ionic strength relationship derived here should be considered qualitative. In addition, the above analysis is based on the data sets collected in Beijing winter and may not apply to other conditions.~~

Formatted: Not Highlight

Formatted: Not Highlight

3.2.2 S curves of semi-volatile species

The S curves of ammonia, nitric acid, and hydrochloric acid describe the relationship between particle pH and their equilibrium fractions in the aqueous phase ($\varepsilon(NH_4^+) = [NH_4^+]/([NH_4^+] + [NH_3])$, $\varepsilon(NO_3^-) = [NO_3^-]/([NO_3^-] + [HNO_3])$, and $\varepsilon(Cl^-) = [Cl^-]/([Cl^-] + [HCl])$) at a given temperature and aerosol water content (AWC), assuming ideal solutions (water activity and all activity coefficients equal to unity). The S curves have been shown as useful tools to qualitatively and conceptually estimate particle pH (Guo et al., 2017a), and are calculated in this study using Henry's law constants and acid–base dissociation constants for each semi-volatile species (details in the Supplement, Sect. S3). We choose very humid conditions (RH > 75%) in the field measurements when particles are most likely in a completely aqueous phase, under which the average temperature and AWC (predicted by ISORROPIA) are 278 K and 144 μg m^{-3}, respectively. As shown in Fig. ~~53~~, the calculated $\varepsilon(NH_4^+)$ increases with pH whereas $\varepsilon(NO_3^-)$ and $\varepsilon(Cl^-)$ decrease with pH. The field measurements suggest that about a half of the total ammonia resides in the condensed phase ($\varepsilon(NH_4^+)$ = 54% ± 12%), and that almost all of the total nitric acid and hydrochloric acid are in the condensed phase ($\varepsilon(NO_3^-)$ = 99.6% ± 0.1% and $\varepsilon(Cl^-)$ = 98.1% ± 0.7%). Thus, the ammonia S curve and the measured $\varepsilon(NH_4^+)$ suggest that the particle pH should be around 4 and is unlikely to exceed 5.5 when $\varepsilon(NH_4^+)$ < 1% or below 1.5 when $\varepsilon(NH_4^+)$ > 99%. The S curves for nitric acid and hydrochloric acid and the measured $\varepsilon(NO_3^-)$ and $\varepsilon(Cl^-)$ also suggest that pH should be greater than 2, as $\varepsilon(NO_3^-)$ and $\varepsilon(Cl^-)$ become close to unity and are consequently insensitive to pH. Note that the assumption of ideal solutions is applied in the above analysis of the S curves. Thermodynamic equilibrium models can calculate the values of activity coefficients (and thus consider the non-ideality of solutions) and are therefore able to provide more quantitative results for particle pH compared to the S curves. As shown in Fig. 5, the forward mode ISORROPIA and E-AIM calculations predict similar average pH values (4.1 and 4.6 respectively), compared to the average number of 3.6 inferred from the S curve of ammonia. Note that calculations using the standard ISORROPIA model with the stable state assumption obtain an unrealistic average pH value of 7.7 due to its coding errors.

Formatted: Not Highlight

Formatted: Not Highlight

Formatted: Not Highlight

3.2.3 Driving factors for particle pH

It has been suggested that ambient RH plays an important role in the evolution of winter haze events (Sun et al., 2013; Wang et al., 2014; Tie et al., 2017) and the phase state of aerosols (Liu et al., 2017b). Thus, we present the pH and AWC values for $PM_{2.5}$ predicted by the ISORROPIA forward mode calculations (in both metastable and stable states) as a function of RH (Figs. 4a6a–b). Note that the revised ISORROPIA model is used for the stable state calculations.

Several previous studies have indicated that the values of AWC predicted by ISORROPIA are in reasonable agreement with those based on measurements of aerosol light scattering coefficients and hygroscopic growth factors (Bian et al., 2014; Guo et al., 2015; Tan et al., 2017; Wu et al., 2018). The predicted AWC increases with RH, and is greater for the metastable state (a completely aqueous solution). The absolute difference of AWC between the two states is minor at either high (> 70%) or low (< 40%) RH but is large at intermediate RH. Most inorganic species deliquesce at RH below 70% and, at a higher RH, particles are liquid for both states. At a very low RH, particles are solid in the stable state (thus the AWC is zero and no prediction of pH is given), but can absorb a small amount of water if they are in the metastable state.

As shown in Fig. 6a and Fig. S7 in the Supplement, the pH values for these two phase states are very similar (ranging from 4 to 5) and of a moderately acidic nature for a wide range of RH. The results are consistent with the qualitative understanding of particle pH ~~obtained~~ inferred from the S curves. Thermodynamic model calculations with either stable or metastable state assumption can provide reasonable estimates of aerosol water pH, at least for the winter haze conditions considered in this study. The pH values predicted by the AMS PM_1 measurements and forward mode ISORROPIA calculations (Fig. S87 in the Supplement) are about 0.2 unit lower than those ~~e pH values~~ of $PM_{2.5}$, due partly to lack of crustal ions (Na^+ and K^+) for the AMS PM_1 measurements.

~~An insignificant (p = 0.14) increasing trend is calculated from the ISORROPIA metastable analysis: pH = 0.01 × RH (%) + 3.9, but this trend may be enhanced if the variability of γ_{H^+} with RH is considered. The pH values predicted by the AMS PM_1 measurements and forward mode ISORROPIA calculations (Fig. S7) are about 0.2 unit lower than the pH values of $PM_{2.5}$, due partly to lack of crustal ions (Na^+ and K^+) for PM_1 measurements.~~

By analyzing the sensitivity of pH to ammonia concentrations, ~~R~~recent studies have emphasized the important role of ammonia in determining winter haze particle pH (Guo et al., 2017b; Liu et al., 2017a). It was suggested, under ammonia-rich conditions, that a 10-fold increase in gas phase NH_3 concentrations roughly corresponds to one unit increase in pH (i.e., a 10-fold decrease in H^+ activity) (Guo et al., 2017b). This is obvious, since the equilibrium of dissolution and dissociation of ammonia in water can be expressed as: $NH_{3(g)} + H^+_{(aq)} \leftrightarrow NH^+_{4(aq)}$. These sensitivity tests have also indicated that atmospheric relevant ammonia concentrations are not high enough to achieve a fully neutralized condition (pH of around 7) for aerosol particles (Guo et al.,

Formatted: Not Highlight
Formatted: Not Highlight
Formatted: Not Highlight
Formatted: Subscript
Formatted: Superscript
Formatted: Font: +Headings (Times New Roman), Not Italic
Formatted: Font: +Headings (Times New Roman), Not Italic
Formatted: Font: +Headings (Times New Roman), Not Italic
Formatted: Font: +Headings (Times New Roman)
Formatted: Font: +Headings (Times New Roman), Not Italic
Formatted: Font: +Headings (Times New Roman), Not Italic
Formatted: Font: +Headings (Times New Roman), Not Italic
Formatted: Font: +Headings (Times New Roman)
Formatted: Font: +Headings (Times New Roman)
Formatted: Font: +Headings (Times New Roman), Not Italic

2017b; Liu et al., 2017a). The sensitivity tests conducted in this study are consistent with these previous studies (Fig. S9 in the Supplement).

The ambient RH has a minor effect on the predicted pH values. An insignificant (p = 0.14) increasing trend is calculated from the ISORROPIA metastable analysis in Fig. 6a: pH = 0.01 × RH (%) + 3.9. A more detailed sensitivity analysis suggests that pH from ISORROPIA is insensitive to RH and the variability of pH is less than 0.3 unit within a RH range of 30%–90% (Fig. S9 in the Supplement). On the other hand, the pH predicted by E-AIM increases by 0.8 unit when RH increases from 30% to 90%, reflecting the systematic difference in pH between ISORROPIA and E-AIM discussed in Sect. 3.2.1.

Our calculations have shown that Beijing winter haze particles are moderately acidic with pH values ranging from 4 to 5 for a wide range of RH. ~~have emphasized the important role of ammonia in determining winter haze particle pH.~~ As shown in Fig. ~~4c~~6c, ~~the~~ our field measurements indicate that the concentrations of CO and total NH_x (the sum of gas phase NH_3 and aerosol phase NH_4^+) exhibit similar increasing trends with ambient RH. CO is usually considered as an inactive chemical species during rapid haze formation and its enhancement with increased RH may be taken to reflect the accumulation of primary pollutants in the shallower boundary layer (Tie et al., 2017). Thus, the total NH_x is accumulated as a primary pollutant and undergoes a considerable gas-to-particle conversion (Wang et al., 2015; Wei et al., 2015). The NH_3 to NH_4^+ ratio decreases from about 3 at a RH of 30% to about 1 at a RH of 80%. However, relatively high levels of NH_3 remain in the gas phase throughout the range of RH considered here. Note that the measured gas phase HNO_3 and HCl mixing ratios were very low. Based on the above evidence, we suggest that the amount of total NH_x is rich enough so as to balance most of the HNO_3, H_2SO_4, and HCl formed in gas and particle phases (Fig. ~~4d~~6d). Comparable NH_3 levels have been measured at multiple ~~stations~~ sites over the NCP ~~during~~ in ~~the~~ winter ~~months~~ (Wang et al., 2016; Xu et al., 2016; Zhao et al., 2016; Liu et al., 2017a), indicating that ammonia-rich conditions are ~~very~~ common. Thus, we suggest that ammonia may strongly affect particle pH over the NCP from clean to hazy conditions (low to high RHs). The ~~The NH_x~~ sources of ammonia include agriculture, fossil fuel use, and green space, and their contributions vary in different environments (Pan et al., 2016; Sun et al., 2017; Teng et al., 2017; Zhang et al., 2017). We note however that the similar behavior of CO and total NH_x does not imply necessarily similar emission sources.

3.3 Summary of existing studies

In the analysis so far, we have examined the impacts of different thermodynamic models (E-AIM vs. ISORROPIA), model configurations (forward vs. reverse), and phase states (stable vs. metastable) on the estimation of fine particle pH using the data sets collected during 2014 winter in Beijing. Here we summarize and compare the existing fine particle pH studies of North China winter haze, highlighting the importance of using an appropriate thermodynamic modeling approach. Figure ~~7~~5 presents predicted pH from these studies. Their experimental details are summarized in Table 1.

Formatted: Not Highlight

Formatted: Not Highlight

Formatted: Not Highlight

Formatted: Not Highlight

Formatted: Not Highlight

The average reverse mode pH reported by previous studies ranged from –1 to 6.2 (Cheng et al., 2011; He et al., 2012; Cheng et al., 2016; Tian et al., 2018). Our calculations show that the reverse mode pH has a bimodal distribution with peaks between –2 and 2 (highly acidic) and between 7 and 10 (basic), and is very sensitive to errors in ionic measurements (Sect. 3.1). In fact, this implies, for an observational study, that the average pH calculated from many individual samples can be any value between –2 and 10 for E-AIM (between –2 and 8 for ISORROPIA), depending on the number of samples with negative and positive ion balances. The mean pH values in our calculations are 5.4 and 4.2 for E-AIM and ISORROPIA, respectively, which happen to show a weakly acidic condition.

The forward mode pH is affected much less by measurement errors and exhibits thus a narrow unimodal distribution according to our calculations. The average pH values are 4.6 (95% confidence interval 4.0 to 5.1) and 4.0 (95% confidence interval 3.6 to 4.4) for ISORROPIA and E-AIM, respectively. ~~The systematic difference relates to the way in which the activity coefficient is estimated for hydrogen ions, as described in Sect. 3.2.1.~~ It is essential to note that the revised ISORROPIA when running in the stable state yields an almost identical distribution as compared to ISORROPIA in the metastable state. The studies using the standard ISORROPIA model with the stable state assumption have predicted unrealistic pH values of around 7 and should be re-evaluated (Wang et al., 2016; He et al., 2017). Previous ISORROPIA calculations using the metastable state assumption obtained average pH values from 4.1 to 5.4 (Cheng et al., 2016; Guo et al., 2017b; He et al., 2017; Liu et al., 2017a; Shi et al., 2017; Tan et al., 2018), agreeing reasonably with our results (an average pH value of 4.6). ~~It is noted that~~The Ca^{2+} and Mg^{2+} concentrations ~~of Ca^{2+} and Mg^{2+}~~ were not measured in this study and a sensitivity test suggests that including these crustal cations in ~~thermodynamic~~ calculations would increase predicted pH values by about 0.1 unit (Fig. S108). Among these studies, the highest pH value of 5.4 was obtained in Beijing in 2013 January (Cheng et al., 2016) and may be related to two factors: the contribution of organics to AWC was considered which might increase the pH values for about 0.1 unit, and the NH_3 concentrations estimated from an empirical relationship with NO_x might be biased high (He et al., 2014; Pan et al., 2016).

The above comparison suggests that the large discrepancy in pH values (from about 0 to about 7) reported in previous studies of North China winter haze may be attributed primarily to differences in the applications of thermodynamic models. We suggest the use of the forward mode rather than the reverse mode in future studies, and the use of the revised ISORROPIA model when the stable state is assumed for particle phase. The appropriate applications of thermodynamic modeling indicate a moderately acidic condition (pH from about 4 to about 5) for fine particles in North China winter haze.

3.4 Assumptions and limitations of thermodynamic modeling

It is important to acknowledge that most thermodynamic equilibrium models, including E-AIM and ISORROPIA, incorporate a few basic assumptions. First, gas and particle phases are assumed to be equilibrated. This seems reasonable given that we use hourly measurement data and that the equilibration timescale for semi-volatile species between gas and submicron particles is estimated to be 15–30 min (Fountoukis et al., 2009). Second, the aerosol curvature effect on equilibrium partial pressures of

Formatted: Not Highlight

Formatted: Not Highlight

Formatted: Not Highlight

Formatted: Not Highlight

semi-volatile species (also known as the Kelvin effect) is ignored. This should have a negligible impact on bulk properties as the effect is important only for particles with sizes smaller than 0.1 μm, a fraction that does not contribute significantly to the mass of $PM_{2.5}$ particles (Nenes et al., 1998). Third, aerosols are assumed to be internally mixed and are treated as bulk properties, meaning that all the particles have the same size and chemical composition (Nenes et al., 1998; Box and Box, 2015). Note that only the measured inorganic components are included in the above calculations, whereas organic compounds, which account for about 30–50% of total fine particle mass during winter haze events (Huang et al., 2014; Zhang et al., 2015; Tan et al., 2018), are not considered. Organics may affect particle pH in several ways: (1) by increasing the absorption of aerosol water; (2) by participating in the charge balance and modifying the activity coefficients of inorganic ions in the aqueous phase; and (3) by changing the aerosol phase state (liquid-liquid phase separation). Next, we will discuss these aspects.

(1) The contribution of organics to aerosol water is parameterized usually based on the hygroscopicity parameter κ_{org} (Guo et al., 2015; Cheng et al., 2016):

$$W_{org} = OM \frac{\rho_w}{\rho_{org}} \frac{\kappa_{org}}{(100\%/RH - 1)}, \quad (6)$$

where W_{org} is the aerosol water associated with organics, OM is the mass concentration of organics, and ρ_w (1.0×10^3 kg m^{-3}) and ρ_{org} (1.4×10^3 kg m^{-3}) are the densities of water and organics, respectively. The average κ_{org} of 0.06 was obtained from an earlier cloud condensation nuclei study in Beijing (Gunthe et al., 2011). Black carbon may also absorb water with an average κ of 0.04 from Peng et al. (2017). Using the OM and BC concentrations measured by the AMS and a $PM_{2.5}/PM_1$ conversion factor of 1.6 (Zhao et al., 2017), we find that the aerosol water associated with these species is only about 14 ± 3% (median ± median absolute deviation) of that associated with inorganic salts, and thus has a very minor impact on the predicted pH values of fine particles (Fig. S11~~9~~). The particle pH values increase by 0.05 ± 0.01 ~~(median ± median absolute deviation)~~, consistent with Liu et al. (2017a). Even with a κ_{org} of 0.2 (a potential upper limit)~~, the change of particle pH (0.13 ± 0.03) is still small~~ (Zhao et al., 2015)~~.~~, the change of particle pH (0.13 ± 0.03) is still small.

(2) It has been suggested that organic compounds (e.g., amines and organic acid salts) may affect particle pH, especially under weakly acidic conditions (Hennigan et al., 2015). Due to lack of detailed measurements of these species, a thorough evaluation of their effect is difficult. Here, we conduct a sensitivity test using the E-AIM model including oxalate ($C_2O_4^{2-}$), which is the most abundant organic acid salt in $PM_{2.5}$ in winter Beijing (Huang et al., 2005; Wang et al., 2017) and is also one of the strongest organic acids (acid dissociation constants pK_{a1} = 1.27 and pK_{a2} = 4.27). Strong positive correlations are measured between oxalate and sulfate and their ratios are about 1–2% (Wang et al., 2017). Considering also the relative concentration levels of oxalate and other organic acid salts (Table S8), the oxalate concentration is set at 20% of sulfate in this test, which may represent the upper limit for the concentration of total organic acids. The pH values predicted by the forward mode E-AIM decrease only by 0.07 ± 0.03 when oxalate is included (Fig. S12~~0~~), indicating that particle pH is not strongly affected by

Formatted: Not Highlight

Formatted: Not Highlight

Formatted: Not Highlight

Formatted: Not Highlight

organic acids if the system is equilibrated. Note that E-AIM assumes that the organics in the aqueous solution do not affect the activity coefficients of inorganic ions (Clegg et al., 2001). Using the AIOMFAC model (*web.meteo.mcgill.ca/aiomfac*), Pye et al. (2018) have recently showed that the interaction of inorganic ions with water-soluble organic compounds resulted in a 0.1 unit increase in pH for aerosols in the southeast United States.

(3) As described earlier, during severe winter haze events at very high RH, the aerosol phase state should be liquid. However, we suggest that the particles very likely undergo liquid-liquid phase separation between the inorganic and organic components. This phase separation is believed to depend primarily on the oxygen-to-carbon (O/C) atomic ratio (a parameter used to roughly describe the oxidation state) of organic aerosols and occurs almost always when the O/C ratio < 0.5 (Guo et al., 2016; Freedman, 2017). The average O/C ratio calculated based on the AMS PM_1 measurements and updated calibrations by Canagaratna et al. (2015) is 0.4 ± 0.1 (Fig. S1~~3~~1), similar to values reported previously in winter Beijing (Hu et al., 2016; Sun et al., 2016). The effect of phase separation on pH values of these two liquid phases remains unclear. It has been suggested in a recent laboratory study that the pH of the organic-rich fraction under phase separation is about 0.4 unit higher than that for a fully mixed aqueous phase ~~it would change pH by about 0.4 unit~~ (Dallemagne et al., 2016).

~~The effect of liquid-liquid phase separation on particle pH remains unclear. It has been suggested in a recent laboratory study that it would change pH by about 0.4 unit (Dallemagne et al., 2016).~~

The above discussion suggests that the assumptions and limitations implicit in the thermodynamic models may not lead to large biases in prediction of the bulk pH of fine particles in North China winter haze, which is supported by the reasonable agreement between the measured and predicted gas-particle partitioning of semi-volatile species such as ammonia.

4 Conclusions

This study suggests that the significant discrepancy of fine particle pH, ranging from about 0 (highly acidic) to about 7 (neutral), calculated in previous studies of North China winter haze is due ~~mainly~~ primarily to differences in the ways in which the E-AIM and ISORROPIA thermodynamic equilibrium models have been applied. The reverse mode calculations (only using aerosol phase composition as inputs) lead to erroneous results of pH since they are strongly affected by ionic measurement errors (especially under ammonia-rich conditions), and therefore should be avoided in future winter haze studies. The forward mode calculations (using the total (gas plus aerosol phase) compositions as inputs) ~~can~~ account for additional constraints imposed by the partitioning of semi-volatile species~~,~~ and are affected ~~therefore~~ much less by the measurement errors, and therefore, should be used in future studies. The forward mode calculations in this and previous studies collectively indicate, during North China winter haze events, that aerosol particles are moderately acidic with pH values ranging from about 4 to about 5. The assumed particle phase state (stable or metastable) do~~es~~es not significantly affect the pH calculations of

Formatted: Font: Italic

Formatted: Not Highlight

Formatted: Font: Italic

ISORROPIA after coding errors in its standard model being fixed. ~~when coding errors are fixed.~~ A few previous studies, in which the standard ISORROPIA model was used and the stable state was assumed, predicted unrealistic pH values of around 7, and should be re-evaluated. ~~The difference in pH values calculated by the forward mode E-AIM and ISORROPIA may be attributed mainly to differences in estimates of the activity coefficient for hydrogen ions.~~ In agreement with previous studies, we confirm that ammonia plays an important role in determining particle pH under winter haze conditions in northern China.

Data availability

The Windows stand-alone executable of the ISORROPIA model is available at *isorropia.eas.gatech.edu*. The web-based E-AIM model is available at *www.aim.env.uea.ac.uk*. The measurement data on gas and particle compositions and meteorology are available upon request to the authors. The revision for the forward stable state in the source codes of ISORROPIA made in this study is available at *wiki.seas.harvard.edu/geos-chem/index.php/ISORROPIA_II*.

Formatted: Font: Italic

Formatted: Not Highlight

Formatted: Not Highlight

Competing interests

Formatted: Not Highlight

The authors declare that they have no conflict of interest.

Acknowledgments

This study was supported by the Harvard Global Institute and the National Natural Science Foundation of China (91744207, 21625701). We thank Athanasios Nenes for helpful discussions and for providing the source codes of ISORROPIA, and Becky Alexander, Michael Battaglia Jr., Simon Clegg, Hongyu Guo, Daniel Jacob, Mingxu Liu, Pengfei Liu, Mario Molina, Rachel Silvern, Gehui Wang, Lin Zhang, and Guangjie Zheng for helpful discussions.

References

Bahreini, R., Ervens, B., Middlebrook, A. M., Warneke, C., de Gouw, J. A., DeCarlo, P. F., Jimenez, J. L., Brock, C. A., Neuman, J. A., Ryerson, T. B., Stark, H., Atlas, E., Brioude, J., Fried, A., Holloway, J. S., Peischl, J., Richter, D., Walega, J., Weibring, P., Wollny, A. G., and Fehsenfeld, F. C.: Organic aerosol formation in urban and industrial plumes near Houston and Dallas, Texas, J. Geophys. Res.-Atmos., 114, D00F16, doi:10.1029/2008JD011493, 2009.

Battaglia, M. A., Douglas, S., and Hennigan, C. J.: Effect of the urban heat island on aerosol pH, Environ. Sci. Technol., 51, 13095-13103, doi:10.1021/acs.est.7b02786, 2017.

Bian, Y. X., Zhao, C. S., Ma, N., Chen, J., and Xu, W. Y.: A study of aerosol liquid water content based on hygroscopicity measurements at high relative humidity in the North China Plain, Atmos. Chem. Phys., 14, 6417-6426, doi:10.5194/acp-14-6417-2014, 2014.

Bougiatioti, A., Nikolaou, P., Stavroulas, I., Kouvarakis, G., Weber, R., Nenes, A., Kanakidou, M., and Mihalopoulos, N.: Particle water and pH in the eastern Mediterranean: source variability and implications for nutrient availability, Atmos. Chem. Phys., 16, 4579-4591, doi:10.5194/acp-16-4579-2016, 2016.

Box, M. A., and Box, G. P.: Physics of radiation and climate, Crc Press, Boca Raton, Florida, 2015.

Canagaratna, M. R., Jimenez, J. L., Kroll, J. H., Chen, Q., Kessler, S. H., Massoli, P., Hildebrandt Ruiz, L., Fortner, E., Williams, L. R., Wilson, K. R., Surratt, J. D., Donahue, N. M., Jayne, J. T., and Worsnop, D. R.: Elemental ratio measurements of organic compounds using aerosol mass spectrometry: characterization, improved calibration, and implications, Atmos. Chem. Phys., 15, 253-272, doi:10.5194/acp-15-253-2015, 2015.

Cheng, S.-h., Yang, L.-x., Zhou, X.-h., Xue, L.-k., Gao, X.-m., Zhou, Y., and Wang, W.-x.: Size-fractionated water-soluble ions, situ pH and water content in aerosol on hazy days and the influences on visibility impairment in Jinan, China, Atmos. Environ., 45, 4631-4640, doi:10.1016/j.atmosenv.2011.05.057, 2011.

Cheng, Y., Zheng, G., Wei, C., Mu, Q., Zheng, B., Wang, Z., Gao, M., Zhang, Q., He, K., Carmichael, G., Pöschl, U., and Su, H.: Reactive nitrogen chemistry in aerosol water as a source of sulfate during haze events in China, Sci. Adv., 2, e1601530, doi:10.1126/sciadv.1601530, 2016.

Clegg, S. L., Pitzer, K. S., and Brimblecombe, P.: Thermodynamics of multicomponent, miscible, ionic solutions. Mixtures including unsymmetrical electrolytes, J. Phys. Chem., 96, 9470-9479, doi:10.1021/j100202a074, 1992.

Clegg, S. L., Seinfeld, J. H., and Brimblecombe, P.: Thermodynamic modelling of aqueous aerosols containing electrolytes and dissolved organic compounds, J. Aerosol. Sci., 32, 713-738, doi:10.1016/S0021-8502(00)00105-1, 2001.

Craig, R. L., Nandy, L., Axson, J. L., Dutcher, C. S., and Ault, A. P.: Spectroscopic determination of aerosol pH from acid–base equilibria in inorganic, organic, and mixed systems, J. Phys. Chem. A, 121, 5690-5699, doi:10.1021/acs.jpca.7b05261, 2017.

Dallemagne, M. A., Huang, X. Y., and Eddingsaas, N. C.: Variation in pH of model secondary organic aerosol during liquid–liquid phase separation, J. Phys. Chem. A, 120, 2868-2876, doi:10.1021/acs.jpca.6b00275, 2016.

DeCarlo, P. F., Kimmel, J. R., Trimborn, A., Northway, M. J., Jayne, J. T., Aiken, A. C., Gonin, M., Fuhrer, K., Horvath, T., Docherty, K. S., Worsnop, D. R., and Jimenez, J. L.: Field-deployable, high-resolution, time-of-flight aerosol mass spectrometer, Anal. Chem., 78, 8281-8289, doi:10.1021/ac061249n, 2006.

Dong, H. B., Zeng, L. M., Hu, M., Wu, Y. S., Zhang, Y. H., Slanina, J., Zheng, M., Wang, Z. F., and Jansen, R.: Technical Note: The application of an improved gas and aerosol collector for ambient air pollutants in China, Atmos. Chem. Phys., 12, 10519-10533, doi:10.5194/acp-12-10519-2012, 2012.

Fang, T., Guo, H., Zeng, L., Verma, V., Nenes, A., and Weber, R. J.: Highly acidic ambient particles, soluble metals, and oxidative potential: a link between sulfate and aerosol toxicity, Environ. Sci. Technol., 51, 2611-2620, doi:10.1021/acs.est.6b06151, 2017.

Fountoukis, C., and Nenes, A.: ISORROPIA II: a computationally efficient thermodynamic equilibrium model for K^+–Ca^{2+}–Mg^{2+}–NH_4^+–Na^+–SO_4^{2-}–NO_3^-–Cl^-–H_2O aerosols, Atmos. Chem. Phys., 7, 4639-4659, doi:10.5194/acp-7-4639-2007, 2007.

Fountoukis, C., Nenes, A., Sullivan, A., Weber, R., Van Reken, T., Fischer, M., Matías, E., Moya, M., Farmer, D., and Cohen, R. C.: Thermodynamic characterization of Mexico City aerosol during MILAGRO 2006, Atmos. Chem. Phys., 9, 2141-2156, doi:10.5194/acp-9-2141-2009, 2009.

Freedman, M. A.: Phase separation in organic aerosol, Chem. Soc. Rev., 46, 7694-7705, doi:10.1039/C6CS00783J, 2017.

Friese, E., and Ebel, A.: Temperature dependent thermodynamic model of the system H^+−NH_4^+−Na^+−SO_4^{2-}−NO_3^-−Cl^-−H_2O, J. Phys. Chem. A, 114, 11595-11631, doi:10.1021/jp101041j, 2010.

Gao, M., Carmichael, G. R., Wang, Y., Saide, P. E., Yu, M., Xin, J., Liu, Z., and Wang, Z.: Modeling study of the 2010 regional haze event in the North China Plain, Atmos. Chem. Phys., 16, 1673-1691, doi:10.5194/acp-16-1673-2016, 2016.

Ghio, A. J., Carraway, M. S., and Madden, M. C.: Composition of air pollution particles and oxidative stress in cells, tissues, and living systems, J. Toxicol. Environ. Health B, 15, 1-21, doi:10.1080/10937404.2012.632359, 2012.

Gunthe, S. S., Rose, D., Su, H., Garland, R. M., Achtert, P., Nowak, A., Wiedensohler, A., Kuwata, M., Takegawa, N., Kondo, Y., Hu, M., Shao, M., Zhu, T., Andreae, M. O., and Pöschl, U.: Cloud condensation nuclei (CCN) from fresh and aged air pollution in the megacity region of Beijing, Atmos. Chem. Phys., 11, 11023-11039, doi:10.5194/acp-11-11023-2011, 2011.

Guo, H., Xu, L., Bougiatioti, A., Cerully, K. M., Capps, S. L., Hite Jr, J. R., Carlton, A. G., Lee, S. H., Bergin, M. H., Ng, N. L., Nenes, A., and Weber, R. J.: Fine-particle water and pH in the southeastern United States, Atmos. Chem. Phys., 15, 5211-5228, doi:10.5194/acp-15-5211-2015, 2015.

Guo, H., Sullivan, A. P., Campuzano-Jost, P., Schroder, J. C., Lopez-Hilfiker, F. D., Dibb, J. E., Jimenez, J. L., Thornton, J. A., Brown, S. S., Nenes, A., and Weber, R. J.: Fine particle pH and the partitioning of nitric acid during winter in the northeastern United States, J. Geophys. Res.-Atmos., 121, 10355-10376, doi:10.1002/2016JD025311, 2016.

Guo, H., Liu, J., Froyd, K. D., Roberts, J. M., Veres, P. R., Hayes, P. L., Jimenez, J. L., Nenes, A., and Weber, R. J.: Fine particle pH and gas–particle phase partitioning of inorganic species in Pasadena, California, during the 2010 CalNex campaign, Atmos. Chem. Phys., 17, 5703-5719, doi:10.5194/acp-17-5703-2017, 2017a.

Guo, H., Weber, R. J., and Nenes, A.: High levels of ammonia do not raise fine particle pH sufficiently to yield nitrogen oxide-dominated sulfate production, Sci. Rep., 7, 12109, doi:10.1038/s41598-017-11704-0, 2017b.

He, H., Wang, Y., Ma, Q., Ma, J., Chu, B., Ji, D., Tang, G., Liu, C., Zhang, H., and Hao, J.: Mineral dust and NOx promote the conversion of SO_2 to sulfate in heavy pollution days, Sci. Rep., 4, 4172, doi:10.1038/srep04172, 2014.

He, K., Zhao, Q., Ma, Y., Duan, F., Yang, F., Shi, Z., and Chen, G.: Spatial and seasonal variability of $PM_{2.5}$ acidity at two Chinese megacities: insights into the formation of secondary inorganic aerosols, Atmos. Chem. Phys., 12, 1377-1395, doi:10.5194/acp-12-1377-2012, 2012.

He, P., Alexander, B., Geng, L., Chi, X., Fan, S., Zhan, H., Kang, H., Zheng, G., Cheng, Y., Su, H., Liu, C., and Xie, Z.: Isotopic constraints on heterogeneous sulphate production in Beijing haze, Atmos. Chem. Phys. Discuss., 2017, 1-25, doi:10.5194/acp-2017-977, 2017.

Hennigan, C. J., Izumi, J., Sullivan, A. P., Weber, R. J., and Nenes, A.: A critical evaluation of proxy methods used to estimate the acidity of atmospheric particles, Atmos. Chem. Phys., 15, 2775-2790, doi:10.5194/acp-15-2775-2015, 2015.

Hu, W., Hu, M., Hu, W., Jimenez, J. L., Yuan, B., Chen, W., Wang, M., Wu, Y., Chen, C., Wang, Z., Peng, J., Zeng, L., and Shao, M.: Chemical composition, sources, and aging process of submicron aerosols in Beijing: Contrast between summer and winter, J. Geophys. Res.-Atmos., 121, 1955-1977, doi:10.1002/2015JD024020, 2016.

Huang, R.-J., Zhang, Y., Bozzetti, C., Ho, K.-F., Cao, J.-J., Han, Y., Daellenbach, K. R., Slowik, J. G., Platt, S. M., Canonaco, F., Zotter, P., Wolf, R., Pieber, S. M., Bruns, E. A., Crippa, M., Ciarelli, G., Piazzalunga, A., Schwikowski, M., Abbaszade, G., Schnelle-Kreis, J., Zimmermann, R., An, Z., Szidat, S., Baltensperger, U., Haddad, I. E., and Prévôt, A. S. H.: High secondary aerosol contribution to particulate pollution during haze events in China, Nature, 514, 218, doi:10.1038/nature13774, 2014.

Huang, X.-F., Hu, M., He, L.-Y., and Tang, X.-Y.: Chemical characterization of water-soluble organic acids in $PM_{2.5}$ in Beijing, China, Atmos. Environ., 39, 2819-2827, doi:10.1016/j.atmosenv.2004.08.038, 2005.

Jang, M., Czoschke, N. M., Lee, S., and Kamens, R. M.: Heterogeneous atmospheric aerosol production by acid-catalyzed particle-phase reactions, Science, 298, 814-817, doi:10.1126/science.1075798, 2002.

Jayne, J. T., Leard, D. C., Zhang, X., Davidovits, P., Smith, K. A., Kolb, C. E., and Worsnop, D. R.: Development of an aerosol mass spectrometer for size and composition analysis of submicron particles, Aerosol Sci. Technol., 33, 49-70, doi:10.1080/027868200410840, 2000.

Jia, B., Wang, Y., Yao, Y., and Xie, Y.: A new indicator on the impact of large-scale circulation on wintertime particulate matter pollution over China, Atmos. Chem. Phys., 15, 11919-11929, doi:10.5194/acp-15-11919-2015, 2015.

Keene, W. C., Pszenny, A. A. P., Maben, J. R., Stevenson, E., and Wall, A.: Closure evaluation of size-resolved aerosol pH in the New England coastal atmosphere during summer, J. Geophys. Res.-Atmos., 109, D23307, doi:10.1029/2004JD004801, 2004.

Khlystov, A., Wyers, G. P., and Slanina, J.: The steam-jet aerosol collector, Atmos. Environ., 29, 2229-2234, doi:10.1016/1352-2310(95)00180-7, 1995.

Li, J., and Jang, M.: Aerosol acidity measurement using colorimetry coupled with a Reflectance UV-Visible spectrometer, Aerosol Sci. Technol., 46, 833-842, doi:10.1080/02786826.2012.669873, 2012.

Lim, S. S., Vos, T., Flaxman, A. D., Danaei, G., Shibuya, K., Adair-Rohani, H., AlMazroa, M. A., Amann, M., Anderson, H. R., Andrews, K. G., Aryee, M., Atkinson, C., Bacchus, L. J., Bahalim, A. N., Balakrishnan, K., Balmes, J., Barker-Collo, S., Baxter, A., Bell, M. L., Blore, J. D., Blyth, F., Bonner, C., Borges, G., Bourne, R., Boussinesq, M., Brauer, M., Brooks, P., Bruce, N. G., Brunekreef, B., Bryan-Hancock, C., Bucello, C., Buchbinder, R., Bull, F., Burnett, R. T., Byers, T. E., Calabria, B., Carapetis, J., Carnahan, E., Chafe, Z., Charlson, F., Chen, H., Chen, J. S., Cheng, A. T.-A., Child, J. C., Cohen, A., Colson, K. E., Cowie, B. C., Darby, S., Darling, S., Davis, A., Degenhardt, L., Dentener, F., Des Jarlais, D. C., Devries, K., Dherani, M., Ding, E. L., Dorsey, E. R., Driscoll, T., Edmond, K., Ali, S. E., Engell, R. E., Erwin, P. J., Fahimi, S., Falder, G., Farzadfar, F., Ferrari, A., Finucane, M. M., Flaxman, S., Fowkes, F. G. R., Freedman, G., Freeman, M. K.,

Gakidou, E., Ghosh, S., Giovannucci, E., Gmel, G., Graham, K., Grainger, R., Grant, B., Gunnell, D., Gutierrez, H. R., Hall, W., Hoek, H. W., Hogan, A., Hosgood, H. D., III, Hoy, D., Hu, H., Hubbell, B. J., Hutchings, S. J., Ibeanusi, S. E., Jacklyn, G. L., Jasrasaria, R., Jonas, J. B., Kan, H., Kanis, J. A., Kassebaum, N., Kawakami, N., Khang, Y.-H., Khatibzadeh, S., Khoo, J.-P., Kok, C., Laden, F., Lalloo, R., Lan, Q., Lathlean, T., Leasher, J. L., Leigh, J., Li, Y., Lin, J. K., Lipshultz, S. E., London, S., Lozano, R., Lu, Y., Mak, J., Malekzadeh, R., Mallinger, L., Marcenes, W., March, L., Marks, R., Martin, R., McGale, P., McGrath, J., Mehta, S., Memish, Z. A., Mensah, G. A., Merriman, T. R., Micha, R., Michaud, C., Mishra, V., Hanafiah, K. M., Mokdad, A. A., Morawska, L., Mozaffarian, D., Murphy, T., Naghavi, M., Neal, B., Nelson, P. K., Nolla, J. M., Norman, R., Olives, C., Omer, S. B., Orchard, J., Osborne, R., Ostro, B., Page, A., Pandey, K. D., Parry, C. D. H., Passmore, E., Patra, J., Pearce, N., Pelizzari, P. M., Petzold, M., Phillips, M. R., Pope, D., Pope, C. A., III, Powles, J., Rao, M., Razavi, H., Rehfuess, E. A., Rehm, J. T., Ritz, B., Rivara, F. P., Roberts, T., Robinson, C., Rodriguez-Portales, J. A., Romieu, I., Room, R., Rosenfeld, L. C., Roy, A., Rushton, L., Salomon, J. A., Sampson, U., Sanchez-Riera, L., Sanman, E., Sapkota, A., Seedat, S., Shi, P., Shield, K., Shivakoti, R., Singh, G. M., Sleet, D. A., Smith, E., Smith, K. R., Stapelberg, N. J. C., Steenland, K., Stöckl, H., Stovner, L. J., Straif, K., Straney, L., Thurston, G. D., Tran, J. H., Van Dingenen, R., van Donkelaar, A., Veerman, J. L., Vijayakumar, L., Weintraub, R., Weissman, M. M., White, R. A., Whiteford, H., Wiersma, S. T., Wilkinson, J. D., Williams, H. C., Williams, W., Wilson, N., Woolf, A. D., Yip, P., Zielinski, J. M., Lopez, A. D., Murray, C. J. L., and Ezzati, M.: A comparative risk assessment of burden of disease and injury attributable to 67 risk factors and risk factor clusters in 21 regions, 1990-2010: a systematic analysis for the Global Burden of Disease Study 2010, Lancet, 380, 2224-2260, doi:10.1016/S0140-6736(12)61766-8, 2012.

Liu, M., Song, Y., Zhou, T., Xu, Z., Yan, C., Zheng, M., Wu, Z., Hu, M., Wu, Y., and Zhu, T.: Fine particle pH during severe haze episodes in northern China, Geophys. Res. Lett., 44, 5213-5221, doi:10.1002/2017GL073210, 2017a.

Liu, Y., Wu, Z., Wang, Y., Xiao, Y., Gu, F., Zheng, J., Tan, T., Shang, D., Wu, Y., Zeng, L., Hu, M., Bateman, A. P., and Martin, S. T.: Submicrometer particles are in the liquid state during heavy haze episodes in the urban atmosphere of Beijing, China, Environ. Sci. Technol. Lett., 4, 427-432, doi:10.1021/acs.estlett.7b00352, 2017b.

Ma, G., Wang, J., Yu, F., Guo, X., Zhang, Y., and Li, C.: Assessing the premature death due to ambient particulate matter in China's urban areas from 2004 to 2013, Front. Env. Sci. Eng., 10, 7, doi:10.1007/s11783-016-0849-7, 2016.

Ma, Q., Wu, Y., Tao, J., Xia, Y., Liu, X., Zhang, D., Han, Z., Zhang, X., and Zhang, R.: Variations of chemical composition and source apportionment of $PM_{2.5}$ during winter haze episodes in Beijing, Aerosol Air Qual. Res., 17, 2791-2803, doi:10.4209/aaqr.2017.10.0366, 2017.

Meskhidze, N., Chameides, W. L., Nenes, A., and Chen, G.: Iron mobilization in mineral dust: Can anthropogenic SO_2 emissions affect ocean productivity?, Geophys. Res. Lett., 30, 2085, doi:10.1029/2003GL018035, 2003.

Murphy, J. G., Gregoire, P. K., Tevlin, A. G., Wentworth, G. R., Ellis, R. A., Markovic, M. Z., and VandenBoer, T. C.: Observational constraints on particle acidity using measurements and modelling of particles and gases, Faraday Discuss., 200, 379-395, doi:10.1039/C7FD00086C, 2017.

Nenes, A., Pandis, S. N., and Pilinis, C.: ISORROPIA: A new thermodynamic equilibrium model for multiphase multicomponent inorganic aerosols, Aquat. Geochem., 4, 123-152, doi:10.1023/a:1009604003981, 1998.

Nguyen, T. K. V., Zhang, Q., Jimenez, J. L., Pike, M., and Carlton, A. G.: Liquid water: ubiquitous contributor to aerosol mass, Environ. Sci. Technol. Lett., 3, 257-263, doi:10.1021/acs.estlett.6b00167, 2016.

Pan, Y., Tian, S., Liu, D., Fang, Y., Zhu, X., Zhang, Q., Zheng, B., Michalski, G., and Wang, Y.: Fossil fuel combustion-related emissions dominate atmospheric ammonia sources during severe haze episodes: evidence from ^{15}N-stable isotope in size-resolved aerosol ammonium, Environ. Sci. Technol., 50, 8049-8056, doi:10.1021/acs.est.6b00634, 2016.

Parworth, C. L., Young, D. E., Kim, H., Zhang, X., Cappa, C. D., Collier, S., and Zhang, Q.: Wintertime water-soluble aerosol composition and particle water content in Fresno, California, J. Geophys. Res.-Atmos., 122, 3155-3170, doi:10.1002/2016JD026173, 2017.

Pathak, R. K., Yao, X., and Chan, C. K.: Sampling artifacts of acidity and ionic species in $PM_{2.5}$, Environ. Sci. Technol., 38, 254-259, doi:10.1021/es0342244, 2004.

Peng, J., Hu, M., Guo, S., Du, Z., Shang, D., Zheng, J., Zheng, J., Zeng, L., Shao, M., Wu, Y., Collins, D., and Zhang, R.: Ageing and hygroscopicity variation of black carbon particles in Beijing measured by a quasi-atmospheric aerosol evolution study (QUALITY) chamber, Atmos. Chem. Phys., 17, 10333-10348, doi:10.5194/acp-17-10333-2017, 2017.

Pitzer, K. S., and Simonson, J. M.: Thermodynamics of multicomponent, miscible, ionic systems: theory and equations, J. Phys. Chem., 90, 3005-3009, doi:10.1021/j100404a042, 1986.

Pye, H. O. T., Liao, H., Wu, S., Mickley, L. J., Jacob, D. J., Henze, D. K., and Seinfeld, J. H.: Effect of changes in climate and emissions on future sulfate-nitrate-ammonium aerosol levels in the United States, J. Geophys. Res.-Atmos., 114, D01205, doi:10.1029/2008JD010701, 2009.

Pye, H. O. T., Zuend, A., Fry, J. L., Isaacman-VanWertz, G., Capps, S. L., Appel, K. W., Foroutan, H., Xu, L., Ng, N. L., and Goldstein, A. H.: Coupling of organic and inorganic aerosol systems and the effect on gas–particle partitioning in the southeastern US, Atmos. Chem. Phys., 18, 357-370, doi:10.5194/acp-18-357-2018, 2018.

Ramanathan, V., Crutzen, P. J., Kiehl, J. T., and Rosenfeld, D.: Aerosols, climate, and the hydrological cycle, Science, 294, 2119-2124, doi:10.1126/science.1064034, 2001.

Rindelaub, J. D., Craig, R. L., Nandy, L., Bondy, A. L., Dutcher, C. S., Shepson, P. B., and Ault, A. P.: Direct measurement of pH in individual particles via Raman Microspectroscopy and variation in acidity with relative humidity, J. Phys. Chem. A, 120, 911-917, doi:10.1021/acs.jpca.5b12699, 2016.

Rood, M. J., Shaw, M. A., Larson, T. V., and Covert, D. S.: Ubiquitous nature of ambient metastable aerosol, Nature, 337, 537-539, doi:10.1038/337537a0, 1989.

Seinfeld, J. H., and Pandis, S. N.: Atmospheric chemistry and physics: from air pollution to climate change, Third ed., John Wiley & Sons, Inc., Hoboken, New Jersey, 2016.

Shi, G., Xu, J., Peng, X., Xiao, Z., Chen, K., Tian, Y., Guan, X., Feng, Y., Yu, H., Nenes, A., and Russell, A. G.: pH of aerosols in a polluted atmosphere: source contributions to highly acidic aerosol, Environ. Sci. Technol., 51, 4289-4296, doi:10.1021/acs.est.6b05736, 2017.

Sun, K., Tao, L., Miller, D. J., Pan, D., Golston, L. M., Zondlo, M. A., Griffin, R. J., Wallace, H. W., Leong, Y. J., Yang, M. M., Zhang, Y., Mauzerall, D. L., and Zhu, T.: Vehicle emissions as an important urban ammonia source in the United States and China, Environ. Sci. Technol., 51, 2472-2481, doi:10.1021/acs.est.6b02805, 2017.

Sun, Y., Wang, Z., Fu, P., Jiang, Q., Yang, T., Li, J., and Ge, X.: The impact of relative humidity on aerosol composition and evolution processes during wintertime in Beijing, China, Atmos. Environ., 77, 927-934, doi:10.1016/j.atmosenv.2013.06.019, 2013.

Sun, Y., Du, W., Fu, P., Wang, Q., Li, J., Ge, X., Zhang, Q., Zhu, C., Ren, L., Xu, W., Zhao, J., Han, T., Worsnop, D. R., and Wang, Z.: Primary and secondary aerosols in Beijing in winter: sources, variations and processes, Atmos. Chem. Phys., 16, 8309-8329, doi:10.5194/acp-16-8309-2016, 2016.

Tan, H., Cai, M., Fan, Q., Liu, L., Li, F., Chan, P. W., Deng, X., and Wu, D.: An analysis of aerosol liquid water content and related impact factors in Pearl River Delta, Sci. Total Environ., 579, 1822-1830, doi:10.1016/j.scitotenv.2016.11.167, 2017.

Tan, T., Hu, M., Li, M., Guo, Q., Wu, Y., Fang, X., Gu, F., Wang, Y., and Wu, Z.: New insight into $PM_{2.5}$ pollution patterns in Beijing based on one-year measurement of chemical compositions, Sci. Total Environ., 621, 734-743, doi:10.1016/j.scitotenv.2017.11.208, 2018.

Teng, X., Hu, Q., Zhang, L., Qi, J., Shi, J., Xie, H., Gao, H., and Yao, X.: Identification of major sources of atmospheric NH_3 in an urban environment in Northern China during wintertime, Environ. Sci. Technol., 51, 6839-6848, doi:10.1021/acs.est.7b00328, 2017.

Tian, S., Pan, Y., and Wang, Y.: Ion balance and acidity of size-segregated particles during haze episodes in urban Beijing, Atmos. Res., 201, 159-167, doi:10.1016/j.atmosres.2017.10.016, 2018.

Tie, X., Huang, R.-J., Cao, J., Zhang, Q., Cheng, Y., Su, H., Chang, D., Pöschl, U., Hoffmann, T., Dusek, U., Li, G., Worsnop, D. R., and O'Dowd, C. D.: Severe pollution in China amplified by atmospheric moisture, Sci. Rep., 7, 15760, doi:10.1038/s41598-017-15909-1, 2017.

Wang, G., Zhang, R., Gomez, M. E., Yang, L., Levy Zamora, M., Hu, M., Lin, Y., Peng, J., Guo, S., Meng, J., Li, J., Cheng, C., Hu, T., Ren, Y., Wang, Y., Gao, J., Cao, J., An, Z., Zhou, W., Li, G., Wang, J., Tian, P., Marrero-Ortiz, W., Secrest, J., Du, Z., Zheng, J., Shang, D., Zeng, L., Shao, M., Wang, W., Huang, Y., Wang, Y., Zhu, Y., Li, Y., Hu, J., Pan, B., Cai, L., Cheng, Y., Ji, Y., Zhang, F., Rosenfeld, D., Liss, P. S., Duce, R. A., Kolb, C. E., and Molina, M. J.: Persistent sulfate formation from London Fog to Chinese haze, Proc. Natl. Acad. Sci. U.S.A., 113, 13630-13635, doi:10.1073/pnas.1616540113, 2016.

Wang, J., Wang, G., Gao, J., Wang, H., Ren, Y., Li, J., Zhou, B., Wu, C., Zhang, L., Wang, S., and Chai, F.: Concentrations and stable carbon isotope compositions of oxalic acid and related SOA in Beijing before, during, and after the 2014 APEC, Atmos. Chem. Phys., 17, 981-992, doi:10.5194/acp-17-981-2017, 2017.

Wang, S., Nan, J., Shi, C., Fu, Q., Gao, S., Wang, D., Cui, H., Saiz-Lopez, A., and Zhou, B.: Atmospheric ammonia and its impacts on regional air quality over the megacity of Shanghai, China, Sci. Rep., 5, 15842, doi:10.1038/srep15842, 2015.

Wang, Y., Zhang, Q., Jiang, J., Zhou, W., Wang, B., He, K., Duan, F., Zhang, Q., Philip, S., and Xie, Y.: Enhanced sulfate formation during China's severe winter haze episode in January 2013 missing from current models, J. Geophys. Res.-Atmos., 119, 10425-10440, doi:10.1002/2013JD021426, 2014.

Weber, R. J., Guo, H., Russell, A. G., and Nenes, A.: High aerosol acidity despite declining atmospheric sulfate concentrations over the past 15 years, Nat. Geosci., 9, 282-285, doi:10.1038/ngeo2665, 2016.

Wei, L., Duan, J., Tan, J., Ma, Y., He, K., Wang, S., Huang, X., and Zhang, Y.: Gas-to-particle conversion of atmospheric ammonia and sampling artifacts of ammonium in spring of Beijing, Sci. China-Earth Sci., 58, 345-355, doi:10.1007/s11430-014-4986-1, 2015.

Wexler, A. S., and Clegg, S. L.: Atmospheric aerosol models for systems including the ions H^+, NH_4^+, Na^+, SO_4^{2-}, NO_3^-, Cl^-, Br^-, and H_2O, J. Geophys. Res.-Atmos., 107, 4207, doi:10.1029/2001JD000451, 2002.

Wu, Z., Wang, Y., Tan, T., Zhu, Y., Li, M., Shang, D., Wang, H., Lu, K., Guo, S., Zeng, L., and Zhang, Y.: Aerosol liquid water driven by anthropogenic inorganic salts: implying its key role in haze formation over the North China Plain, Environ. Sci. Technol. Lett., 5, 160-166, doi:10.1021/acs.estlett.8b00021, 2018.

Xu, L., Guo, H., Boyd, C. M., Klein, M., Bougiatioti, A., Cerully, K. M., Hite, J. R., Isaacman-VanWertz, G., Kreisberg, N. M., Knote, C., Olson, K., Koss, A., Goldstein, A. H., Hering, S. V., de Gouw, J., Baumann, K., Lee, S.-H., Nenes, A., Weber, R. J., and Ng, N. L.: Effects of anthropogenic emissions on aerosol formation from isoprene and monoterpenes in the southeastern United States, Proc. Natl. Acad. Sci. U.S.A., 112, 37-42, doi:10.1073/pnas.1417609112, 2015a.

Xu, W., Wu, Q., Liu, X., Tang, A., Dore, A. J., and Heal, M. R.: Characteristics of ammonia, acid gases, and $PM_{2.5}$ for three typical land-use types in the North China Plain, Environ. Sci. Pollut. Res., 23, 1158-1172, doi:10.1007/s11356-015-5648-3, 2016.

Xu, W. Q., Sun, Y. L., Chen, C., Du, W., Han, T. T., Wang, Q. Q., Fu, P. Q., Wang, Z. F., Zhao, X. J., Zhou, L. B., Ji, D. S., Wang, P. C., and Worsnop, D. R.: Aerosol composition, oxidation properties, and sources in Beijing: results from the 2014 Asia-Pacific Economic Cooperation summit study, Atmos. Chem. Phys., 15, 13681-13698, doi:10.5194/acp-15-13681-2015, 2015b.

Yao, X., Ling, T. Y., Fang, M., and Chan, C. K.: Size dependence of in situ pH in submicron atmospheric particles in Hong Kong, Atmos. Environ., 41, 382-393, doi:10.1016/j.atmosenv.2006.07.037, 2007.

Yin, Z., Wang, H., and Chen, H.: Understanding severe winter haze events in the North China Plain in 2014: roles of climate anomalies, Atmos. Chem. Phys., 17, 1641-1651, doi:10.5194/acp-17-1641-2017, 2017.

Young, L.-H., Li, C.-H., Lin, M.-Y., Hwang, B.-F., Hsu, H.-T., Chen, Y.-C., Jung, C.-R., Chen, K.-C., Cheng, D.-H., Wang, V.-S., Chiang, H.-C., and Tsai, P.-J.: Field performance of a semi-continuous monitor for ambient $PM_{2.5}$ water-soluble inorganic ions and gases at a suburban site, Atmos. Environ., 144, 376-388, doi:10.1016/j.atmosenv.2016.08.062, 2016.

Zaveri, R. A., Easter, R. C., Fast, J. D., and Peters, L. K.: Model for Simulating Aerosol Interactions and Chemistry (MOSAIC), J. Geophys. Res.-Atmos., 113, D13204, doi:10.1029/2007JD008782, 2008.

Zhang, L., Chen, Y., Zhao, Y., Henze, D. K., Zhu, L., Song, Y., Paulot, F., Liu, X., Pan, Y., and Huang, B.: Agricultural ammonia emissions in China: reconciling bottom-up and top-down estimates, Atmos. Chem. Phys. Discuss., 2017, 1-36, doi:10.5194/acp-2017-749, 2017.

Zhang, Q., Jimenez, J. L., Worsnop, D. R., and Canagaratna, M.: A case study of urban particle acidity and its influence on secondary organic aerosol, Environ. Sci. Technol., 41, 3213-3219, doi:10.1021/es061812j, 2007.

Zhang, Q., Duan, F., He, K., Ma, Y., Li, H., Kimoto, T., and Zheng, A.: Organic nitrogen in $PM_{2.5}$ in Beijing, Front. Env. Sci. Eng., 9, 1004-1014, doi:10.1007/s11783-015-0799-5, 2015.

Zhao, D. F., Buchholz, A., Kortner, B., Schlag, P., Rubach, F., Kiendler-Scharr, A., Tillmann, R., Wahner, A., Flores, J. M., Rudich, Y., Watne, Å. K., Hallquist, M., Wildt, J., and Mentel, T. F.: Size-dependent hygroscopicity parameter (κ) and chemical composition of secondary organic cloud condensation nuclei, Geophys. Res. Lett., 42, 10920-10928, doi:10.1002/2015GL066497, 2015.

Zhao, M., Wang, S., Tan, J., Hua, Y., Wu, D., and Hao, J.: Variation of urban atmospheric ammonia pollution and its relation with $PM_{2.5}$ chemical property in winter of Beijing, China, Aerosol Air Qual. Res., 16, 1378-1389, doi:10.4209/aaqr.2015.12.0699, 2016.

Zhao, P., Chen, Y., and Su, J.: Size-resolved carbonaceous components and water-soluble ions measurements of ambient aerosol in Beijing, J. Environ. Sci., 54, 298-313, doi:10.1016/j.jes.2016.08.027, 2017.

Zheng, G. J., Duan, F. K., Su, H., Ma, Y. L., Cheng, Y., Zheng, B., Zhang, Q., Huang, T., Kimoto, T., Chang, D., Pöschl, U., Cheng, Y. F., and He, K. B.: Exploring the severe winter haze in Beijing: the impact of synoptic weather, regional transport and heterogeneous reactions, Atmos. Chem. Phys., 15, 2969-2983, doi:10.5194/acp-15-2969-2015, 2015.

Figures

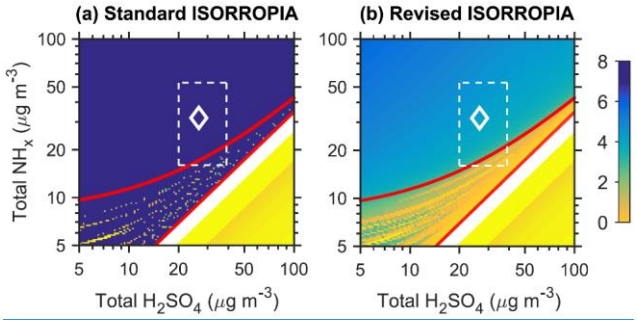

Figure 1. Sensitivity of particle pH to the total (gas + aerosol) NH_x and H_2SO_4 concentrations predicted by the standard and revised ISORROPIA model. Model calculations are conducted in the forward mode with the stable state assumption. The red curves indicate the NH_3-rich (above the curve) and NH_3-poor (below the curve) regions. The red straight lines are used to distinguish the different subregimes in the ISORROPIA solution domain (G1 above the line, and I3 and J3 below the line, details in the supplement, Sect. S1). The input data (total Na = 0 μg m^{-3}, total HNO_3 = 26 μg m^{-3}, total HCl = 1.7 μg m^{-3}, RH = 56%, and T = 274.1 K) of an NH_3–Na–H_2SO_4–HNO_3–HCl–H_2O aerosol system reflect the average $PM_{1.0}$ measurements for Beijing winter haze pollution episodes reported in Wang et al. (2016). The white boxes define the observed concentration ranges for the Beijing winter haze pollution episodes and diamonds represent the average Beijing haze conditions (total NH_x = 32 μg m^{-3}, total H_2SO_4 = 26 μg m^{-3}) reported in Wang et al. (2016). The noises in pH between the two red lines are due very likely to the instability of numerical solver currently used in the ISORROPIA model (more information can be found at *wiki.seas.harvard.edu/geos-chem/index.php/ISORROPIA_II*).

Formatted: Normal, Centered

Formatted: Font: 小五, Bold, English (United Kingdom)

Formatted ...

Formatted: Normal, Justified

Formatted ...

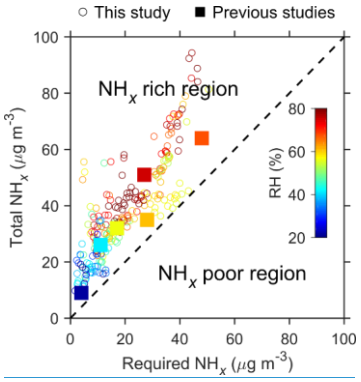

Figure 2. Relationship between required NH_x and total NH_x concentrations under Beijing winter haze conditions. The circles indicate hourly measurements in this study and the filled squares indicate measurement results from previous studies (Wang et al., 2016; Liu et al., 2017a) in winter Beijing. The dash line indicates a 1:1 relationship and defines the NH_x-rich region (above) and NH_x-poor region (below).

Formatted: Centered, Space After: 0 pt, Line spacing: 1.5 lines

Formatted: Font: Italic, Subscript

Formatted: Font: Italic, Subscript

Formatted: Font: Not Bold

Formatted: Caption

Formatted: Font: Not Bold, Italic, Subscript

Formatted: Font: Not Bold

Formatted: Font: Not Bold, Italic, Subscript

Formatted: Font: Not Bold

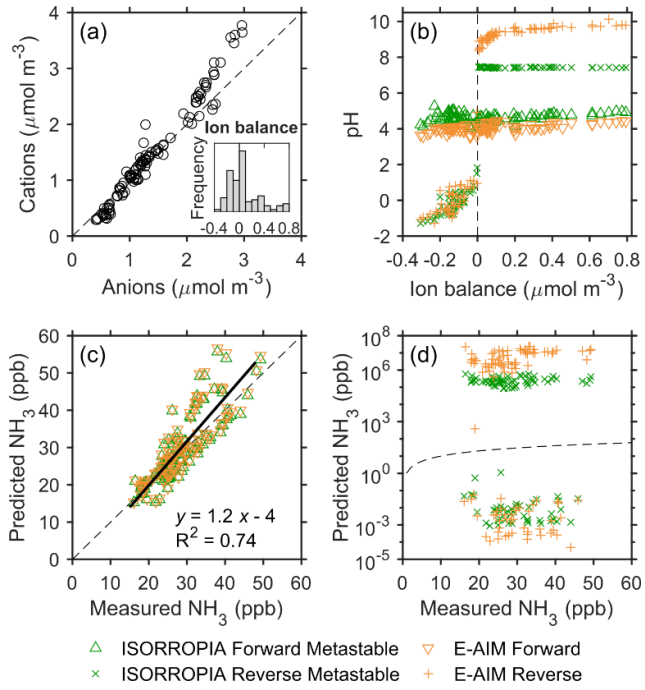

Figure 3~~1~~. Relationship between ion balance and predicted particle pH in forward mode and reverse mode calculations, and a comparison of measured and predicted gas phase NH_3 mixing ratios. (a) Cation-to-anion equivalent ratios in $PM_{2.5}$ during the field measurements. The inserted figure displays the frequency distribution of ion balance values. The dash line indicates a 1:1 relationship. (b) Predicted pH vs. ion balance. The dash line indicates ion balance equal to zero. (c–d) Comparisons of predicted and measured gas phase NH_3 mixing ratios. The dash lines indicate a 1:1 relationship. The solid line in (c) represents the linear correlation between predicted and measured NH_3 levels (the ISORROPIA forward metastable and E-AIM forward calculations have essentially the same results). The eligible number of samples (n = 106) is limited by the requirement in E-AIM that RH > 60%.

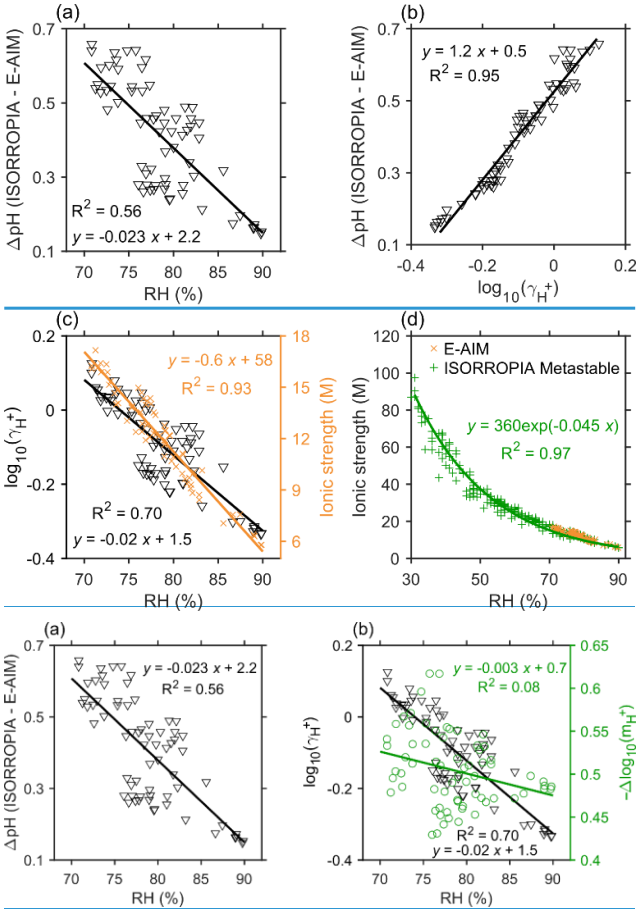

Figure 24. pH difference between forward mode E-AIM and ISORROPIA, calculations and the its relationship with hydrogen ion activity coefficient, ionic strength, and RH. (a) ΔpH vs. RH. (b) The relationship between RH and hydrogen ion activity coefficient from E-AIM (left) and difference in predicted H^+ concentrations (right). (a) ΔpH (ISORROPIA – E-AIM) vs. RH. (b) ΔpH vs. hydrogen ion activity coefficient from E-AIM. (c) RH vs. hydrogen ion activity coefficient (left) and ionic strength (right) both from E-AIM. (d) RH vs. ionic strength. TThe solid linesss in each panel indicate linear regressionss and their expressions are also shown. For a more appropriate comparison, we choose the samples (n = 68) that are in a completely aqueous phase predicted by E-AIM, and K^+ is accounted for as equivalent Na^+ in ISORROPIA. The ISORROPIA calculations are carried out assuming the a metastable state, but the pH results are very similar for the stable state when the revised ISORROPIA model is applied.

Formatted: Font: Not Bold

Formatted: Superscript

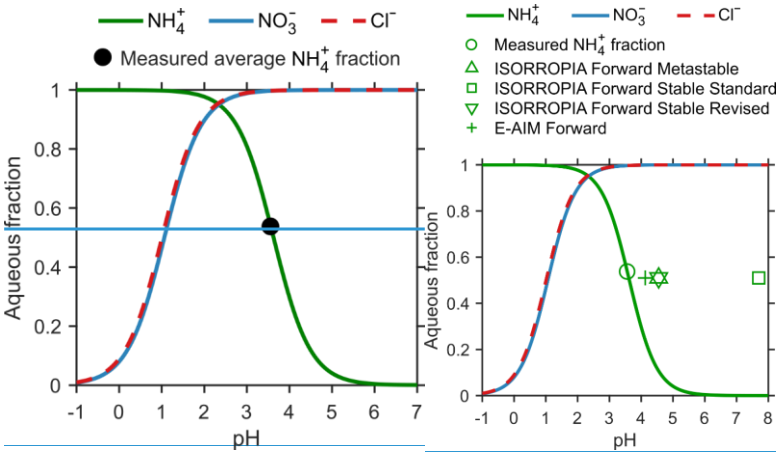

Figure ~~3~~5. Equilibrium fraction of total ammonia, nitric acid, and hydrochloric acid in the aqueous phase as a function of particle pH. The average temperature (278 K) and aerosol water content (144 μg m^{-3}) during severe haze conditions (RH > 75%) are used to calculate these S curves. The ~~black dot~~circle on top of the ammonia curve indicates the measured average aqueous fraction, which is calculated with the gas phase NH_3 and $PM_{2.5}$ NH_4^+ concentrations. The corresponding results from different model calculations are also shown as scatter plots: the *x* axis is the calculated average pH value and the *y* axis is the calculated average NH_4^+ aqueous fraction.

Formatted: Subscript
Formatted: Subscript
Formatted: Subscript
Formatted: Superscript
Formatted: Font: Italic
Formatted: Font: Italic
Formatted: Subscript
Formatted: Superscript

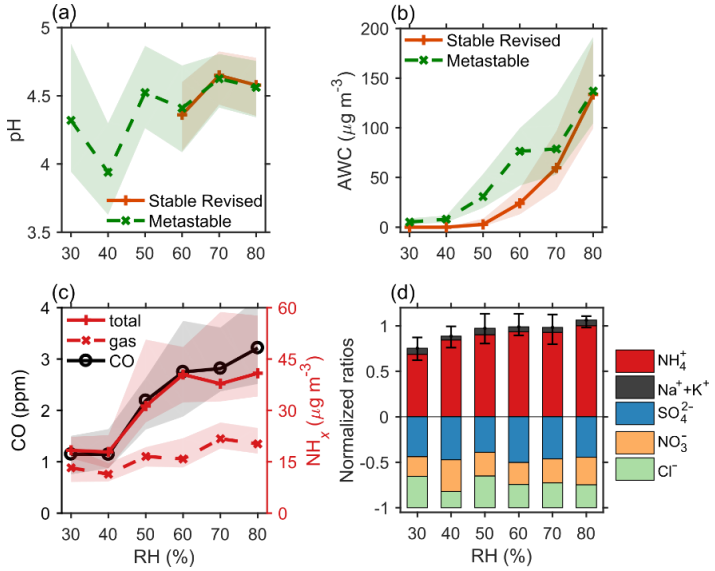

Figure 46. Variations of several chemical and physical parameters as a function of RH. (a–b) $PM_{2.5}$ pH and AWC predicted from forward mode ISORROPIA calculations in both stable and metastable states. (c) Measured ~~mass~~ concentrations of CO, total (gas + aerosol) NH_x, and gas phase NH_3. For NH_3, 1 μg $m^{-3} \approx 1.3$ ppb at standard temperature and pressure. (d) Equivalent ratios of different ions normalized by the levels of total anions. The data are grouped in RH bins (10% increment). The shaded regions in (a–c) and error bars in (d) indicate the 25th and 75th percentiles. The measurement uncertainties of ions and gases are considered in pH and AWC calculations using a Monte Carlo approach.

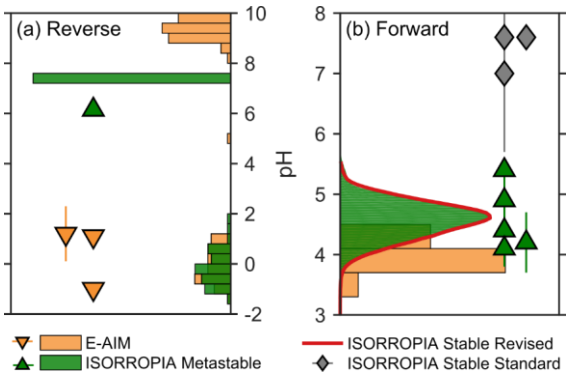

Figure 57. pH predictions during North China winter haze events from this and previous studies. Note differences in pH scales for the reverse mode (a) and forward mode (b) calculations. The frequency distributions and symbols reflect results from this and previous studies, respectively. Here we include only our samples during winter haze events (RH > 60%), with a Monte Carlo approach used in the ISORROPIA forward mode calculations to better account for the ionic and gas measurement uncertainties.

Tables

Table 1. Previously reported cation-to-anion equivalent ratios and particle pH values during winter haze periods in North China.

City	Year	Time Resolution	Size	Model	Equivalent Ratio	pH	Note	Reference
				Forward (closed)				
Beijing	2015	1 h	PM_1	ISORROPIA Stable[c]	1.09±0.11	7.6±0.0	$PM_{2.5}$=114±44 μg m^{-3}; RH=56±14%	Wang et al. (2016)
Beijing[a]	2014/ 2015	12 h	$PM_{2.5}$	ISORROPIA Stable	1.16	7.6±0.1	$PM_{2.5}$>75 μg m^{-3}; RH=62±12%	He et al. (2017)
Xi'an	2012	1 h	$PM_{2.5}$	ISORROPIA Stable[c]	1.06±0.06	7.0±1.3	$PM_{2.5}$=250±120 μg m^{-3}; RH=68±14%	Wang et al. (2016)
Beijing	2013	2 h	$PM_{2.5}$	ISORROPIA Metastable	1.08	5.4	Average of January[e]	Cheng et al. (2016)
Beijing	2015/ 2016	1 h	$PM_{2.5}$	ISORROPIA Metastable	0.99	4.2±0.5	RH=68±16%	Liu et al. (2017a)
Beijing[a]	2014/ 2015	12 h	$PM_{2.5}$	ISORROPIA Metastable	1.16	4.4±0.6	$PM_{2.5}$>75 μg/m^{-3}; RH=62±12%	He et al. (2017)
Beijing	2014	1 d	$PM_{2.5}$	ISORROPIA Metastable	1.2	4.1	$PM_{2.5}$>150 μg m^{-3}	Tan et al. (2018)
Tianjin	2014/ 2015	1 h	$PM_{2.5}$	ISORROPIA Metastable	1.13	4.9±0.4	RH=72±10%	Shi et al. (2017)
				Reverse (open)				
Beijing	2013	2 h	$PM_{2.5}$	ISORROPIA Metastable	1.08	6.2	Average of January[e]	Cheng et al. (2016)
Beijing	2013	1 d	$PM_{2.1}$	E-AIM	1.16	1.1	$PM_{2.5}$>150 μg m^{-3}; RH>60%	Tian et al. (2018)
Beijing[b]	2005/ 2006	7 d	$PM_{2.5}$	E-AIM[d]	1.09	1.2±1.1	RH=63±15%	He et al. (2012)
Jinan	2006/ 2007	1 d	PM_1	E-AIM[d]	Not Available	−1	$PM_{1.8}$=193 μg m^{-3}	Cheng et al. (2011)

All measurements were made in the urban region except [a]suburban and [b]both urban and rural. Thermodynamic models were ISORROPIA (version II) or E-AIM (version IV) except for [d]E-AIM version II. [c]Personal communication with G. Wang. [e]Personal communication with G. Zheng.

Supplement

Contents:

Section S1. Revised ISORROPIA-II Model and Influence on pH Prediction

The revised ISORROPIA-II model in this study has fixed some coding errors in the standard ISORROPIA-II model (*http://isorropia.eas.gatech.edu/*, last accessed: 2017/12/17). These errors are found to be closely related to aerosol water pH calculations under North China winter haze conditions. Note that only the forward stable state pH predictions are affected. Details are given in this section. ~~The~~ The standard ISORROPIA-II model source code is password protected, but there is a version of ISORROPIA-II source code, implemented by Pye et al. (2009) into the GEOS-Chem chemical transport model and publicly accessible at *http://acmg.seas.harvard.edu/geos/doc/man/*. The code revision is available at *http://wiki.seas.harvard.edu/geos-chem/index.php/ISORROPIA_II#Bug_fixes_for_ISORROPIA_II_stable_mode* (last accessed: 2018/04/02). ~~Details are given in this section.~~

Formatte

S1.1 General Solution Procedure of ISORROPIA-II

As shown in the reference manual (*http://nenes.eas.gatech.edu/ISORROPIA/Version2_1/ISORROPIA21Manual.pdf*, last accessed: 2017/12/17), the ISORROPIA-II model consists of eight submodels according to the type of problem defined (forward or reverse) and the input chemical species (Table S1). For example, the submodel ISRP3F solves the forward problem for the NH_3–Na–H_2SO_4–HNO_3–HCl–H_2O aerosol system.

Under each submodel, there are several subregimes determined by the molar ratios of basic chemical species (NH_3, Na, K, Ca, and Mg) to sulfuric acid (Table S2). These molar ratios are referred as "sulfate ratios". Table S3 presents the subregimes under the submodels ISRP3F and ISRP4F. Different major and minor species potentially present in the solution are assumed by different subregimes, which reduces the number of thermodynamic reactions required. For example, gas phase NH_3 is considered as a minor species for "sulfate rich" and "sulfate super-rich" aerosols, whereas bisulfate ion HSO_4^- (l) is a minor species for "sulfate poor" aerosols.

Formatte

Table S1. Eight submodels in ISORROPIA-II

Input Chemical Species	Submodel
NH_3, H_2SO_4	ISRP1F (forward) or ISRP1R (reverse)
NH_3, H_2SO_4, HNO_3	ISRP2F (forward) or ISRP2R (reverse)
NH_3, H_2SO_4, HNO_3, Na, HCl	ISRP3F (forward) or ISRP3R (reverse)
NH_3, H_2SO_4, HNO_3, Na, HCl, K, Ca, Mg	ISRP4F (forward) or ISRP4R (reverse)

~~Under each submodel, there are several subregimes determined by the molar ratios of basic chemical species (NH_3, Na, K, Ca, and Mg) to sulfuric acid (Table S2). These molar ratios are referred as "sulfate ratios". Table S3 presents the subregimes under the submodels ISRP3F and ISRP4F. Different major and minor species potentially present in the solution are assumed by different subregimes, which reduces the number of thermodynamic reactions required. For example, gas phase NH_3 is considered as a minor species for "sulfate rich" and "sulfate super rich" aerosols, whereas bisulfate ion HSO_4^- (1) is a minor species for "sulfate poor" aerosols.~~

Table S2. Definition of different sulfate ratios

Sulfate Ratio	Equation
Total sulfate molar ratio	$R_{Total} = \frac{[NH_3{}^{gas+aerosol} + Na^{gas+aerosol} + Ca^{gas+aerosol} + K^{gas+aerosol} + Mg^{gas+aerosol}]}{[H_2SO_4{}^{gas+aerosol}]}$
Ammonia & Sodium molar ratio	$R_{NH_3+Na} = \frac{[NH_3{}^{gas+aerosol} + Na^{gas+aerosol}]}{[H_2SO_4{}^{gas+aerosol}]}$
Crustal & Sodium molar ratio	$R_{Crustal+Na} = \frac{[Na^{gas+aerosol} + Ca^{gas+aerosol} + K^{gas+aerosol} + Mg^{gas+aerosol}]}{[H_2SO_4{}^{gas+aerosol}]}$
Crustal molar ratio	$R_{Crustal} = \frac{[Ca^{gas+aerosol} + K^{gas+aerosol} + Mg^{gas+aerosol}]}{[H_2SO_4{}^{gas+aerosol}]}$
Sodium molar ratio	$R_{Na} = \frac{[Na^{gas+aerosol}]}{[H_2SO_4{}^{gas+aerosol}]}$

Table S3. Subregimes under the submodels ISRP3F and ISRP4F

Aerosol Type	Sulfate Ratio	Subregime	Subcase
ISRP3F (NH_3–Na–H_2SO_4–HNO_3–HCl–H_2O aerosol)			
Sulfate Poor, Sodium Rich	$R_{Na} \geq 2$	H	H1–H6
Sulfate Poor, Sodium Poor	$R_{NH_3+Na} \geq 2$, $R_{Na} < 2$	G	G1–G5
Sulfate Rich	$1 \leq R_{NH_3+Na} < 2$	I	I1–I6
Sulfate Super-Rich	$R_{NH_3+Na} < 1$	J	J1–J3
ISRP4F (K–Ca–Mg–NH_3–Na–H_2SO_4–HNO_3–HCl–H_2O aerosol)			
Sulfate Poor, Crustal & Sodium Rich, Crustal Rich	$R_{Crustal} > 2$	P	P1–P13
Sulfate Poor, Crustal & Sodium Rich, Crustal Poor	$R_{Crustal+Na} \geq 2$, $R_{Crustal} \leq 2$	M	M1–M8
Sulfate Poor, Crustal & Sodium Poor	$R_{Total} \geq 2$, $R_{Crustal+Na} < 2$	O	O1–O7
Sulfate Rich	$1 \leq R_{Total} < 2$	L	L1–L9
Sulfate Super-Rich	$R_{Total} < 1$	K	K1–K4

Further, each subregime includes several subcases which depend on the input relative humidity (RH). This is because the possible solid salts have different associated deliquescence relative humidities (DRH). The RH ranges and possible solid and aqueous phases are shown in Table S4 (for subcases G1–G5) and Table S5 (for subcases O1–O7). For the stable state solution, RH increases gradually from G1 to G5 and from O1 to O7, and the solid salts are dissolved one

by one (depending on their DRH). When the input RH is larger than the DRH for all possible salts, an aqueous phase always exists (G5 and O7). G5 and O7 are used thus also for the metastable state solution (no precipitate is formed).

Table S4. Subcases G1–G5

Subcase	RH Subdomain	Notes
G1	RH < DRNH4NO3	Solids: $(NH_4)_2SO_4$, NH_4NO_3, NH_4Cl, Na_2SO_4; Aqueous phase: Present when RH ≥ MDRH.
G2	DRNH4NO3 ≤ RH < DRNH4CL	Solids: $(NH_4)_2SO_4$, NH_4Cl, Na_2SO_4; Aqueous phase: Present when there is NH_4NO_3 (which deliquesces) or when RH ≥ MDRH.
G3	DRNH4CL ≤ RH < DRNH42S4	Solids: $(NH_4)_2SO_4$, Na_2SO_4; Aqueous phase: Present when there is NH_4NO_3 or NH_4Cl (which deliquesces) or when RH ≥ MDRH.
G4	DRNH42S4 ≤ RH < DRNA2SO4	Solids: Na_2SO_4; Aqueous phase: Present.
G5	RH ≥ DRNA2SO4	Solids: None; Aqueous phase: Present; *This subroutine is used for the metastable mode calculation.*

DRNH4NO3, DRNH4CL, DRNH42S4 and DRNA2SO4 represent the deliquescence relative humidity (DRH) of $NH_4NO_{3(s)}$, $NH_4Cl_{(s)}$, $(NH_4)_2SO_{4(s)}$, and $Na_2SO_{4(s)}$, respectively. The MDRH (mutual deliquescence relative humidity) for each subdomain represents the deliquescence point of the corresponding salt mixture and thus varies from case to case.

Table S5. Subcases O1–O7

Subcase	RH Subdomain	Notes
O1	RH < DRNH4NO3	Solids: $CaSO_4$, $(NH_4)_2SO_4$, NH_4NO_3, NH_4Cl, $MgSO_4$, Na_2SO_4, K_2SO_4; Aqueous phase: Present when RH ≥ MDRH.
O2	DRNH4NO3 ≤ RH < DRNH4CL	Solids: $CaSO_4$, $(NH_4)_2SO_4$, NH_4Cl, $MgSO_4$, Na_2SO_4, K_2SO_4; Aqueous phase: Present when there is NH_4NO_3 (which deliquesces) or when RH ≥ MDRH.
O3	DRNH4CL ≤ RH < DRNH42S4	Solids: $CaSO_4$, $(NH_4)_2SO_4$, $MgSO_4$, Na_2SO_4, K_2SO_4; Aqueous phase: Present when there is NH_4NO_3 or NH_4Cl (which deliquesces) or when RH ≥ MDRH.
O4	DRNH42S4 ≤ RH < DRMGSO4	Solids: $CaSO_4$, $MgSO_4$, Na_2SO_4, K_2SO_4; Aqueous phase: Present.
O5	DRMGSO4 ≤ RH < DRNA2SO4	Solids: $CaSO_4$, Na_2SO_4, K_2SO_4; Aqueous phase: Present.
O6	DRNA2SO4 ≤ RH < DRK2SO4	Solids: $CaSO_4$, K_2SO_4; Aqueous phase: Present.
O7	RH ≥ DRK2SO4	Solids: $CaSO_4$; Aqueous phase: Present; *This subroutine is used for the metastable mode calculation.*

DRNH4NO3, DRNH4CL, DRNH42S4, DRMGSO4, DRNA2SO4 and DRK2SO4 represent the deliquescence relative humidity (DRH) of $NH_4NO_{3(s)}$, $NH_4Cl_{(s)}$, $(NH_4)_2SO_{4(s)}$, $MgSO_{4(s)}$, $Na_2SO_{4(s)}$, and $K_2SO_{4(s)}$, respectively. The MDRH (mutual deliquescence relative humidity) for each subdomain represents the deliquescence point of the corresponding salt mixture and thus varies from case to case. $CaSO_4$ is assumed completely insoluble (Fountoukis and Nenes, 2007).

S1.2 Coding Errors within Several Subcases

For the subcase G2 (an NH_3–Na–H_2SO_4–HNO_3–HCl–H_2O aerosol, $R_{NH_3+Na} \geq 2$, $R_{Na} < 2$, DRNH4NO3 ≤ RH < DRNH4CL), an aqueous phase exists if NH_4NO_3 is present (which deliquesces). The problem is solved iteratively in ISORROPIA-II. For each iteration, it calculates the levels of solids, gases (NH_3, HNO_3, HCl), and aqueous ions. The major ions include Na^+, NH_4^+, H^+, SO_4^{2-}, NO_3^-, and Cl^- (HSO_4^- and OH^- are considered minor species under such conditions) (Fountoukis and Nenes, 2007). The objective function is the departure of $Cl^-_{(l)}$, $NH_4^+{}_{(l)}$, $HCl_{(g)}$, and $NH_{3(g)}$ from the equilibrium reaction $NH_{3(g)} + HCl_{(g)} \leftrightarrow NH_4^+{}_{(l)} + Cl^-_{(l)}$. The aerosol water pH is calculated based on ion balance:

$$\mathrm{IB} = \left[Na^+{}_{(l)}\right] + \left[NH_4^+{}_{(l)}\right] - \left[Cl^-{}_{(l)}\right] - \left[NO_3^-{}_{(l)}\right] - 2\times\left[SO_4^{2-}{}_{(l)}\right] \quad \text{(S1)}$$

Here, $\left[Na^+{}_{(l)}\right]$ is assumed to be zero as the RH is lower than the DRH of $Na_2SO_{4(s)}$ and its dissolution does not affect pH. Eq. (S1) indicates that $\left[NH_4^+{}_{(l)}\right]$, $\left[Cl^-{}_{(l)}\right]$, $\left[NO_3^-{}_{(l)}\right]$, and $\left[SO_4^{2-}{}_{(l)}\right]$ should be known in order to calculate pH.

The solution procedure begins by assuming that a very small amount of $Cl^-_{(l)}$ exists. $\left[NO_3^-{}_{(l)}\right]$ is computed taking advantage of the equilibrium reactions $HNO_{3(g)} \leftrightarrow H^+_{(l)} + NO_3^-{}_{(l)}$ and $HCl_{(g)} \leftrightarrow H^+_{(l)} + Cl^-_{(l)}$:

$$\left[NO_3^-{}_{(l)}\right] = \frac{\left[HNO_{3(T)}\right]}{1 + \frac{K_2}{K_1}\times\frac{\gamma^2_{HNO_3}}{\gamma^2_{HCl}}\times\frac{\left[HCl_{(T)}\right]-\left[Cl^-{}_{(l)}\right]}{\left[Cl^-{}_{(l)}\right]}} \quad \text{(S2)}$$

where K_1 and K_2 are the equilibrium constants for $HNO_{3(g)} \leftrightarrow H^+_{(l)} + NO_3^-{}_{(l)}$ and $HCl_{(g)} \leftrightarrow H^+_{(l)} + Cl^-_{(l)}$, respectively. The symbol γ represents the activity coefficient. The subscript $_{(T)}$ defines the total input.

Then, $\left[NH_4^+{}_{(l)}\right]$ is calculated, which consists of two parts, $\left[NH_4^+{}_{(l),NC}\right]$ (associated with $NO_3^-{}_{(l)}$ and $Cl^-_{(l)}$) and $\left[NH_4^+{}_{(l),S}\right]$ (associated with $SO_4^{2-}{}_{(l)}$). Thus, $\left[NH_4^+{}_{(l)}\right] = \left[NH_4^+{}_{(l),NC}\right] + \left[NH_4^+{}_{(l),S}\right]$. $\left[SO_4^{2-}{}_{(l)}\right]$ and $\left[NH_4^+{}_{(l),S}\right]$ are computed from the equilibrium reaction $(NH_4)_2SO_{4(s)} \leftrightarrow 2NH_4^+{}_{(l)} + SO_4^{2-}{}_{(l)}$ solving a cubic equation. Note that $\left[NH_4^+{}_{(l),S}\right] = 2\times\left[SO_4^{2-}{}_{(l)}\right]$. Accordingly, Eq. (S1) becomes:

$$\mathrm{IB} = \left[NH_4^+{}_{(l),NC}\right] - \left[Cl^-{}_{(l)}\right] - \left[NO_3^-{}_{(l)}\right] \quad \text{(S3)}$$

Eq. (S3) indicates that the estimation of $\left[NH_4^+{}_{(l),NC}\right]$ is important for pH calculation. However, we find, in the subcase G2 of the standard ISORROPIA-II model, that $\left[NH_4^+{}_{(l),NC}\right]$ is wrongly calculated by Eq. (S4):

$$\left[NH_4^+{}_{(l),NC}\right] = \mathrm{MIN}\left(\left[Cl^-{}_{(l)}\right] + \left[NO_3^-{}_{(l)}\right], C_1\right) \quad \text{(S4)}$$

where $C_1 = \left[NH_{3(T)}\right] + \left[Na_{(T)}\right] - 2\times\left[H_2SO_{4(T)}\right]$. As the iteration begins with a very small $\left[Cl^-_{(l)}\right]$ (and thus a very small $\left[NO_{3(l)}^-\right]$), Eq. (S4) is usually reduced to Eq. (S5):

$$\left[NH_{4(l),NC}^+\right] = \left[Cl^-_{(l)}\right] + \left[NO_{3(l)}^-\right] \quad \text{(S5)}$$

Consequently, the ion balance IB obtained from Eq. (S3) becomes zero in the subcase G2 and the pH is very often around 7 (i.e., neutral). On the other hand, the subcases G3, G4, and G5 in the ISORROPIA-II subregime G correctly calculate $\left[NH_{4(l),NC}^+\right]$ based on the equilibrium reaction $NH_{3(g)} + H^+_{(l)} \leftrightarrow NH_4^+{}_{(l)}$ (with an equilibrium constant K_3) and the ion balance equation, Eq. (S1). The following equations are derived:

$$\frac{C_3\left(\left[NH_{4(l),NC}^+\right]+C_2\right)}{\left(C_1-\left[NH_{4(l),NC}^+\right]\right)} + \left[NH_{4(l),NC}^+\right] - \left[Cl^-_{(l)}\right] - \left[NO_{3(l)}^-\right] = 0 \quad \text{(S6)}$$

$$\left[NH_{4(l),NC}^+\right]^2 - \left(C_1 + C_3 + \left[Cl^-_{(l)}\right] + \left[NO_{3(l)}^-\right]\right)\left[NH_{4(l),NC}^+\right] + C_1\left(\left[Cl^-_{(l)}\right] + \left[NO_{3(l)}^-\right]\right) - C_2C_3 = 0 \quad \text{(S7)}$$

where $C_2 = 2\times\left[H_2SO_{4(T)}\right] - \left[Na_{(T)}\right]$, $C_3 = \frac{1}{K_3RT}\times\frac{\gamma^2_{NH_4NO_3}}{\gamma^2_{HNO_3}}$, R is the gas constant, and T is the temperature. Eq. (S7) is a quadratic equation in which $\left[NH_{4(l),NC}^+\right]$ is the only unknown.

The difference in calculating $\left[NH_{4(l),NC}^+\right]$ between G2 (using Eq. (S5)) and G3–G5 (using Eq. (S7)) is that Eq. (S7) accounts for NH_3 evaporation. Note that if $K_3 \rightarrow \infty$ (i.e., NH_3 does not evaporate), then $C_3 \rightarrow 0$, and Eq. (S7) is reduced to Eq. (S8), which is essentially the same as Eq. (S4).

$$\left(\left[NH_{4(l),NC}^+\right] - \left[Cl^-_{(l)}\right] - \left[NO_{3(l)}^-\right]\right)\left(\left[NH_{4(l),NC}^+\right] - C_1\right) = 0 \quad \text{(S8)}$$

The coding errors in the subcase G2 also affect the pH calculation for the subcase G1 ($R_{NH_3+Na} \geq 2$, $R_{Na} < 2$, RH < DRNH4NO3). An aqueous phase is present only for G1 when the RH is larger than the mutual deliquescence relative humidity (MDRH) of the salt mixture ($(NH_4)_2SO_4$, NH_4NO_3, NH_4Cl, Na_2SO_4) (Table S4). In this situation, the ISORROPIA model calculates a "dry" solution of chemical composition (no aqueous phase) and a "wet" solution (assuming the deliquescence of NH_4NO_3) using results from the subcase G2. The actual gas/liquid/solid composition is then a weighted average of the "dry" and "wet" solutions (Fountoukis and Nenes, 2007). The molar concentrations of chemical species in the aqueous phase are the same as the results from G2, and thus the aerosol water pH in G1 is the same as that in G2.

Similar coding errors are found also for the subcases O1 and O2 (K–Ca–Mg–NH_3–Na–H_2SO_4–HNO_3–HCl–H_2O aerosol, $R_{Total} \geq 2$, $R_{Crustal+Na} < 2$; see Tables S3 and S5). Because the standard ISORROPIA-II model fails to account for NH_3 evaporation, the calculated aerosol water pH is very often ~ 7 for O1 and O2.

Overall, we have identified coding errors in the standard ISORROPIA-II model which are related to the calculation of aerosol water pH for the four subcases (G1, G2, O1, and O2). It is important to note that only the forward stable mode calculations are affected by these errors. The forward metastable mode solutions remain the same since other subcases (G5 and O7) are used. It is also important to note that these errors have little effect on the predicted gas phase NH_3 levels. In ISORROPIA-II, the gas phase NH_3 is computed from the difference between the total NH_3 and aqueous phase NH_4^+. The difference caused by these coding errors is equal to $\left[H^+_{(l)}\right]$, much smaller than $\left[NH^+_{4(l)}\right]$. In addition, the same coding issues also exist in previous ISORROPIA versions 1.5 and 1.7.

In this study, the ISORROPIA-II model with these coding errors fixed is denoted as the revised ISORROPIA-II model, which is used to predict aerosol water and pH in the stable state.

S1.3 Sensitivity Tests

In order to explore the effect of our model revisions on the aerosol water pH calculations in ISORROPIA-II, we have carried out two sets of sensitivity tests. The first is for an NH_3–Na–H_2SO_4–HNO_3–HCl–H_2O aerosol system (Fig. S1). The forward metastable mode and forward stable mode simulations are performed for the standard ISORROPIA-II model; for the revised ISORROPIA-II model, only the forward stable mode simulations are made. The input data of Na, HNO_3, HCl, RH, and temperature are fixed, which represent the average PM_1 (particles with size smaller than 1 μm) observations of Beijing winter haze pollution episodes reported by Wang et al. (2016), and are summarized in Table S6. The levels of H_2SO_4 and NH_3 are varied over large ranges. As shown in Fig. S1d, three subcases (G1, I3, and J3) are included in these sensitivity tests. Our model revisions have no effect on I3 and J3. For G1, the standard forward stable mode simulations almost always predict pH around 7 (Fig. S1b), whereas the standard forward metastable mode simulations and the revised forward stable mode simulations predict similar values for pH < 7 (Fig. S1a–c). It is also seen from Fig. S1 that Beijing winter haze conditions fall within the subcase G1. Thus, our model revisions have a significant impact on estimating Beijing winter haze aerosol pH.

The second set of sensitivity tests is for a K–Ca–Mg–NH_3–Na–H_2SO_4–HNO_3–HCl–H_2O aerosol. The ISORROPIA-II model simulations are analogous to those in the first set. The levels of H_2SO_4 and NH_3 are varied whereas the other inputs which represent the average $PM_{2.5}$ observations of Xi'an winter haze pollution episodes reported by Wang et al. (2016) are fixed. As shown in Fig. S2, our model revisions change the pH output (from ~ 7 to < 7) in the subcase O1 (most of the Xi'an winter haze conditions fall within O1), but do not affect the other subcases (P5, M1, L3, and K3). In addition, some non-monotonic features (i.e., noises) of the pH output are observed in Figs. S1 and S2 for all of the ISORROPIA-II simulations, when the total molar concentrations of basic species ($[K_{(T)}] + 2\times[Ca_{(T)}] + 2\times[Mg_{(T)}] + [Na_{(T)}] + [NH_{3(T)}]$) are smaller than those of acidic species ($2\times[H_2SO_{4(T)}] + [HNO_{3(T)}] + [HCl_{(T)}]$). Such noises are due likely to instability of the numerical solver used in ISORROPIA-II. This issue is currently being investigated by Dr. Sebastian D. Eastham (*wiki.seas.harvard.edu/geos-chem/index.php/ISORROPIA_II*, last accessed: 2017/12/01). Fortunately, this issue does not strongly affect the pH calculation results under North China winter haze conditions.

Table S6. Summary of gases and aerosol measurements in Beijing and Xi'an reported by Wang et al. (2016)

	Beijing Polluted		Xi'an Polluted	
Year	2015		2012	
PM size	PM_1		$PM_{2.5}$	
	Mean	Range	Mean	Range
SO_4^{2-}, μg m^{-3}	26	20–38	38	20–83
NO_3^-, μg m^{-3}	26	4.5–48	33	12–55
Cl^-, μg m^{-3}	1.7	0.0–4.5	14	2.6–34
NH_4^+, μg m^{-3}	20	9.1–30	25	3.2–44
Na^+, μg m^{-3}	NA	NA	4.2	0.5–17
K^+, μg m^{-3}	NA	NA	4.6	1.8–8.3
Ca^{2+}, μg m^{-3}	NA	NA	2.3	0.2–5.9
Mg^{2+}, μg m^{-3}	NA	NA	0.3	0.0–0.8
NH_3, ppb	17	10–32	23	9.3–61
T, °C	0.9	−1.7–8.2	4.1	−3.1–14
RH, %	56	22–72	68	41–93

NA = Not Available. The polluted condition is defined by the concentration of SO_4^{2-} > 20 μg m^{-3}.

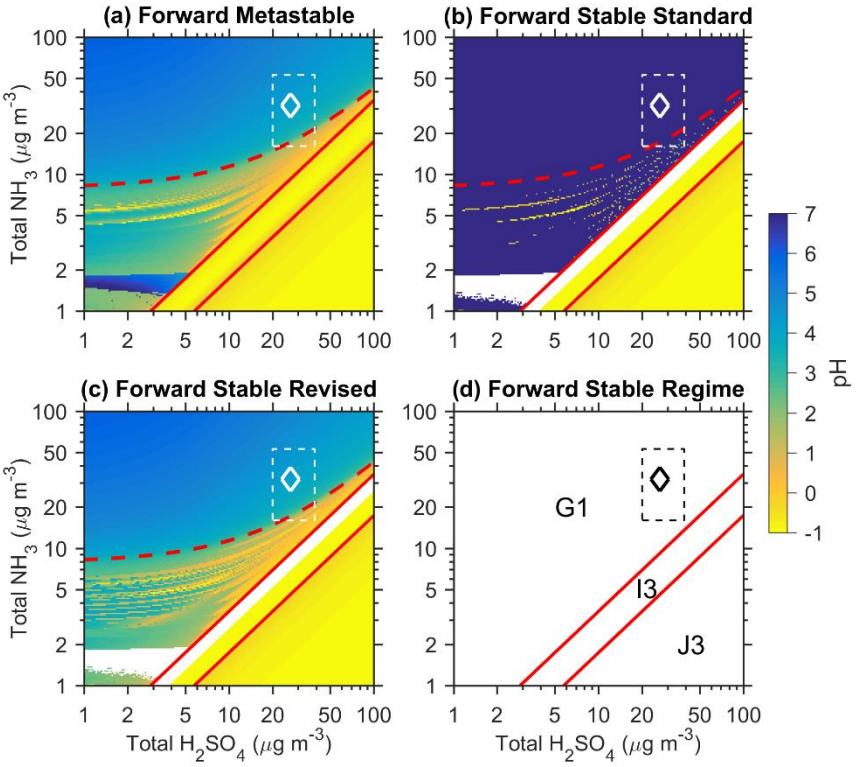

Figure S1. Sensitivity of pH to the total (gas + aerosol) NH_3 and H_2SO_4 concentrations. The results reflect thermodynamic equilibrium predictions with different ISORROPIA-II model assumptions: (a) forward metastable mode, (b) standard forward stable mode, and (c) revised forward stable mode. The subregimes of the ISORROPIA-II forward stable mode are shown in panel (d). The solid red curves are used to distinguish different subregimes. The chemical and meteorological input data (total Na = 0 μg m^{-3}, total HNO_3 = 26 μg m^{-3}, total HCl = 1.7 μg m^{-3}, RH = 56%, T = 274.1 K) for the NH_3–Na–H_2SO_4–HNO_3–HCl–H_2O aerosol

system reflect average PM_1 measurements for Beijing winter haze pollution episodes reported by Wang et al. (2016). The dashed red curves indicate the situation in which the total molar concentrations of acidic and basic species are equal ($[Na_{(T)}] + [NH_{3(T)}] = 2\times[H_2SO_{4(T)}] + [HNO_{3(T)}] + [HCl_{(T)}]$). Boxes define observed concentration ranges for the Beijing winter haze pollution episodes and diamonds represent the average Beijing haze conditions (total NH_3 = 32 μg m^{-3}, total H_2SO_4 = 26 μg m^{-3}).

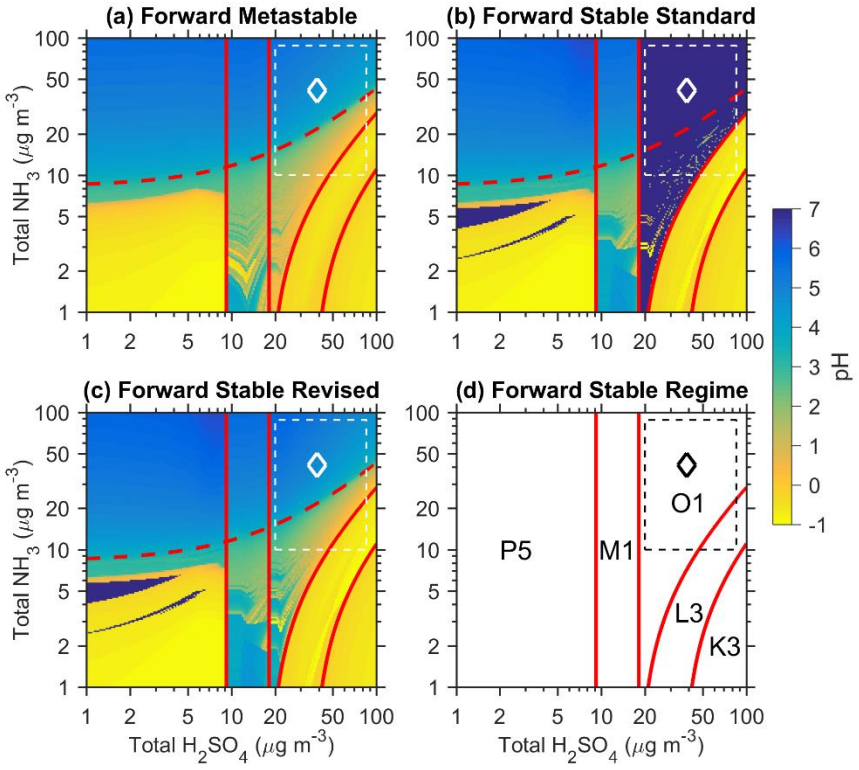

Figure S2. Sensitivity of pH to the total (gas + aerosol) NH_3 and H_2SO_4 concentrations. The results reflect thermodynamic equilibrium predictions with different ISORROPIA-II model assumptions: (a) forward metastable mode, (b) standard forward stable mode, and (c) revised forward stable mode. The subregimes of the ISORROPIA-II forward stable mode are shown in panel (d). The solid red curves are used to distinguish different subregimes. The chemical and meteorological input data (total Na = 4.2 μg m^{-3}, total K = 4.6 μg m^{-3}, total Ca = 2.3 μg m^{-3}, total Mg = 0.3 μg m^{-3}, total HNO_3 = 34 μg m^{-3}, total HCl = 14 μg m^{-3}, RH = 68%, T = 277.3 K) for the K–Ca–Mg–NH_3–Na–H_2SO_4–HNO_3–HCl–H_2O aerosol system reflect average $PM_{2.5}$ measurements for Xi'an winter haze pollution episodes reported by Wang et al. (2016). The dashed red curves indicate the situation in which the total molar concentrations of acidic and basic species are equal ($[K_{(T)}] + 2\times[Ca_{(T)}] + 2\times[Mg_{(T)}] + [Na_{(T)}] + [NH_{3(T)}] = 2\times[H_2SO_{4(T)}] + [HNO_{3(T)}] + [HCl_{(T)}]$). Boxes define observed concentration ranges for Xi'an winter haze pollution episodes and diamonds represent the average Xi'an haze conditions (total NH_3 = 41 μg m^{-3}, total H_2SO_4 = 39 μg m^{-3}).

We also calculate particle pH using our observational data collected during 2014 winter in Beijing and the standard and revised ISORROPIA-II models (Fig. S3). As expected, predicted pH values are different for the subcases G1, G2, O1, and O2. The predicted $NH_{3(g)}$ from the standard and revised calculations are similar and thus it is impossible to differentiate them by comparing the $NH_{3(g)}$ concentrations. Similarly, predicted particle NH_4^+ concentrations from the standard and revised model calculations should also be similar (because in the forward-mode calculations the total (gas + aerosol) quantity is fixed). Therefore, we believe that the measurement–model comparisons of NH_3 gas-particle partitioning for the standard ISORROPIA-II forward stable mode calculations cannot be used to evaluate the success or failure of pH predictions, in contrast to previous studies (Wang et al., 2016; Guo et al., 2017). The subtle difference ΔNH_3 ($< 1\times10^{-3}$ ppb) shown in Figs. S3c and f suggests that incorporating the partitioning of NH_3 in the revised calculations pushes a little more ammonia to the gas phase, and thus more H^+ is needed in the aqueous phase and the solution is more acidic.

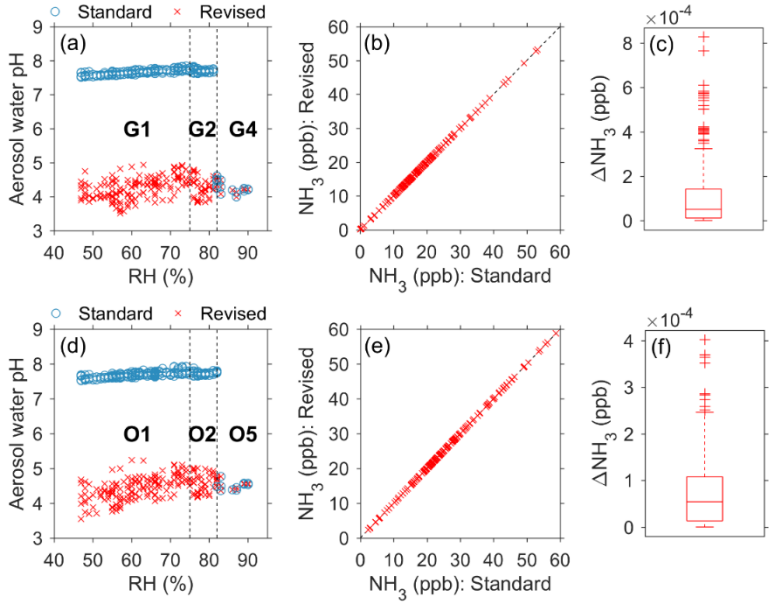

Figure S3. Comparisons of the predicted pH and gas phase NH_3 concentrations between the standard and revised ISORROPIA-II models with the stable state assumptions. (a–c) show the results using the AMS PM_1 measurements (an NH_3–H_2SO_4–HNO_3–HCl–H_2O aerosol), and (d–f) show the results using the GAC-IC $PM_{2.5}$ measurements (a K–NH_3–Na–H_2SO_4–HNO_3–HCl–H_2O aerosol).

Section S2. Uncertainties of the AMS Measurements

The AMS measurement uncertainty arises from inaccuracies in the ionization efficiency of nitrate (IE_{NO_3}), the relative ionization efficiency of a species *X* relative to nitrate (RIE_X), the collection efficiency (CE), flow rate (Q), and the transmission efficiency (TE):

$$\frac{\Delta_X}{X} = \sqrt{\left(\frac{\Delta_{IE_{NO_3}}}{IE_{NO_3}}\right)^2 + \left(\frac{\Delta_{RIE_X}}{RIE_X}\right)^2 + \left(\frac{\Delta_{CE}}{CE}\right)^2 + \left(\frac{\Delta_Q}{Q}\right)^2 + \left(\frac{\Delta_{TE}}{TE}\right)^2} \quad \text{(S9)}$$

where $\frac{\Delta_{IE_{NO_3}}}{IE_{NO_3}}$, $\frac{\Delta_{CE}}{CE}$, $\frac{\Delta_Q}{Q}$, and $\frac{\Delta_{TE}}{TE}$ are estimated to be 10%, 30%, <0.5%, and 10%, respectively; and $\frac{\Delta_{RIE_X}}{RIE_X}$ depends on the species *X* (10% for ammonium, 15% for sulfate and 20% for organics) (Bahreini et al., 2009). Using the above equation, we estimate that the overall relative uncertainties of the AMS measurements are 33% (nitrate), 35% (ammonium), 36% (sulfate), and 39% (organics). The relative uncertainties for chloride and black carbon have not been quantified and are assumed to be 40% in this study.

Section S3. S-curves for gas-particle partitioning of NH_3, HNO_3, and HCl

Note that we assume water activity and all of the activity coefficients equal to unity (i.e., an ideal aqueous solution).

S3.1 NH_3

The ammonia–water equilibrium is (Seinfeld and Pandis, 2016)

$$NH_3\,(g) + H_2O \leftrightarrow NH_3{\cdot}H_2O\,(l) \tag{S10}$$

$$NH_3{\cdot}H_2O\,(l) \leftrightarrow NH_4^+ + OH^- \tag{S11}$$

Their equilibrium constants can be expressed as $H_{NH_3} = \frac{[NH_3{\cdot}H_2O_{(l)}]}{p_{NH_3}}$ and $K_a = \frac{[NH_{4(l)}^+][OH^-]}{[NH_3{\cdot}H_2O_{(l)}]} = \frac{[NH_{4(l)}^+][H^+]}{K_w[NH_3{\cdot}H_2O_{(l)}]}$, where H_{NH_3} (M atm^{-1}) is the Henry's law constant for NH_3, p_{NH_3} (atm) is the partial pressure for NH_3, K_a (M) is the dissociation equilibrium constant for $NH_3{\cdot}H_2O$, K_w (M^2) is the dissociation equilibrium constant for water, and [X] represents aqueous concentrations of the species X (M). Thus, the total ammonia concentration in the liquid phase is

$$[NH_{4(Tl)}^+] = [NH_3{\cdot}H_2O_{(l)}] + [NH_{4(l)}^+] = H_{NH_3}p_{NH_3}\left(1+\frac{K_a}{[OH^-]}\right) = H_{NH_3}p_{NH_3}\left(1+\frac{K_a[H^+]}{K_w}\right) \tag{S12}$$

Under neutral or acidic conditions, $\frac{K_a[H^+]}{K_w} \gg 1$, and thus $[NH_{4(Tl)}^+] \cong \frac{H_{NH_3}K_a}{K_w}[H^+]p_{NH_3}$. The aqueous fraction of total (gas + particle) ammonia, $\varepsilon(NH_4^+)$, is calculated as

$$\varepsilon(NH_4^+) = \frac{\frac{H_{NH_3}K_a}{K_w}[H^+]p_{NH_3}W}{\frac{H_{NH_3}K_a}{K_w}[H^+]p_{NH_3}W + \frac{p_{NH_3}}{RT}} = \frac{H_{NH_3}^*WRT}{1 + H_{NH_3}^*WRT} \tag{S13}$$

where W is the aerosol water content, R is the ideal gas constant, T is the ambient temperature, and $H_{NH_3}^* = \frac{H_{NH_3}K_a}{K_w}[H^+]$ is known as the effective Henry's law coefficient for NH_3.

S3.2 HNO_3

The nitric acid-water equilibrium is (Seinfeld and Pandis, 2016)

$$HNO_3\,(g) \leftrightarrow HNO_3\,(l) \tag{S14}$$

$$HNO_3\,(l) \leftrightarrow NO_3^- + H^+ \tag{S15}$$

The equilibrium constants for these two equations are $H_{HNO_3} = \frac{[HNO_{3(l)}]}{p_{HNO_3}}$ and $K_{n1} = \frac{[NO_{3(l)}^-][H^+]}{[HNO_{3(l)}]}$, where H_{HNO_3} (M atm^{-1}) is the Henry's law constant of HNO_3, p_{HNO_3} (atm) is the partial pressure of HNO_3, and K_{n1} is the dissociation equilibrium constant. The total nitrate in the liquid phase can be expressed as

$$\left[NO_{3\,(l)}^{-}\right] = \frac{H_{HNO_3} K_{n1}}{[H^+]} p_{HNO_3} \quad \text{(S16)}$$

The aqueous fraction of total (gas + particle) nitric acid, $\varepsilon(NO_3^-)$, is calculated as

$$\varepsilon(NO_3^-) = \frac{\frac{H_{HNO_3} K_{n1}}{[H^+]} p_{HNO_3} W}{\frac{H_{HNO_3} K_{n1}}{[H^+]} p_{HNO_3} W + \frac{p_{HNO_3}}{RT}} = \frac{H^*_{HNO_3} WRT}{1 + H^*_{HNO_3} WRT} \quad \text{(S17)}$$

where W is the aerosol water content, R is the ideal gas constant, T is the ambient temperature, and $H^*_{HNO_3} = \frac{H_{HNO_3} K_{n1}}{[H^+]}$ is the effective Henry's law coefficient.

S3.3 HCl

Similar to the nitric acid-water equilibrium, the hydrochloric acid-water equilibrium is (Seinfeld and Pandis, 2016)

$$HCl\,(g) \leftrightarrow HCl\,(l) \quad \text{(S18)}$$

$$HCl\,(l) \leftrightarrow Cl^- + H^+ \quad \text{(S19)}$$

The equilibrium constants for these two equations are $H_{HCl} = \frac{[HCl_{(l)}]}{p_{HCl}}$ and $K_{n2} = \frac{[Cl^-][H^+]}{[HCl_{(l)}]}$, where H_{HCl} (M atm^{-1}) is the Henry's law constant of HCl, p_{HCl} (atm) is the partial pressure of HCl, K_{n2} is the dissociation equilibrium constant of $HCl_{(l)}$. The total $[Cl^-]$ in the liquid phase can be expressed as

$$\left[Cl^-_{(l)}\right] = \frac{H_{HCl} K_{n2}}{[H^+]} p_{HCl} \quad \text{(S20)}$$

The aqueous fraction of total (gas + particle) hydrochloric acid, $\varepsilon(Cl^-)$, is calculated as

$$\varepsilon(Cl^-) = \frac{\frac{H_{HCl} K_{n2}}{[H^+]} p_{HCl} W}{\frac{H_{HCl} K_{n2}}{[H^+]} p_{HCl} W + \frac{p_{HCl}}{RT}} = \frac{H^*_{HCl} WRT}{1 + H^*_{HCl} WRT} \quad \text{(S21)}$$

where W is the aerosol water content, R is the ideal gas constant, T is the ambient temperature, and $H^*_{HCl} = \frac{H_{HCl} K_{n2}}{[H^+]}$ is known as the effective Henry's law coefficient for hydrochloric acid.

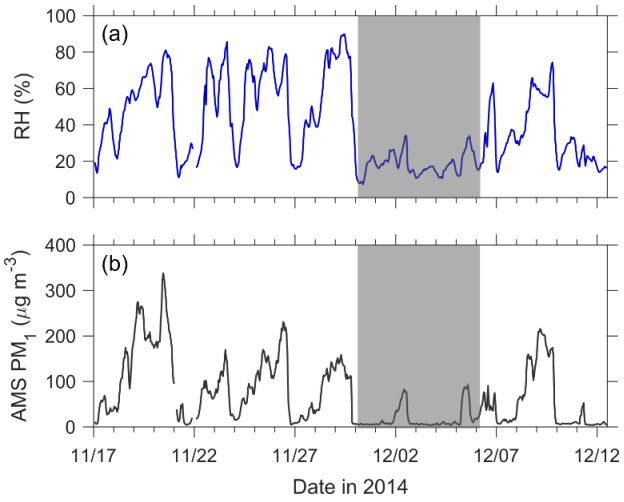

Figure S4. Time series of measured RH (a) and AMS PM_1 concentrations (b). The shaded area indicates a time period of ~ 6 days which were very dry (with RH from 7% to 34%) and relatively clean, and thus were not included in the thermodynamic analysis.

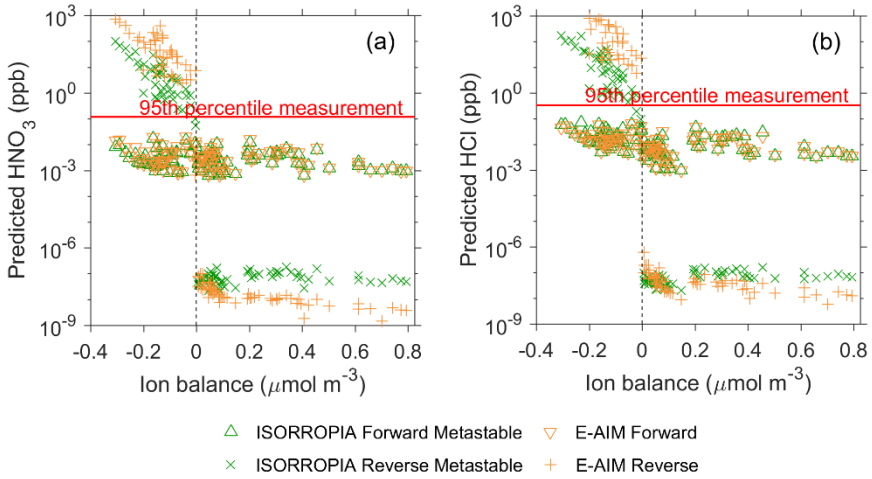

Figure S5. Relationship between ion balance and gas phase HNO_3 (a) and HCl (b) mixing ratios predicted using forward and reverse mode calculations. It is seen that the reverse mode calculations predict either very high or very low levels of HNO_3 and HCl depending on the sign (negative or positive) of the ion balance, whereas forward mode predictions are insensitive to ion balance. Because the measured mixing ratios of HNO_3 and HCl are very low and sometimes below detection limits, we do not present a quantitative comparison but show the 95% percentile of the HNO_3 and HCl data in our measurement period. As shown, the very high levels of HNO_3 and HCl in the reverse mode calculations (corresponding to negative ion balance, cations < anions, and low pH values, see Fig. 1 in the main text) are unlikely to be detected in the atmosphere.

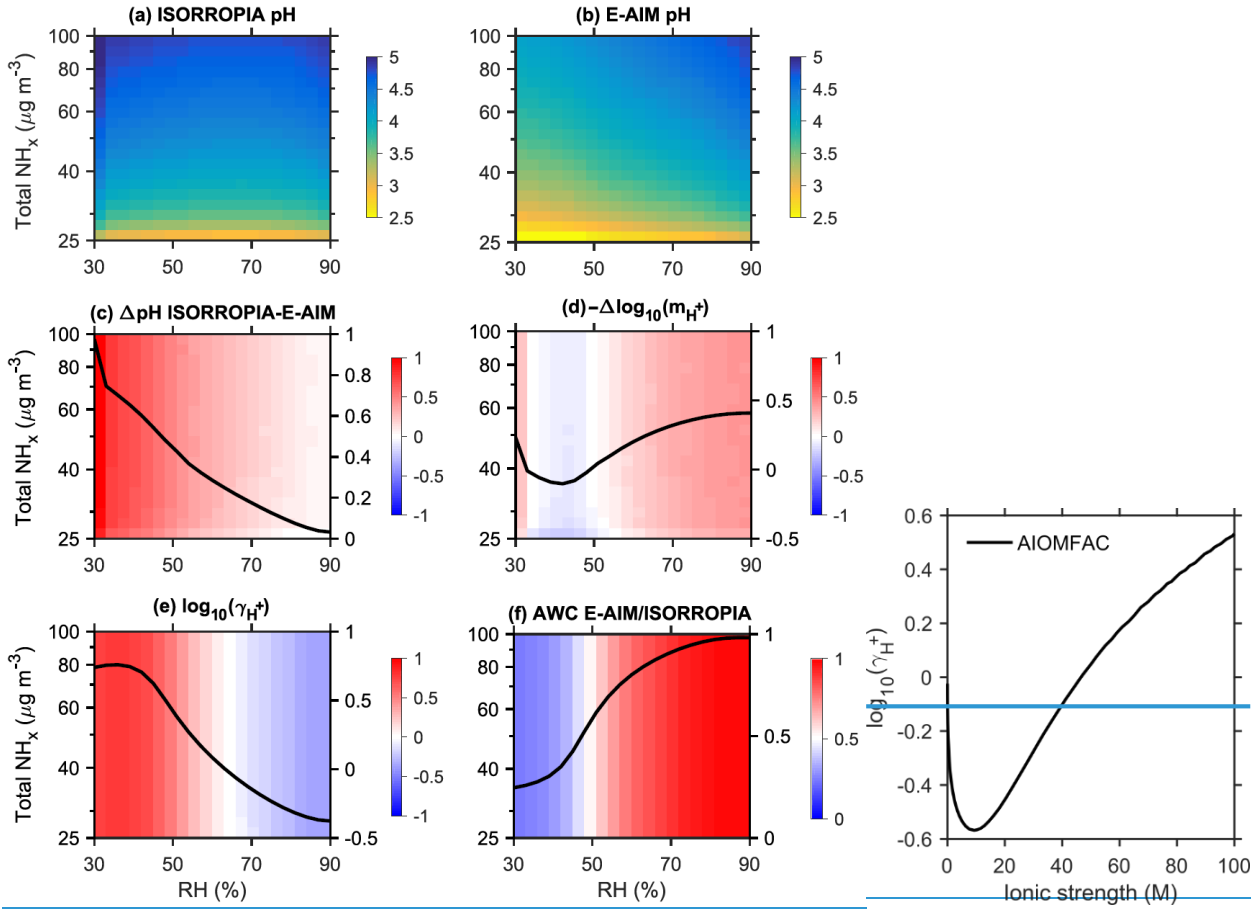

Figure S6. Comparison of predicted pH and several other parameters by ISORROPIA and E-AIM (version II) under representative Beijing winter haze conditions (NH_x-rich). These variables are shown as a function of RH and total NH_x concentrations. pH from ISORROPIA (a), pH from E-AIM (b), ΔpH (ISORROPIA − E-AIM) (c), $-\Delta \log_{10} m_{H^+}$ (d), $\log_{10} \gamma_{H^+}$ (e), and the ratio of AWC between E-AIM and ISORROPIA (f). The curve in each panel (c–f) shows the average value for each bin of RH. E-AIM (version II) and ISORROPIA are run in the forward metastable mode. The model inputs are calculated as the average values during haze episodes (RH > 60%) from our field measurements in Beijing, which include total (gas + particle) H_2SO_4 = 30 μg m^{-3}, total HNO_3 = 51 μg m^{-3}, and temperature = 278 K. The total NH_x concentrations and RH vary from 25 to 100 μg m^{-3} and from 30% to 90%, respectively. Na^+ and K^+ are accounted for as equivalent NH_4^+, and Cl^- as equivalent NO_3^-. The average total NH_x concentration in our measurements is 47 μg m^{-3}. Note that the *y* axis is in log scale.

Formatte
Formatte
Formatte
Formatte
Formatte
Formatte
Formatte
Formatte
Formatte
Formatte
Formatte
Formatte
Formatte
Formatte
Formatte

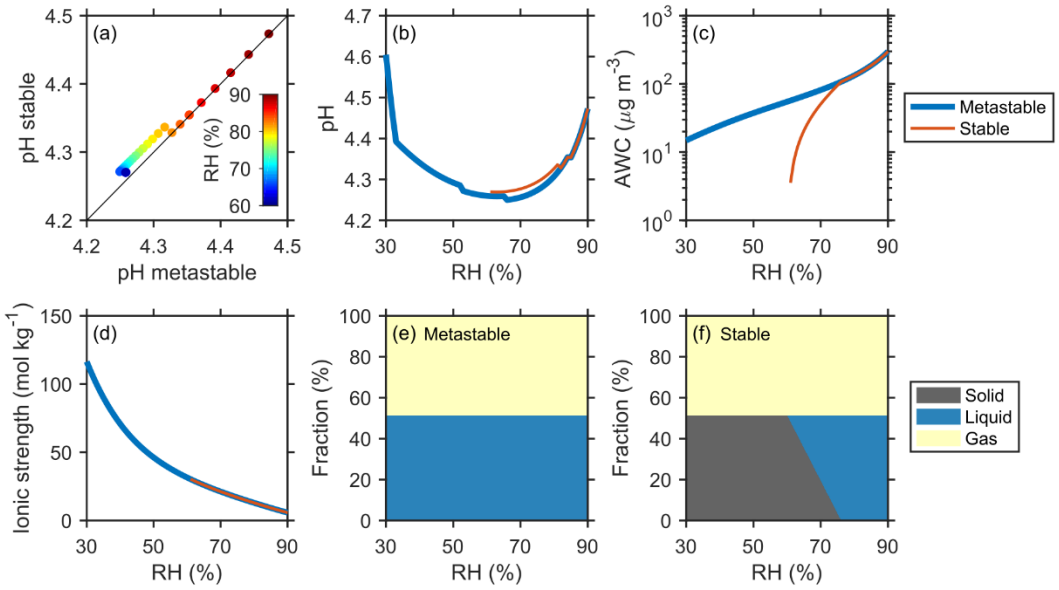

Figure S7. Comparisons of the ISORROPIA predicted pH (a–b), AWC (c), ionic strength (d), and partitioning of NH_3 (e–f) under assumptions of the metastable and stable phase states. The model inputs include total H_2SO_4 = 30 μg m^{-3}, total HNO_3 = 51 μg m^{-3}, total NH_x = 47 μg m^{-3}, temperature = 278 K, and varied RH values. The inputs are calculated from our field measurements during haze episodes (RH > 60%) as the average temperature and the average concentrations of total H_2SO_4, HNO_3, and NH_x. Na^+ and K^+ are accounted for as equivalent NH_4^+, and Cl^- as equivalent NO_3^-. When the RH is between about 60% and about 80% (when both aqueous and solid phases are present for the stable solution), the predicted pH values for the stable solution are on average 0.02 ± 0.00 greater than those for the metastable solution. This difference in pH is small relative to the uncertainty resulting from other factors (e.g., measurements of gas and aerosol species and meteorological parameters).

~~Relationship between the ionic strength and hydrogen ion activity coefficient predicted by the AIOMFAC model under representative winter haze conditions (the relative abundance of NH4+, SO42−, NO3−, Cl−, Na+, K+, and H+ in the aerosol solution is obtained from our field measurements). The AIOMFAC calculations are made at a temperature of 288 K (the applicable range of AIOMFAC is 298 ± 10 K), higher than the measured average ambient temperature (278 K) in this study, but activity coefficients are rather weak functions of temperature (web.meteo.mcgill.ca/aiomfac/).~~

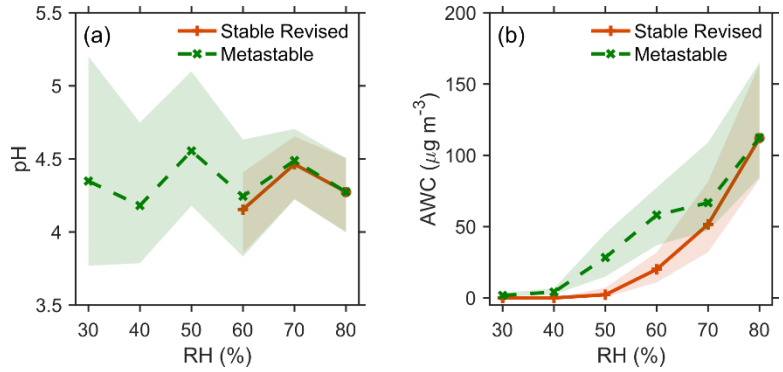

Figure S~~8~~7. pH (a) and AWC (b) predicted by the AMS PM_1 measurements and forward-mode ISORROPIA calculations using both stable and metastable state assumptions. Data are grouped in RH bins (10% increment). The shaded regions indicate the 25th and 75th percentiles. Note that the revised ISORROPIA model is used for the stable state. The uncertainties of ionic and gas measurements are considered using a Monte Carlo approach.

Formatte

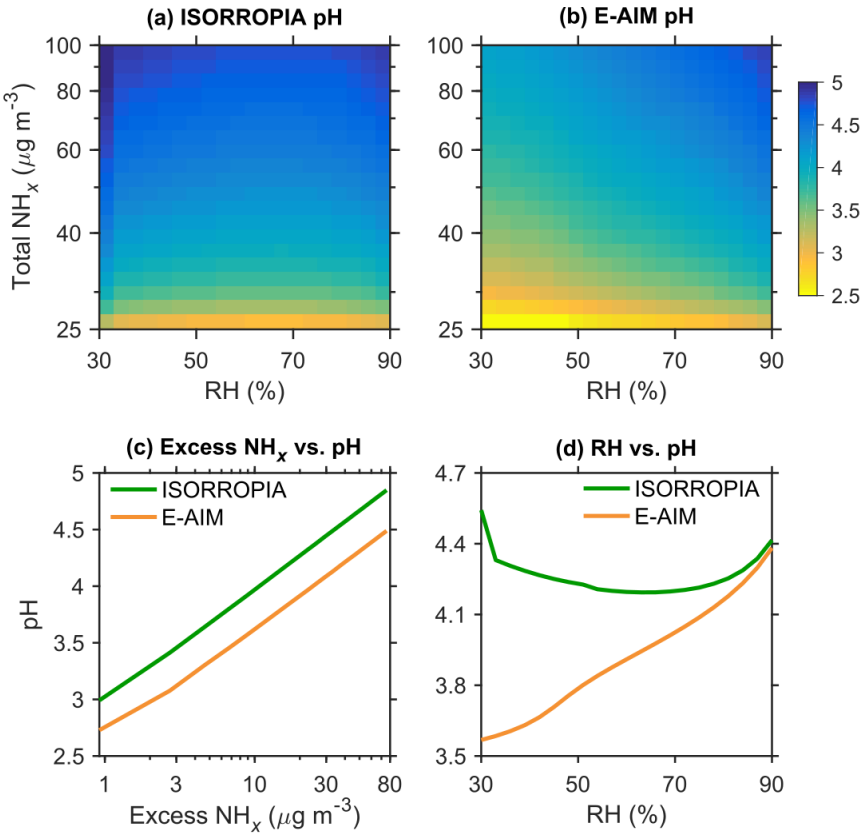

Figure S9. Sensitivity of particle pH to excess NH_x and RH. The model simulations conducted are the same as in Fig. S6. The required NH_x concentrations calculated for the input total H_2SO_4 and HNO_3 concentrations are 24 μg m^{-3}. The curves in panels (c and d) show the average pH in each bin of NH_x concentrations or RH. Note that the *y* axis in panel (a–b) and the *x* axis in panel (c) are in log scale.

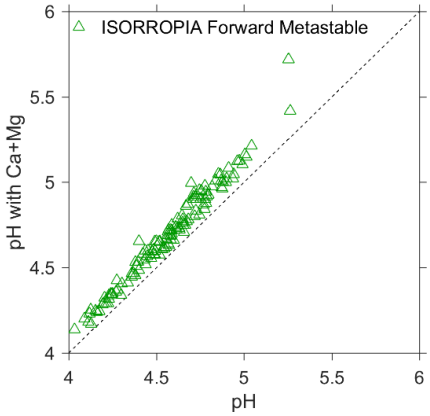

Figure S810. Sensitivity of Ca and Mg on particle pH evaluated using ISORROPIA forward metastable calculations. Based on the measured mass concentrations of Na^+, K^+, Ca^{2+}, and Mg^{2+} in previous studies (summarized in Table S7), the concentration of Ca^{2+} is rarely higher than K^+, and Mg^{2+} is rarely higher than 20% of K^+ concentration. Thus we make a sensitivity test by assuming that Ca^{2+} equals to K^+ and that the concentration of Mg^{2+} is 20% of K^+. Results show, during winter haze events (RH > 60%), that including Ca^{2+} and Mg^{2+} in the calculations increases the predicted particle pH by 0.12 ± 0.05 unit.

Table S7. Mass concentrations of crustal species in $PM_{2.5}$ measured in Beijing during winter haze events (μg m^{-3})

Studies/Species	Na^+	K^+	Ca^{2+}	Mg^{2+}
Jiang et al. (2016)	2.0±0.9	2.9±0.4	2.9±1.8	0.4±0.2
Yang et al. (2015)	0.9±0.3	1.4±0.9	0.5±0.3	0.1±0.1
Huang et al. (2014)	1.0±0.5	4.2± 2.1	0.4± 0.3	0.2±0
Liu et al. (2017) case 1	0.9±0.2	1.8±0.5	0.8±0.2	0.1±0.0
Liu et al. (2017) case 2	0.5±0.1	0.4±0.2	0.1±0.1	0.1±0.0
Liu et al. (2017) case 3	0.8±0.2	0.6±0.3	0.04	0.04

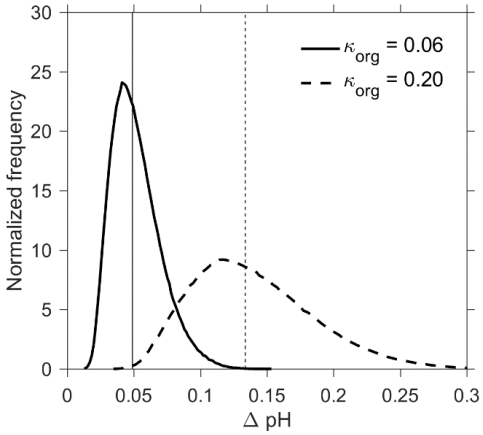

Figure S11~~9~~. The potential impact of aerosol water associated with organic compounds and black carbon on the predicted fine particle pH. The pH values are obtained from the ISORROPIA forward mode metastable calculations. The uncertainties of ionic and gas measurements are considered using a Monte Carlo approach. The solid and dashed curves use κ_{org} of 0.06 and 0.20, respectively, and both use a κ of 0.04 for black carbon. The vertical lines indicate the average ΔpH values of 0.05 and 0.13, respectively.

Table S8. Mass concentrations of major organic acid salts in $PM_{2.5}$ measured in urban Beijing during winter (ng m^{-3})

Reference	Wang et al. (2007)	Huang et al. (2005)	Du et al. (2014)	Jiang et al. (2016)	Wang et al. (2017)
Year	2002	2003	2010	2014	2014
Oxalic	477±304	107±35	195±137	441±429	166±157
Malonic		28±12			16±11
Succinic		24±7			36±26
Glutaric		10±4			5±4
Formic	178±81				
Acetic	3±3				
Glyoxylic		18±5			20±23
Pyruvic		31±14			15±9

Blank means not measured.

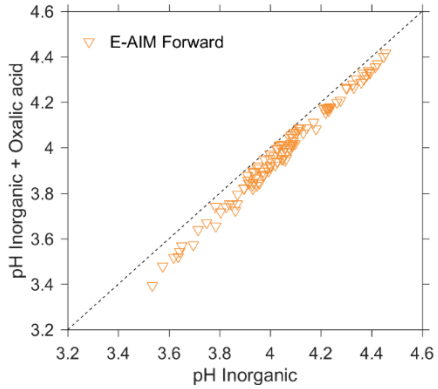

Figure S102. The potential impact of oxalic acid on particle pH evaluated using the E-AIM forward-mode calculations. The *x* axis defines the pH values when only inorganic species (Na^+, NH_4^+, SO_4^{2-}, NO_3^-, and Cl^-) are included in the aerosol system, and the *y* axis indicates the pH values when oxalate is also included. The dashed line indicates a 1:1 relationship.

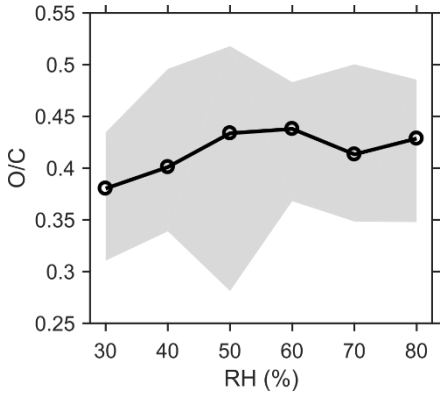

Figure S131. Submicron particle organic aerosol atomic O/C ratios as a function of RH. Data are measured by the AMS and grouped in RH bins (10% increment). The shaded region indicates the 25th and 75th percentiles.

Reference

Bahreini, R., Ervens, B., Middlebrook, A. M., Warneke, C., de Gouw, J. A., DeCarlo, P. F., Jimenez, J. L., Brock, C. A., Neuman, J. A., Ryerson, T. B., Stark, H., Atlas, E., Brioude, J., Fried, A., Holloway, J. S., Peischl, J., Richter, D., Walega, J., Weibring, P., Wollny, A. G., and Fehsenfeld, F. C.: Organic aerosol formation in urban and industrial plumes near Houston and Dallas, Texas, J. Geophys. Res.-Atmos., 114, D00F16, doi:10.1029/2008JD011493, 2009.

Du, Z., He, K., Cheng, Y., Duan, F., Ma, Y., Liu, J., Zhang, X., Zheng, M., and Weber, R.: A yearlong study of water-soluble organic carbon in Beijing I: Sources and its primary vs. secondary nature, Atmos. Environ., 92, 514-521, doi:10.1016/j.atmosenv.2014.04.060, 2014.

Fountoukis, C., and Nenes, A.: ISORROPIA II: a computationally efficient thermodynamic equilibrium model for K^+–Ca^{2+}–Mg^{2+}–NH_4^+–Na^+–SO_4^{2-}–NO_3^-–Cl^-–H_2O aerosols, Atmos. Chem. Phys., 7, 4639-4659, doi:10.5194/acp-7-4639-2007, 2007.

Guo, H., Weber, R. J., and Nenes, A.: High levels of ammonia do not raise fine particle pH sufficiently to yield nitrogen oxide-dominated sulfate production, Sci. Rep., 7, 12109, doi:10.1038/s41598-017-11704-0, 2017.

Huang, K., Zhuang, G., Wang, Q., Fu, J. S., Lin, Y., Liu, T., Han, L., and Deng, C.: Extreme haze pollution in Beijing during January 2013: chemical characteristics, formation mechanism and role of fog processing, Atmos. Chem. Phys. Discuss., 2014, 7517-7556, doi:10.5194/acpd-14-7517-2014, 2014.

Huang, X.-F., Hu, M., He, L.-Y., and Tang, X.-Y.: Chemical characterization of water-soluble organic acids in $PM_{2.5}$ in Beijing, China, Atmos. Environ., 39, 2819-2827, doi:10.1016/j.atmosenv.2004.08.038, 2005.

Jiang, B., Kuang, B. Y., Liang, Y., Zhang, J., Huang, X. H. H., Xu, C., Yu, J. Z., and Shi, Q.: Molecular composition of urban organic aerosols on clear and hazy days in Beijing: a comparative study using FT-ICR MS, Environ. Chem., 13, 888-901, doi:10.1071/EN15230, 2016.

Liu, M., Song, Y., Zhou, T., Xu, Z., Yan, C., Zheng, M., Wu, Z., Hu, M., Wu, Y., and Zhu, T.: Fine particle pH during severe haze episodes in northern China, Geophys. Res. Lett., 44, 5213-5221, doi:10.1002/2017GL073210, 2017.

Pye, H. O. T., Liao, H., Wu, S., Mickley, L. J., Jacob, D. J., Henze, D. K., and Seinfeld, J. H.: Effect of changes in climate and emissions on future sulfate-nitrate-ammonium aerosol levels in the United States, J. Geophys. Res.-Atmos., 114, D01205, doi:10.1029/2008JD010701, 2009.

Seinfeld, J. H., and Pandis, S. N.: Atmospheric chemistry and physics: from air pollution to climate change, Third ed., John Wiley & Sons, Inc., Hoboken, New Jersey, 2016.

Wang, G., Zhang, R., Gomez, M. E., Yang, L., Levy Zamora, M., Hu, M., Lin, Y., Peng, J., Guo, S., Meng, J., Li, J., Cheng, C., Hu, T., Ren, Y., Wang, Y., Gao, J., Cao, J., An, Z., Zhou, W., Li, G., Wang, J., Tian, P., Marrero-Ortiz, W., Secrest, J., Du, Z., Zheng, J., Shang, D., Zeng, L., Shao, M., Wang, W., Huang, Y., Wang, Y., Zhu, Y., Li, Y., Hu, J., Pan, B., Cai, L., Cheng, Y., Ji, Y., Zhang, F., Rosenfeld, D., Liss, P. S., Duce, R. A., Kolb, C. E., and Molina, M. J.: Persistent sulfate formation from London Fog to Chinese haze, Proc. Natl. Acad. Sci. U.S.A., 113, 13630-13635, doi:10.1073/pnas.1616540113, 2016.

Wang, J., Wang, G., Gao, J., Wang, H., Ren, Y., Li, J., Zhou, B., Wu, C., Zhang, L., Wang, S., and Chai, F.: Concentrations and stable carbon isotope compositions of oxalic acid and related SOA in Beijing before, during, and after the 2014 APEC, Atmos. Chem. Phys., 17, 981-992, doi:10.5194/acp-17-981-2017, 2017.

Wang, Y., Zhuang, G., Chen, S., An, Z., and Zheng, A.: Characteristics and sources of formic, acetic and oxalic acids in $PM_{2.5}$ and PM_{10} aerosols in Beijing, China, Atmos. Res., 84, 169-181, doi:10.1016/j.atmosres.2006.07.001, 2007.

Yang, Y., Zhou, R., Wu, J., Yu, Y., Ma, Z., Zhang, L., and Di, Y.: Seasonal variations and size distributions of water-soluble ions in atmospheric aerosols in Beijing, 2012, J. Environ. Sci., 34, 197-205, doi:10.1016/j.jes.2015.01.025, 2015.